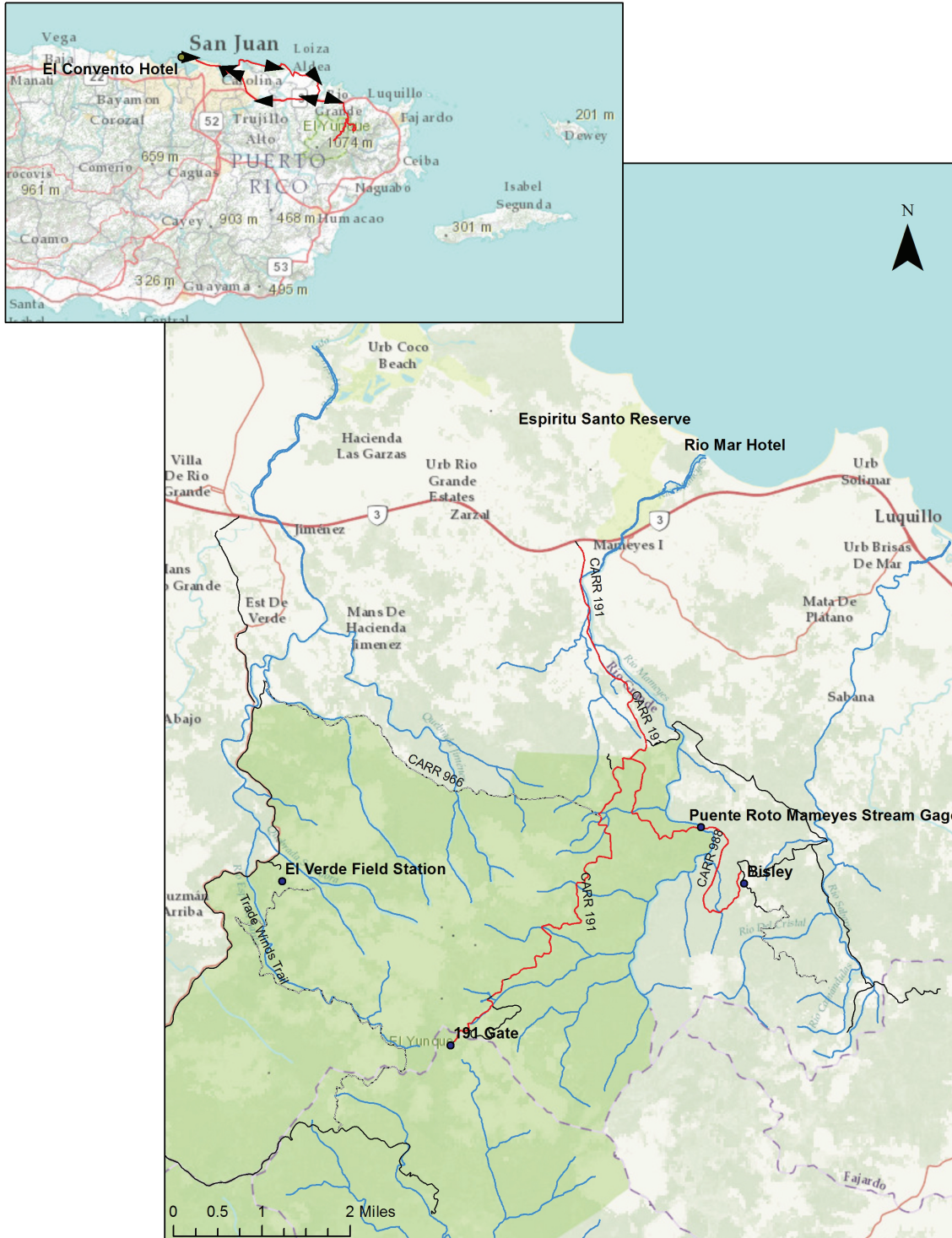


CZO PI Annual Meeting Luquillo Mountains Field Trip Guide

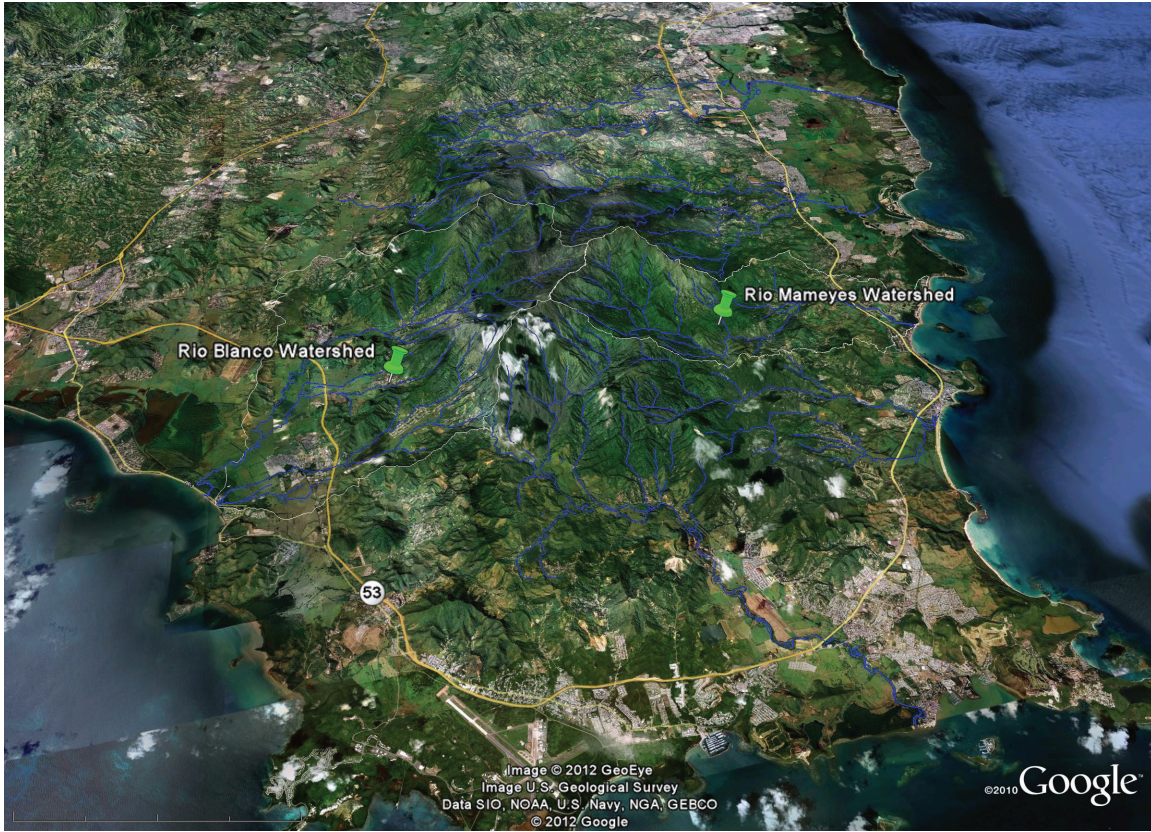
May 31st, 2012

Stop at: Puente Roto, Bisley Watersheds
Upper Luquillo Mountains at Route 191

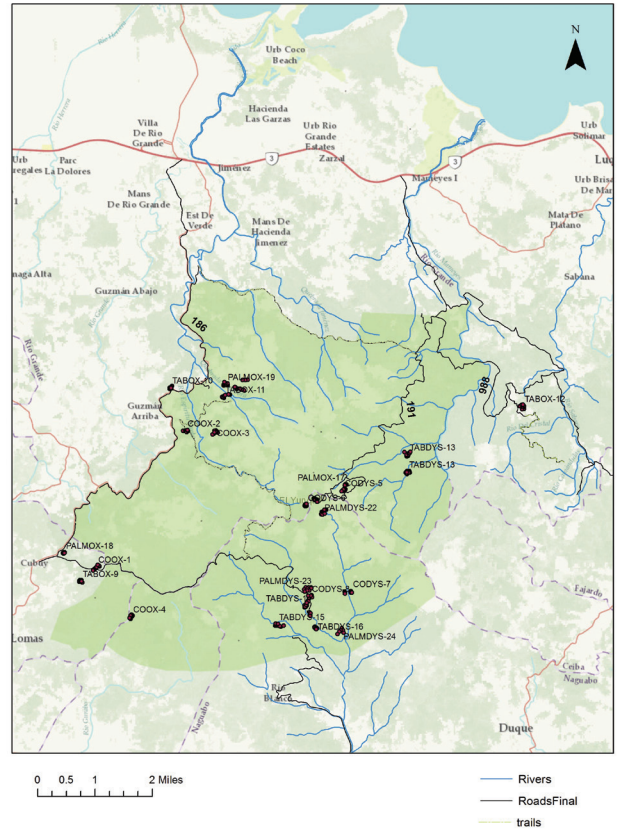


This work is supported by the National Science Foundation's Critical Zone Observatory Program. Additional support is provided by the USGS-WEBB program and the USFS International Institute of Tropical Forestry.

Luquillo Mountains



Luquillo Mountain Infrastructure



LCZO Soil Network

More than 8 stream gages, 3 walk-up canopy towers, 4 meteorological stations, 3 deep observations wells, lysimeter nests, an extensive GIS system and numerous long-term vegetation plots are available for researchers. Datasets generated from this infrastructure are available online. www.sas.upenn.edu/lczodata

Luquillo Critical Zone Observatory Field Guide

Table of Contents

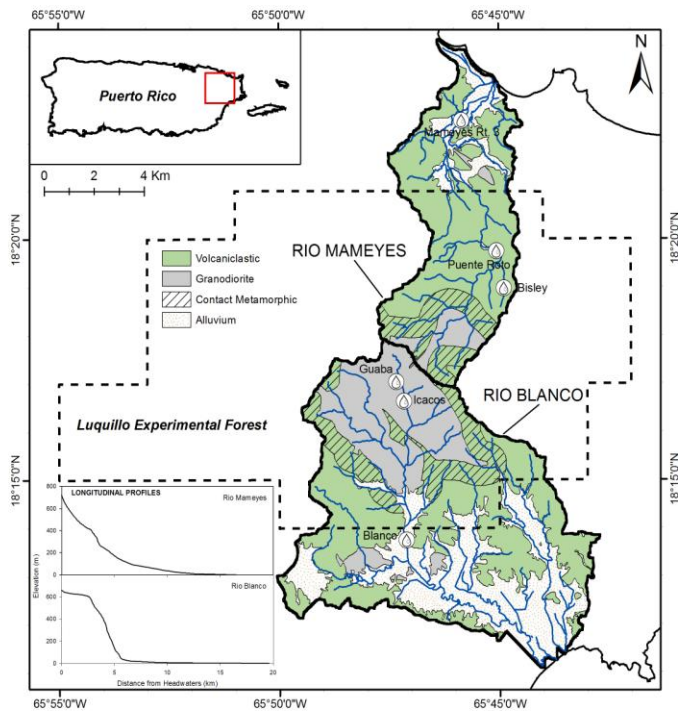
Page	
1-2	Route and Additional site overview maps
3-4	Table of Contents
5-15	Field Guide Overview of LCZO
16-17	Balan S.A., Amundson R., Buss H.L., Sulfur Cycling in the Rainforest of Puerto Rico.
18-19	Brereton R.L., McDowell W.H., Carbon, nitrogen and solute export from high-elevation watersheds in the Luquillo CZO.
20-21	Brocard G., Willenbring J., Scatena F.N., Long-term landscape evolution of the Luquillo Mountains and its effects on today's variability in erosion rates.
22-23	Buss H.L., Brantley S., et al. Probing the Depth of the Critical Zone: Chemical and Physical Weathering of Deep Fractured Bedrock in the Bisley Watersheds.
24-25	Buss H.L., Lara M.C., Application of a Novel Mg-Li Dual Isotopic Tracer to Biogeochemical Cycles in the Critical Zone.
26-27	Buss H.L., White A., Blum A., Lithological Influences on Weathering Processes and Rates.
28-29	Evaristo J., Scatena F.N., Stable isotopes of water as riparian indicators of flow frequency in a tropical montane stream network and the role of microclimates on stable isotopes of water.
30-31	Hall S., Silver W., Linkages between redox processes and surface soil carbon cycling.
32-33	Johnson A.H., Hao X.X., Scatena F.N., Landscape-Scale Controls on C,N, and exchangeable Ca ⁺⁺ , Mg ⁺⁺ and K ⁺ in Soils of the Luquillo CZO Forest.
34-35	Jiménez R.A., Mastropaolo C., et al. A Geochemical Model of Redox Reactions in a Sandy Tropical Rain Forest floodplain Stream Riparian Zone: DOC Oxidation, Respiration and Denitrification.
36-37	Khan N., Horton B.P., Vane C., et al. The reconstruction of Holocene sea level and paleoenvironmental change.
38-39	Kurtz A., Takagi K., A $\delta^{44}\text{Ca}$ based comparison of Ca cycling in tropical and temperate ecosystems.

- 40-41 Leon M., Scatena F.N.,
Real time rainfall-induced landslide risk assessment System for the Luquillo Mountains of Puerto Rico.
- 42-44 Liermann L., Brantley S., Albert I., Buss H., Minyard M.,
Microbiota versus geochemistry in regolith in the Rio Icacos and Bisley watersheds.
- 45-46 Litwin K., Jerolmack D.J.,
Relative importance of sediment abrasion in downstream fining of grains and production of fine sediment.
- 47-48 Malvadkar U., Scatena F.N., Leon M.C.,
Landscape connectivity indices of Luquillo Watershed.
- 49-50 Occhi M.E., Willenbring J., et al.
Determining the Provenance of Suspended Sediment: Storm Sampling in NE Puerto Rico.
- 51-55 Orlando J., Brantley S., et al.
The architecture of the weathering of the Rio Icacos watershed.
- 56-57 Phillips C.B., Scatena F.N.,
Stream channel response to urbanization in the humid tropical region of NE Puerto Rico.
- 58 Phillips C.B., Jerolmack D.J.,
Coarse Sediment tracers and flood scale bed load transport.
- 59-60 Porder S., Mage S.,
Parent material and topography drive soil P status across the Luquillo Mountains.
- 61-62 Scholl M.,
Isotope Hydrology Research in the Luquillo Critical Zone Observatory.
- 63-64 Shanley J.B.,
Mercury research at Luquillo Critical Zone study.
- 65-66 Stachowiak L., Scatena F.N., Doheny E., Tomlin D.
Influences of bedrock lithology and vegetation on flow hydrology in the Luquillo Mountains.
- 67-68 Stone M., Ali L., Plante A.,
Soil Organic matter quantity, quality and microbial activity in deep soil profiles
- 69-70 Thompson A., Meile C., Schere M., et al.
Redox cycling and Fe atom exchange in the Bisley Watershed.
- 71-72 Wordell E., Ohno T., Plante A.,
Differences in soil organic matter quality by biological, chemical and physical fractionation.

Luquillo Critical Zone Observatory Overview April 2012

How critical zone processes, water balances, and mass fluxes differ in landscapes with contrasting lithology but similar climatic and environmental histories is the overarching focus of the Luquillo Critical Zone Observatory (LCZO). Although bedrock lithology and chemistry have been considered primary state factors in landscape and soil development for over a century, the influences of lithology on denudation, hydrologic routing, and geochemical processing is poorly constrained in most studies. To address this challenge the LCZO uses the natural laboratory of the Luquillo Mountains to quantify and contrast how critical zone processes in watersheds underlain by quartzdiorite (QD) and volcanoclastic (VC) bedrock are coupled and decoupled with climatic conditions and hydrologic, geochemical and biogeochemical cycles (Figure 1). A set of interrelated hypothesis (Figure 2, Table 1), sampling sites (Table 2) and a unified data management system allow critical zone processes to be contrasted by bedrock (QD, VC), landscape position (ridge, hillslope, riparian), depth (surface to bedrock), forest type (Tabonuco, Colorado, Cloud) and location (upland to coastal).

Figure 1; Luquillo Critical Zone focus watersheds



Short term responses (e.g. days to seasons) being investigated include the influence of lithology on biogeochemical responses to storms and droughts, and the influence of lithology on hydrologic routing and watershed scale hydrologic budgets. Recent research indicates there are greater seasonal variations in the chemistry of atmospheric inputs and soils processes than previously expected (Heartsill et al 2007, Shanley 2008, Scholl et al 2009). These responses are being quantified using an improved network of weather stations, nested stream gages and multi-investigator event sampling campaigns. Basin

responses at intermediate time scales (e.g. decades to centuries) are being evaluated by quantifying stream channel dynamics and the depositional records in floodplains and coastal zones. The long-term influences of lithology on sediment generation, hillslope and landscape development are evaluated in studies of bedrock weathering rates and rates of saprolite and soil formation (Buss et al 2010).

Figure 2: Conceptual framework and relationships between the hypothesis and sampling nodes for the Luquillo Critical Zone Observatory. Infrastructure is in red while hypothesis are in green.

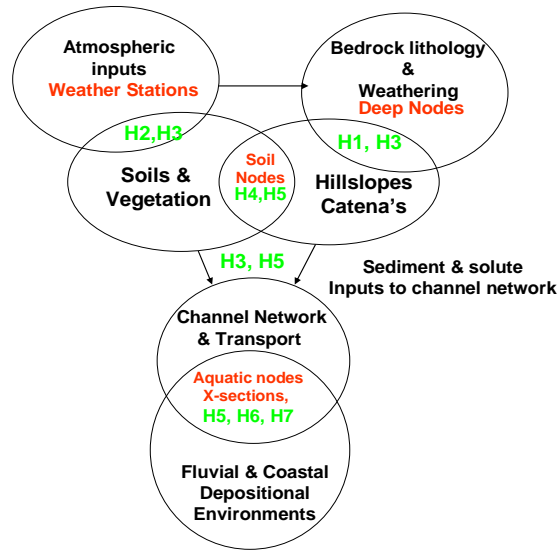


Table 1: Guiding Hypothesis for the Luquillo Critical Zone Observatory

Hypothesis 1: The rate of saprolite advance varies with regolith thickness and landscape position and is fastest in QD valleys and slowest on VC ridges. Over large areas, the rate of saprolite advance will equal the rate of denudation and can be predicted from bedrock chemistry, porefluids, and physical rock properties (Brantley, Buss, White, Heimsath, Willenbring.).

Hypothesis 2: In surface soils, chemical transformations of atmospheric inputs are decoupled from bedrock lithology and influenced by soil carbon, surface redox, and plant nutrient cycling. Biotic influences on soil biogeochemistry decrease with storm intensity and soil depth and are greatest in surface soils of the VC during low intensity rainfalls (Johnson, Shanley, Silver, Scatena, UPR).

Hypothesis 3: The residence time and routing of water varies with bedrock lithology and will be longest in areas underlain by the QD and shortest in areas underlain by VC. However these differences will decrease with storm intensity and duration (Scholl, Scatena, Shanley, McDowell).

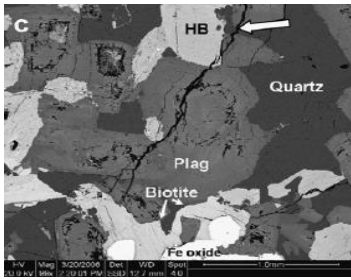
Hypothesis 4: Over seasonal time scales, iron reduction and related CO₂ production will be greatest in VC surface soils and lowest at depth on stable QD ridge tops. Over large areas and longer time scales deep weathering rates and surface soils properties are closely linked to the frequency of low redox events and the magnitude of iron reduction (Silver, Brantley, Plante)

Hypothesis 5: The morphology, and soil biogeochemistry of riparian and colluvial deposits varies systematically with lithology and in a downstream direction, while their vegetation and soil organic matter chemistry varies systematically with rainfall and temperature (McDowell, Plante, Silver, Scatena, Jerolmack).

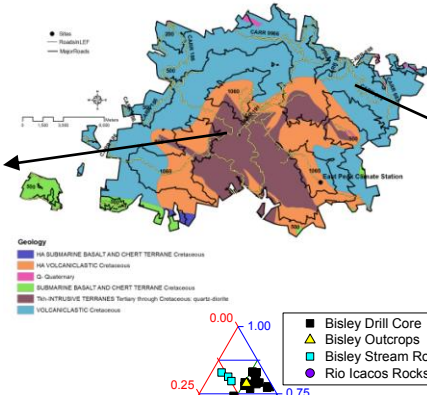
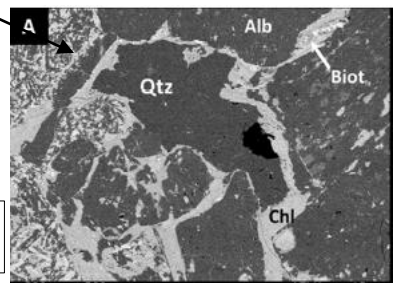
Hypothesis 6: Sediment supply and transport within the stream channel network is dominated by surface erosion associated with rainfalls of moderate intensity in the VC and landslides associated with high intensity events in the QD (Jerolmack, Horton, Willenbring, Scatena, Shanley).

Hypothesis 7: The depositional environments of coastal and fluvial sediments draining the QD will have a higher resolution record of climatic disturbances and land use changes than corresponding environments in the VC (Horton, Willenbring, Jerolmack, Heimsath, Scatena).

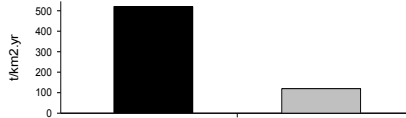
Quartz-Diorite



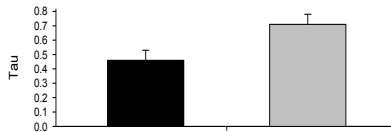
Volcano-Clastic



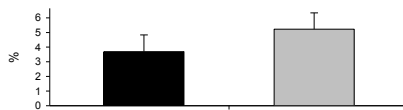
Suspended Sediment



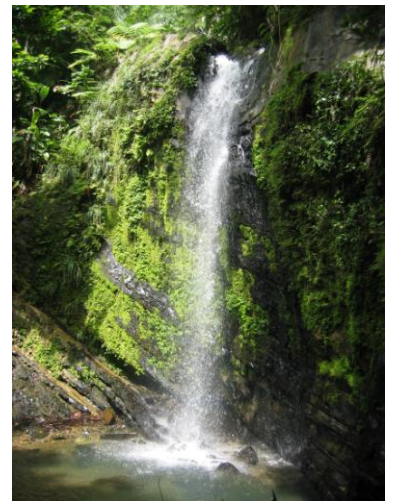
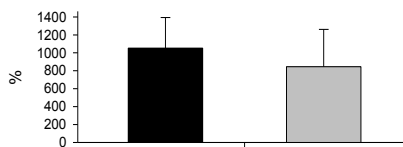
Tau P, Valleys



Soil % C. Ridges



Soil Ca0-20, Valleys



Observatory Geology

Three principal rock types underlay the LM: volcanoclastic (VC), quartzdiorite (QD), and contact metamorphic hornfels (HF). Smaller outcrops of basalt, mafic dikes, and alluvium also occur. Both types of bedrock were derived from a genetically related andesitic magma that was active in the lower Tertiary (Brocard this volume). The VC bedrock consists of thick layers of volcanic debris interbedded with shallow marine clays. The Luquillo Quartz Diorites are part of a system of felsic batholiths that outcrop across PR. Their emplacement was not accompanied by significant host rock folding but the associated contact metamorphism did produce the erosion resistant hornfels (HF) that currently forms the divide between the 2 watersheds and the highest peaks in the LM

In general, areas underlain by the GD have faster weathering rates, sandy eutropeptic soils, and relatively deep subsurface flow paths (McDowell et al 1992, Brown et al 1995, White et al 1998, Peters et al 2006). These areas also have a higher frequency of landslides, well defined floodplains, and lower gradient, sandy bedded streams (Ahmad, et al. 1993, Larsen et al 1998, Pike 2006). In contrast, areas underlain by VC rocks weather to deep, clayey tropohumultic soils that have shallow subsurface flow paths (Silver et al 1994, Schellekens 2004), steeper hillslopes, fewer and smaller landslides, and relatively steep, boulder lined stream. Annual suspended sediment discharge can be 5 to 16 times higher under the GD that comparable VC watersheds (McDowell et al 1994, [Figure 3](#)).

Observatory Climate

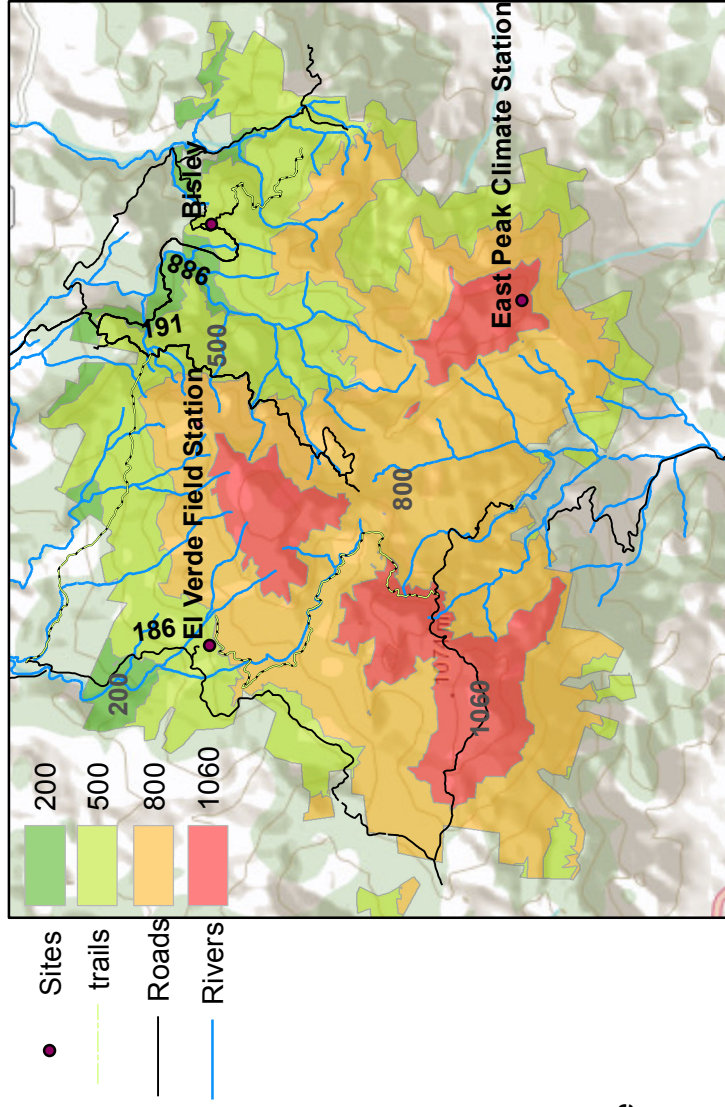
The Luquillo Critical Zone Observatory is located in the windward, Northeastern portion of Puerto Rico and in one of the wettest regions of the Caribbean. Over a distance of 10 to 20 km, this mountain range rises from sea level to an elevation of 1075 meters. The Observatory has a subtropical, humid, maritime climate that is influenced by both orographic and global-scale synoptic weather systems. Rainfall is relatively evenly distributed throughout the year and increases from 1000 mm/yr in the lowlands to nearly 5000 mm/yr at the highest elevations. Rainfall events at mid-elevations are generally small (median daily rainfall 3 mm/day) but numerous (267 rain days per year) and of relatively low intensity (< 5mm/hr). Nevertheless, individual storms with greater than 125 mm/day occur annually, and daily rainfalls greater than 600 mm have been recorded. The most common disturbance-generating weather systems that affect the Luquillo Mountains are (1) cyclonic systems, (2) noncyclonic intertropical systems, (3) extratropical frontal systems, and (4) large-scale, coupled ocean-atmospheric events (e.g., North Atlantic Oscillation, El Niño-Southern Oscillation). Unlike some tropical forests, the Luquillo Mountains do not commonly have disturbances associated with the passage of the Inter-Tropical Convergence Zone (ITCZ) or monsoonal rains.

Observatory Hydrology

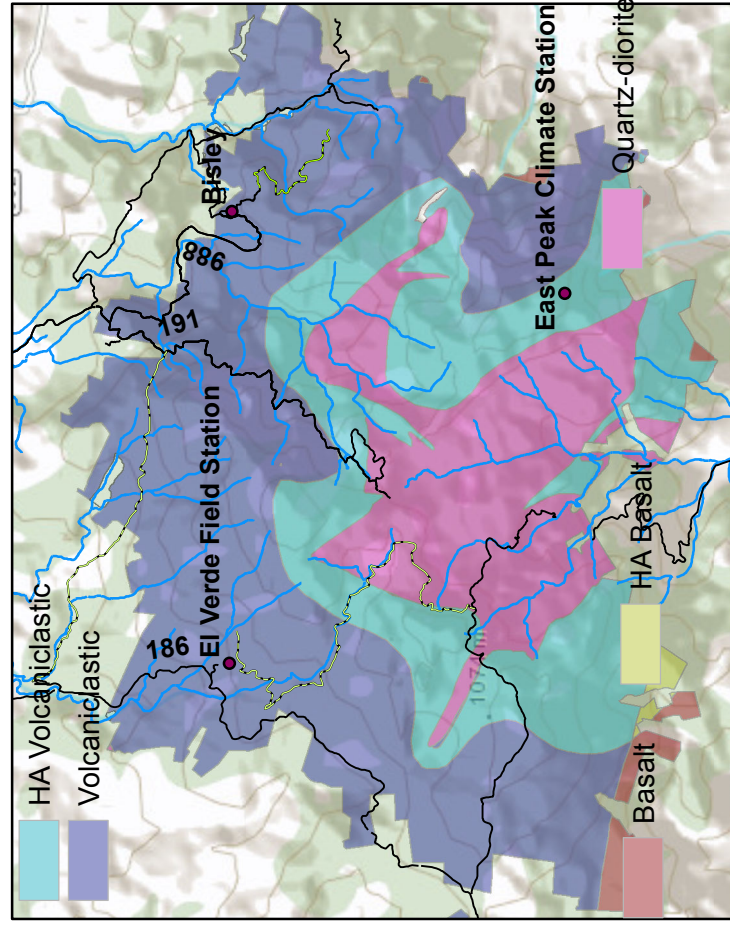
The Luquillo Mountains are the headwaters to 9 rivers that flow through steep, bedrock and boulder-lined channels until they reach their coastal plain alluvial reaches. High stream flows are common and tenfold increases in discharge have been recorded within an hour. The frequency of daily discharges is highly skewed as peak discharges are several hundred times average daily discharge. Short term, flash floods occur at least once a month and the annual peak discharge can occur in any month of the year but are

Figure 4

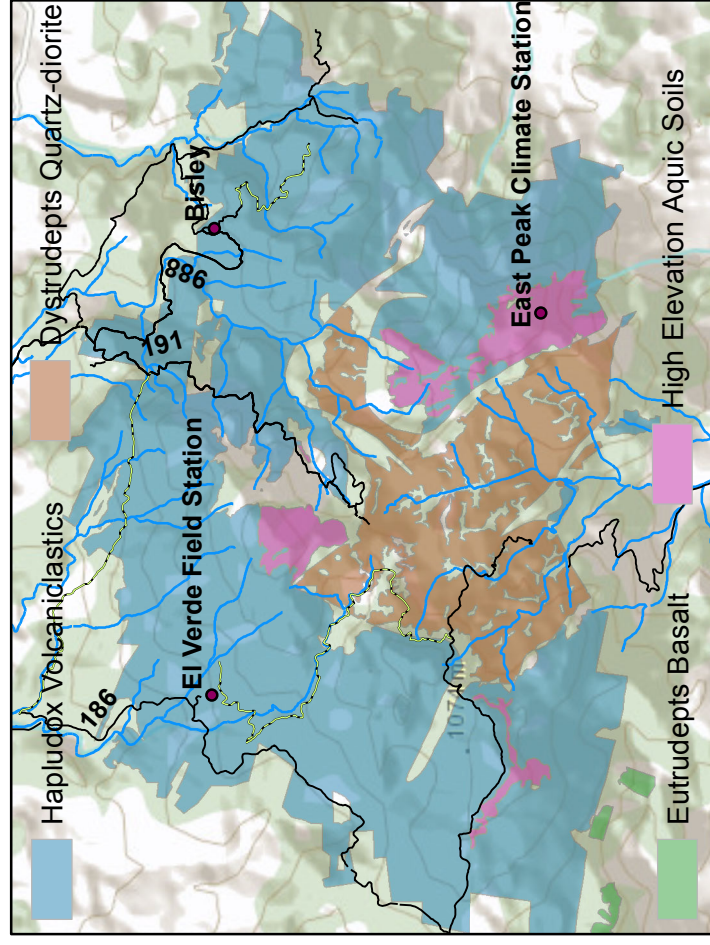
Elevation



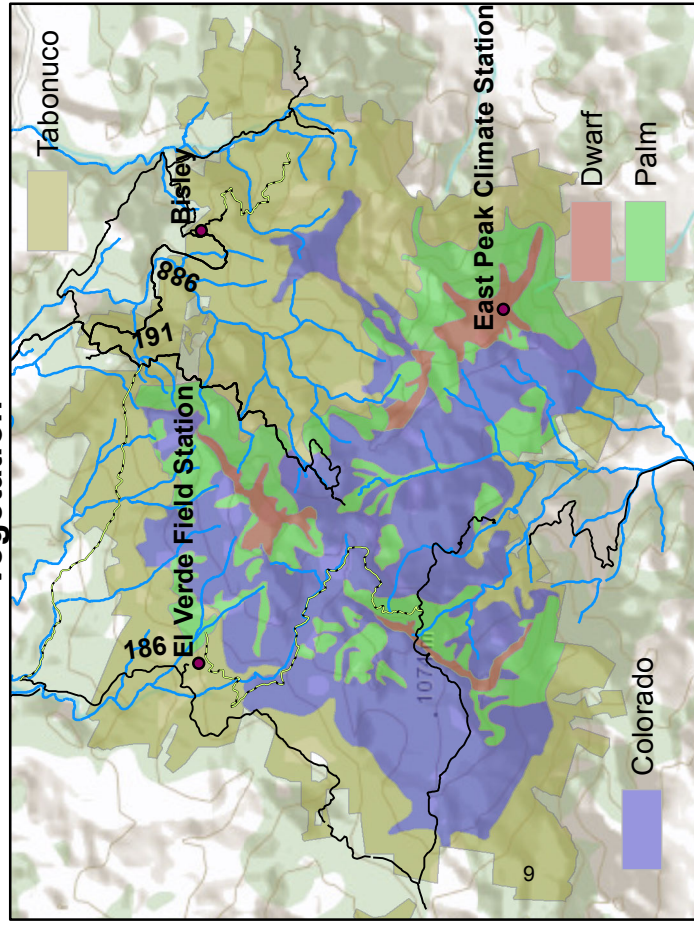
Geology



Soil



Vegetation



most common in the late summer and fall. The largest floods are often, but not always associated with hurricanes. Water temperature in headwater streams is relatively consistent throughout the year and ranges between 18 and 24 °C. The average pH of stream water is 7.2.

Significant relationships exist between elevation, mean annual rainfall and runoff. Of the average annual rainfall input, 65% (2526 mm/yr) is converted to runoff. The remaining 35% (1338 mm/yr) is lost from the system by evapotranspiration and other abstractions (Schellekens et al 2000, Peters et al 2006). In comparison to other tropical forests, the Luquillo Mountains as a whole has more evapotranspiration than many tropical montane forests but less than many lowland tropical forests

Observatory infrastructure and sampling design

The LCZO infrastructure, sampling strategy, and integrated data management system are designed to provide a platform whereby collaborators can put geochemistry and biogeochemistry into a geomorphic and hydrologic perspective. The basic infrastructure of the LCZO is an integrated set of sampling sites (e.g. nodes in Table 2). These sampling sites are built upon existing study sites that have long-term and ongoing records of rainfall, throughfall, litterfall, and streamflow (Schellekens et al 2004, Peters et al 2006, Heartsill et al 2007, Wei et al 2007). Atmospheric sampling nodes consist of 8 weather stations and an additional 8 rain gages that will monitor climatic and geochemical inputs to the different lithologies and forest types across a precipitation gradient that ranges from 1000 mm/yr to 5000 mm/yr. Atmospheric inputs are monitored at existing climate stations that are maintained by the LCZO with support from the USGS, the USFS, and UC Berkeley. Although these stations cover the entire matrix of elevation, lithology, and forest types, most of these stations were established with previous funding that no longer exists. LCZO funding has been used to upgrade, calibrate, and integrate these stations into a network that for the first time constrains variations in precipitation along the elevation gradient and thereby improves water budgets for the individual study basins (see Balan, Scholl write-ups in this volume).

Observation of deep critical zone processes are made at a series of instrumented bore holes in VC, QD, and hornfel lithology (Buss et al 2012, and Buss, Orlando, Brantley write-ups in this volume). Soil and regolith water and gas samples are sampled using suction samplers installed according to our previous studies and CZEN standards (see <http://www.sas.upenn.edu/lczo/> and CZEN.ORG).

Luquillo Critical Zone Soil Network consists of soils collected from 216 profiles from 24 sub-watersheds (Figure 4). Profiles were stratified by two different parent materials (VC and QD), three different forest types (Tabonuco, Palm, and Colorado), and three hillslope positions (ridgetops, slopes, and valleys). See Johnson, and Porder write-ups in this volume.

Aquatic nodes of the observatory focus on quantifying the fluxes of water, sediment, and solutes from the basin and how they are transformed as they move from pore spaces in the lithologic matrix to the coastal zone. These nodes include 8 stream gages and numerous georeferenced cross-sections and riparian sampling sites (see Phillips, Litwin, Malvadkar write-ups in this volume). A major limitation to previous studies has been the ability to monitor storm events and temporal variations in exports. To overcome this limitation, the LCZO has added temperature, conductivity and turbidity

sensors to existing stream gages to obtain continuous records of conductivity, and temperature (Shanley et al 2008). Water chemistry is sampled weekly and during coordinated sampling campaigns (see Occhi in this volume). All samples are processed at the USGS WEBB laboratories and at the University of New Hampshire in collaboration with the Luquillo LTER site.

The late Holocene response to storms and sea-level change of the Luquillo Mountains is being deciphered by studying the sedimentary records of coastal plain sediments (see Khan in this volume). This research uses micro-fossils, isotopes and stratigraphic indicators from shallow sediment cores taken in the coastal zones of both rivers. The environmental histories developed from the coastal plain sediments will then be compared to the historical record and the geologic recorded in upland floodplains and landscapes.

Site Management:

The LCZO will be managed via subcontracts administered through the University of Pennsylvania. While PI's will be responsible for their own research component, daily management is the responsibility of F.N. Scatena. LCZO information management is managed by Miguel Leon, a full time data manager based at UPENN. Technical and administrative oversight is provided by an Executive Management Team (Scatena, Brantley, Buss). Each hypothesis also has a leader (marked in bold in Table 1) who is responsible for organizing synthesis activities and reporting on the progress of the hypothesis.

The LCZO has annual researcher meetings in Puerto Rico during late May or early June where researchers will report on their progress and archive data and samples collected in the previous year. An External Advisory Committee (Larsen, Bras, Lugo) is invited to these meetings to critique our progress and provide technical advice. These senior-level individuals have worked in the area and/or on similar problems and have agreed to advise the group. Funds are also allocated to allow potential collaborators and outreach groups to participate in these annual meetings. Additional hypothesis-based meetings and meetings at AGU and similar conferences are also be held when needed and convenient.

Data and Information Management:

The information management system of the LCZO will be dedicated to preserving and distributing high quality data that can be used in cross-site comparisons and predictive modeling. Our data management philosophy is also based on the premise that the best form of data management involves data that has been synthesized in peer reviewed journals and made widely available online. To accomplish this, a full time data manager, Miguel Leon, manages a central LCZO website that is maintained at UPenn. This site is the central portal for the site and is link to the National CZO Portal, and the CZO San Diego Super Computer data base.

Synthesis and cross-site activities:

A major goal of the LCZO is to promote synthesis within the geosciences and between the various institutions and students involved with the project. While the focus

and study areas of the LCZO are distinct to that of the Luquillo LTER and Puerto Rico NEON site, there will be ample opportunities to collaborate with those groups. Likewise, LCZO members already have unfunded and informal collaborations with the proposed Delaware CZO and various LTER sites in the study of carbon dynamics and quality (Plante, Silver, McDowell, Stroud Water Resource Center and others) and with the coastal site Delaware (Horton) as well as with an investigation of granite weathering with C. Rasmussen (Arizona CZO).

Contact Information:

Luquillo-CZO@sas.upenn.edu

Luquillo Critical Zone Observatory

Department of Earth and Environmental Science

University of Pennsylvania

<http://www.sas.upenn.edu/lczo>

Table 2. Location of existing and proposed infrastructure for the Luquillo Critical Zone Observatory. Ex = existing, no upgrade required, Ux = upgrade of existing infrastructure required, Nx = new installations, x = year of planned upgrade or installation.

Sampling Node (Principal)	Infrastructure and Measurements	Volcaniclastic (Bisley/Mameyes)	Granodiorite (Guaba/Iacos/Rio Blanco)
Soil and Deep Weathering Nodes			
Deep Weathering (Brantley)	Surface to bedrock lysimeters, tensiometers, & gas samplers. Periodic & event sampling, XRF, mineralogy, archived soils	Bisley Ridge (N1) Bisley Slope (N2) Bisley Riparian (N3)	Guaba Ridge (U1) Guaba Slope (U2) Iacos Riparian (N2)
Redox (Silver)	Surface to bedrock Apogee oxygen sensors, trace gas, H ₂ O content, samplers,	Bisley Ridge (N1) Bisley Slope (N2) Bisley Riparian (N3)	Guaba Ridge (U1) Guaba Slope (U1) Iacos Riparian (N2)
Soil (Johnson)	Quantitative pits & bore holes, SOM, total and extractable nutrients, X-ray, grainsize, hydrologic properties	Multiple quantitative soil pits at the intensive research sites and throughout the Luquillo Mountains, stratified by climate, bedrock, and land cover (N1-2)	
Aquatic Sampling Nodes			
Fluvial (Jerlomack, Scatena McDowell Shanley)	Upgrade gages with permanent cross-sections (U1,2), bedload transport estimates (U1-3), Be10 denudation rates (N2-5) expand water sampling (U1), sensors for conductivity & temp (N1,2)	USGS 655 (U1) Bisley Q1-3 (U2) USGS 660 (E) USGS 670 (E)	Iacos USGS 750 (U1) Guaba USGS 749 (U2) Rio Blanco USGS (E)
Riparian (McDowell)	Piezometers, tensiometers, lysimeters & gas samplers, Periodic & event sampling	Bisley (U1,2) Multiple sites along R. Mameyes	Iacos (U1,2) Multiple sites along R. Blanco
Coastal (Horton)	Short cores and surface samples	Mameyes estuary and coastal zone	Rio Blanco estuary and coastal zone
Atmospheric Sampling Nodes			
Atmospheric Climate Stations (E) (Shanley, Scholl, UPR)	Hourly & daily climate (precip, temp., radiation, RH, wind, soil moisture etc.) Periodic & event sampling of chemistry, stable isotopes	Upgrade and standardize existing network supported by USGS WEBB, USFS IITF, and UCB at Iacos, Bisley and Sabana. Isotope samplers will be established as needed. 8 stations and 8 rain gages will be operational	
Data Management (Scatena)	Web site at UPENN (http://www.sas.upenn.edu/lczo/) will provide the portal to all LCZO activities. Data will be managed by an integrated data management system that is linked to National CZO portal.		

Literature Cited

- Ahmad, R., Scatena F.N., Gupta A. 1993. Morphology and sedimentation in Caribbean montane streams: examples from Jamaica and Puerto Rico *Sedimentary Geology* 85: 157-169.
- Buss H.L., Brantley S.L., Scatena F.N., Bazilievskaya E.A., Blum A., Schulz M., Jimenez R., White A.F., 2012 (submitted) Probing the deep critical zone beneath the Luquillo Experimental Forest, Puerto Rico. *Earth Surface Process and Landforms*
- Buss H.L.; Mathur R., White A.F., Brantley S.L., 2010. Phosphorus and iron cycling in deep saprolite, Luquillo Mountains, Puerto Rico *Chemical Geology* Volume: 269 Issue: 1-2 Pages: 52-61 DOI: 10.1016/j.chemgeo.2009.08.001
- Heartsill-Scalley T., Scatena F.N., Estrada C., McDowell W.H., Lugo A.E., 2007. Disturbance and long-term patterns of rainfall and throughfall nutrient fluxes in a subtropical forest in Puerto Rico. *Journal of Hydrology*, 33:472-485
- Larsen, M. C., Torres-Sánchez A.J., 1998. The frequency and distribution of recent landslides in three montane tropical regions of Puerto Rico. *Geomorphology* 24: 309-331.
- McDowell, W. H., Asbury C.E., (1994). "Export of carbon, nitrogen, and major ions from three tropical montane watersheds." *Limnology and Oceanography* 39: 111-125.
- Peters N.E., Shanley J.B., Aulenback B.T., Webb R.M., Campbell, Huny R., Larsen M.C., Stallard R.F., Troester J., Walker J.F. 2006. Water and solute mass balances of five relatively undisturbed watersheds in the U.S. *Science of the Total Environment* 358:221-242
- Scatena, F.N., Gupta, A., 2012. Streams of the montane humid tropics. In: Shroder, J., Jr., Wohl, E. (Eds.), *Treatise on Geomorphology*. Academic Press, San Diego, CA, vol. 9
- Scatena F.N., Blanco J.B., Beard K., Waide R., Lugo A.E., Brokaw N., Silver W., Haines B., Zimmerman J., in press. The Luquillo Disturbance Regime. Chapter 4 in *A Caribbean Forest Tapestry: A Multidimensional Nature of Disturbance and Response*. Luquillo LTER Synthesis Book, Cambridge University Press
- Scholl, M.A., Shanley J.B., Zegarra J.P., Coplen T., 2009 A new explanation for the stable isotope amount effect using NEXRAD echo tops: Luquillo Mountains, Puerto Rico. *Water Resources Research* Volume: 45 Article Number: W12407 DOI: 10.1029/
- Schellekens J., Scatena F.N., Bruijnzeel L.A., van Dijk A.I. J.M., Groen M.M.A., van Hoogezand R.J.P., 2004. Stormflow generation in a small rain-forest catchment in the Luquillo Experimental Forest, Puerto Rico. *Hydrological Processes* 18. 505-530

Schellekens, J., Bruijnzeel, L.A., Scatena, F.N., Bink, N.J., Holwerda, F. (2000). Evaporation from a tropical rain forest, Luquillo Experimental Forest, Puerto Rico. *Water Resources Research*, 36(8):2183-2196

Shanley J.B., Mast M.A., Campbell D., Aiken G.R., et al. 2008 Comparison of total mercury and methylmercury cycling at five sites using the small watershed approach. *Environmental Pollution* 154: 1-12

Seiders, V.M., 1971a, Geologic map of the El Yunque quadrangle, Puerto Rico: U.S. Geological Survey Miscellaneous Geologic Investigations Map I-658, scale 1:20,000.

Wei Wu, Hall C.A.S., Scatena F.N., 2007 Modeling the impact of land use change on the stream flows at the meso-scale watershed level in North-Eastern Puerto Rico. *Hydrological Processes* V21 DOI: 10.1002/hyp.6515

Sulfur Cycling in the Rainforest of Puerto Rico

Simona A. Balan (sbalan@berkeley.edu), Ronald Amundson (earthly@berkeley.edu), Heather L. Buss (h.buss@bristol.ac.uk)

Key Science Questions Involved:

1. What are the sources of S inputs to the Luquillo Forest soils?
2. Do topography and parent material influence the cycling of S in the Luquillo Forest soils?
3. Is S cycling in the Luquillo Forest biologically mediated?

Methods, Preliminary Results and Next Steps:

1. East Peak rain water samples were collected over 20 months (from June 2010 to February 2012). Anion chemistry was measured via IC in the Coates Lab, UC Berkeley, and the $\delta^{34}\text{S}^1$ values were measured on a GV Isoprime isotope ratio mass spectrometer coupled with a Eurovector elemental analyzer (EuroEA3028-HT) in the Laboratory for Environmental and Sedimentary Isotope Geochemistry (LESIG) at the Department of Earth and Planetary Science, UC Berkeley.

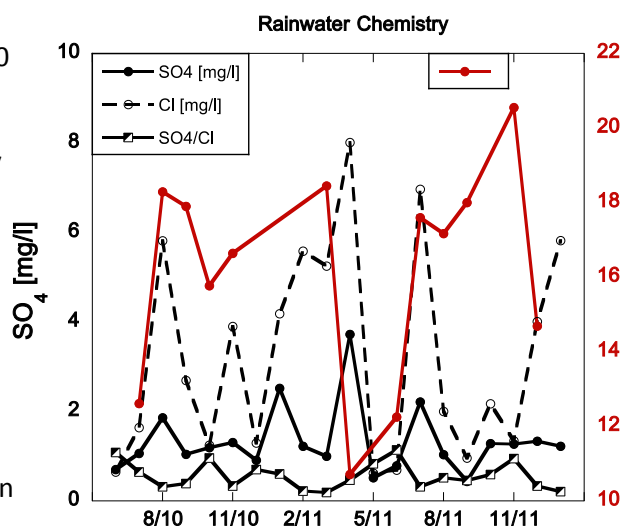
Assuming all Cl is derived from seasalt, on average the rainwater is a mix of 42% seasalt sulfate ($\delta^{34}\text{S}$ of 21‰ (Rees et al., 1978)) and 58% non-seasalt sulfate with an average $\delta^{34}\text{S}$ of 7.4‰. The highest percentage of non-seasalt sulfate sources to rainwater is in May-June, coinciding with the wet season, lowest non-seasalt % in February-March (dry season). Sulfate concentrations in soil pore water match closely those in rainwater, suggesting that rain inputs dominate the amount and isotopic composition of sulfate S in these soils.

Assuming all Cl is derived from seasalt, on average the rainwater is a mix of 42% seasalt sulfate ($\delta^{34}\text{S}$ of 21‰ (Rees et al., 1978)) and 58% non-seasalt sulfate with an average $\delta^{34}\text{S}$ of 7.4‰. The highest percentage of non-seasalt sulfate sources to rainwater is in May-June, coinciding with the wet season, lowest non-seasalt % in February-March (dry season). Sulfate concentrations in soil pore water match closely those in rainwater, suggesting that rain inputs dominate the amount and isotopic composition of sulfate S in these soils.

Next step: correlate the anion chemistry and $\delta^{34}\text{S}$ values with East Peak weather station data to determine if the low $\delta^{34}\text{S}$ rain water sulfate could have been transported from North America.

2. In summer 2010 we collected horizon-based soil samples, six soil cores down to 1.5 m, and representative plant litter samples at two sites: one on quartz diorite (Rio Icacos) and one on volcanoclastic sandstone (Bisley). At each site we sampled along a topographic gradient from ridgetop to the adjacent drainages. We also collected monthly pore water samples from those locations from February 2011 until February 2012.

The soil at Bisley has more total S but less SO_4 than the soil at Icacos, therefore it must have more organic and/or reduced S. Sulfate decreases with depth in both soils. The Bisley soil has higher NO_3 concentrations at the surface (up to 20 mg/kg), whereas NO_3 in the Icacos soil peaks between 20 and 60



¹ $\delta^{34}\text{S}$ values represent the ratios, R, of ^{34}S to ^{32}S ($\delta(\text{‰}) = (R_{\text{sample}}/R_{\text{standard}} - 1) \times 1000$). The standard is Canon Diablo Troilite (CDT).

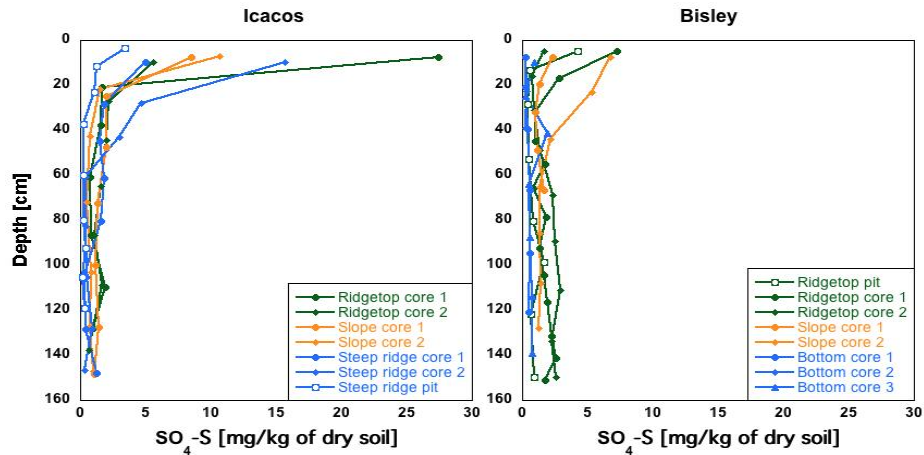
cm (up to 4 mg/kg). Cl content decreases with depth in both soils, but is slightly higher in the Icacos soil (up to 35 mg/kg). C% is similar in both soils, though slightly higher in the Bisley soil in the top 40 cm. Because these differences are apparent mostly at the soil surface they are likely not due to differences in soil parent material

but rather due to differences in inputs from plants and rain. The Icacos soil is at higher elevation, therefore it gets more rain (so more SO₄ and Cl). The Bisley soil appears to be getting a higher organic matter input from litter.

All soils sampled on the ridgetop and hillslope

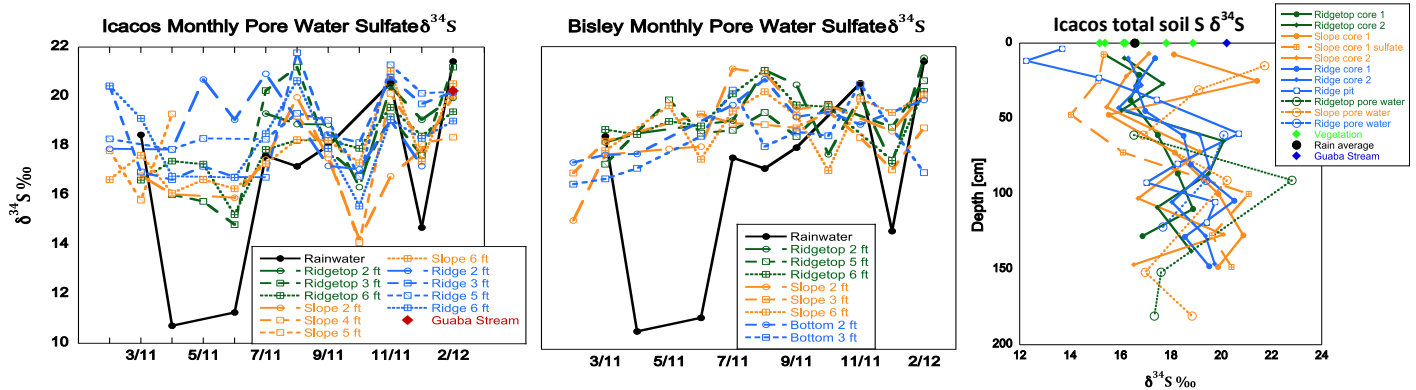
show similar S content. Topography affects these parameters only at the foot of the slope, close to a stream on the volcanoclastic bedrock, where sulfate concentrations are significantly lower than at all other sites. This is not surprising, since this site is frequently saturated.

Next steps: Measure total C, N and S concentrations and stable isotopes ratios in the Bisley and Icacos soils (method in development at the Center for Stable Isotope Biogeochemistry, UC Berkeley).



3. Based on our data so far, it appears that soils and plants retain the isotopic signal of S inputs, and the losses lack significant isotopic fractionation. δ³⁴S is similar in topsoil and plants, evidencing little to no fractionation during plant uptake. In most months, there's no significant difference between the δ³⁴S value of pore water and rain. The pore water maintains a fairly constant δ³⁴S value corresponding to the average rain δ³⁴S, and doesn't reflect all the monthly fluctuations in δ³⁴S. Also, in February 2012 (the only month for which we have stream water data thus far), there was no significant difference between East Peak rainwater, Icacos pore water and Guaba stream water. This all points to little to no microbial fractionation. Alternatively, the frequent rains might simply overwhelm and reset any isotopic signal due to biological reactions. The only biological process that is evident in the isotopic data is mineralization of organic S, which causes an increase in soil δ³⁴S values with depth.

Next steps: Measure δ³⁴S also in the Bisley soil and stream to compare to the Icacos data.



Carbon, nitrogen, and solute export from high-elevation watersheds in the Luquillo CZO

Richard L. Brereton, Univ. of New Hampshire
rich.brereton@unh.edu

William H. McDowell, Univ. of New Hampshire
bill.mcdowell@unh.edu

Key Science Questions

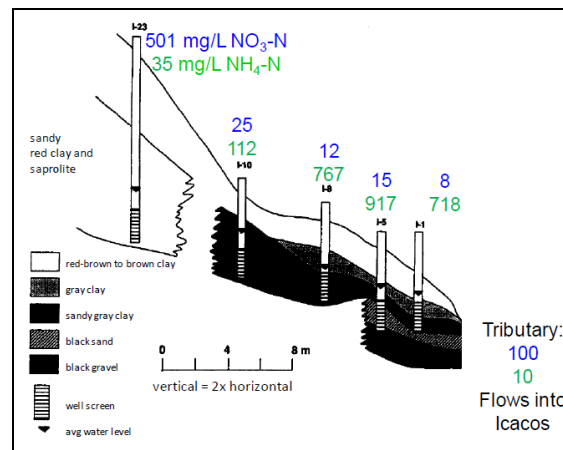
- How does shallow groundwater chemistry evolve across the catena in the Rio Icacos watershed, and how does this differ from the Rio Mameyes?
- What mechanisms are responsible for nitrogen (N) removal from groundwater flow paths through riparian zones in the Rio Icacos watershed?
- In the Rio Icacos and the Rio Mameyes, how do different carbon (C) fractions behave on intra-annual timescales? What is the total C flux from these watersheds?

Shallow groundwater chemistry

Hill slope groundwater carries oxygen and redox conditions are oxidizing. Floodplain groundwater is anoxic and reducing conditions dominate. Concentrations of major anions, cations, and dissolved organic carbon (DOC) remain constant across the hydrologic flow path from the hill slope through the floodplain.

N speciation is dominated by nitrate-N in hill slope wells and by ammonium-N in floodplain wells (Fig. 1). Release of reduced iron and manganese by mineral dissolution or microbial processes is hypothesized to control redox conditions in floodplain groundwater.

Figure 1. Cross-sectional view of Rio Icacos tributary well field, with groundwater N chemistry.



Groundwater concentrations of reduced iron and manganese are being measured at different positions across the catena to assess their role in determining redox conditions.

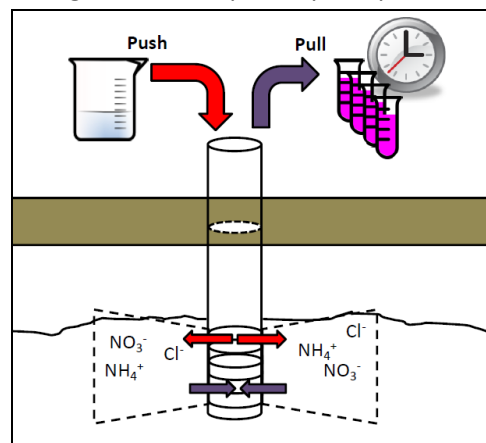
Riparian nitrogen dynamics

Riparian zones have been noted as areas in which N retention and removal occur and thus exert control on watershed N export. Stream total dissolved N (TDN) concentrations are much lower (20%) than riparian groundwater TDN. Is shallow groundwater responsible for only 20% of base flow? Or is ammonium-N being removed before reaching the stream channel? What mechanism is responsible for the observed pattern in N species in the Rio Icacos watershed?

- Denitrification (which requires anoxic conditions) is hypothesized to remove nitrate-N entering the floodplain from hill slope groundwater.
- DON from vegetation and soils is hypothesized to break down and supply ammonium-N to the floodplain aquifer.
- Annamox (anaerobic ammonium oxidation, the reaction of ammonium with nitrite to form N_2 gas) is hypothesized to remove ammonium-N from floodplain groundwater.

These hypotheses are being tested using groundwater push-pull tests (Fig. 2). In the 'push' phase, ammonium and nitrate are pumped into the well casing along with chloride (used as a conservative tracer). Positive hydraulic head pushes the slug downward into the aquifer, where reactive species diffuse and react. The well is sampled at regular intervals (the 'pull' phase) and a reaction rate is inferred. Reaction rates for consumption (or production) of nitrate and ammonium will be quantified for hill slope and floodplain wells.

Figure 2. Diagram of a simplified push-pull methodology.



Temporal variation in C flux: the 'Year of Carbon'

Tropical rivers play a major role in the global C cycle and in delivery of solutes to the oceans. Weathering rates in the Rio Icacos are the fastest documented on silicate terrain in the world. Previous studies here have shown that dissolved C is a crucial linkage between vegetation, soils, and weathering in the LCZO. This new data set will provide an important comparison with DOC, POC, and DIC flux data from the 1980s. Additional parameters for DOC quality (absorbance/fluorescence/EEMS) and dissolved gas flux (carbon dioxide, methane, and nitrous oxide) will increase our understanding of watershed processes and export. Particulate and dissolved lignin will also be quantified in cooperation with Dr. Peter Hernes of UC-Davis.

This effort, which is coordinated with the Luquillo LTER's long-running weekly stream sampling program, will help us answer crucial questions:

- What is the total stream export of C from these two watersheds?
- Does C flux display seasonal trends?
- How do inorganic C fractions behave with discharge? Are higher flows important for inorganic C export?
- Do large storm events affect the flux of C fractions afterward?
- Do absorbance/fluorescence characteristics vary with discharge? Is there evidence of source switching?



Long-term landscape evolution of the Luquillo Mountains: [uplift, waterfalls and trees](#)

Gilles Brocard (gbrocard@sas.upenn.edu); Jane Willenbring (erosion@sas.upenn.edu), Fred Scatena

Key Science Questions Involved:

- 1 – Large scale: When where the Luquillo Mountains uplifted to their present height?
- 2 – Mesoscale: The last 500-600 m of uplift generated a conspicuous wave of erosion still propagating toward the mountain tops. What is the magnitude of the spatial variability in erosion rate associated with this wave?
- 3 – Microscale: Upstream of the erosion wave, slowly eroding crest lines covered by an old growth Palo Colorado forest, alternate with corestone-choked gullies occupied by the Palm forest. Is water-table seepage responsible for gully development or is it the competition between the two types of forests?

The island of Puerto Rico has emerged incrementally from the sea for the last five million years ago. Extensive wave-cut platforms formed at intervals during this uplift, and have been uplifted at high elevations. They provide valuable markers of the island's growth. One extensive platform is encountered around the Luquillo Mountains at an elevation of 500-600 m asl. It now encloses 1100 m high summits that once formed an island 10 km in diameter and only 500 m high. Uplift of this island allowed the establishment of the altitudinal vegetation zoning that we observe today. To determine the minimum age of this event (estimated at 3-5 millions of years), we sampled river borne quartz located in caves that have formed below the wave-cut platforms shortly after they rose above the sea. Dating is achieved by measuring the differential decay of cosmogenic ^{10}Be and ^{26}Al in quartz carried into the caves by rivers that drained the crystalline core of the central range of Puerto Rico. Following uplift, vigorous erosion propagated headward along the streams of the Luquillo Mountains. The wave of incision has not propagated to the divide everywhere, in particular above a stock of quartz diorite located in the core of massif. The preserved upper reaches are separated from the deeply incised downstream reaches by dramatic waterfalls (Figure1). Early works (Brown *et al.*, 1995; Brown *et al.*, 1998) used cosmogenic ^{10}Be contained in river borne quartz and soils to evidence slow erosion rates in the uplands (50-150 m/My). To address question 2 we have undertaken a more systematic inventory of ^{10}Be in river borne quartz to characterize erosion rates over the entire uplands., we also measured erosion rates in streams located downstream of the front of the incision wave, and find a doubling to tripling of erosion rate associated with the passage of the wave (Figure 2). The landscape in the uplands seems to become more dissected with time, with a deepening of seepage-controlled gullies, progressive back wearing and crosscutting of the weathering front at the base of the saprolite. This creates a dual landscape with slowly eroding ridges covered by the Palo Colorado forest and intervening coves occupied by the palm forest. The rapidity of this phenomenon is evaluated using spot measurements of erosion rates in the forest (20 sites) and catchment-wide erosion rates in sub-catchment affected by ground sapping (10 sites).

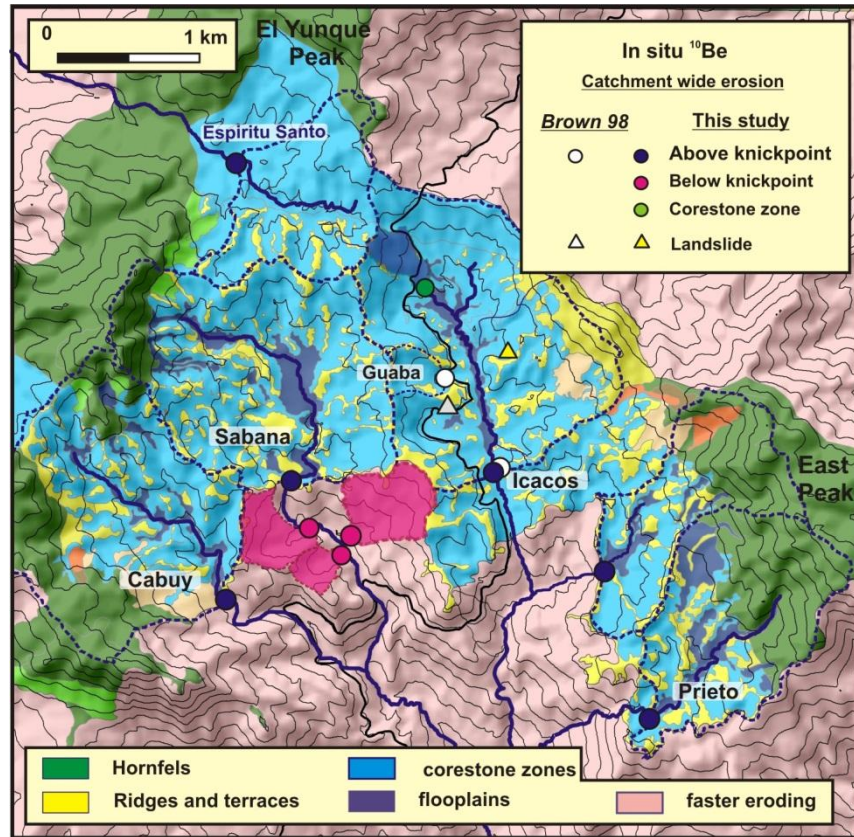


Figure 1. Geomorphic map with sampling sites of Figure 2 and their catchments.

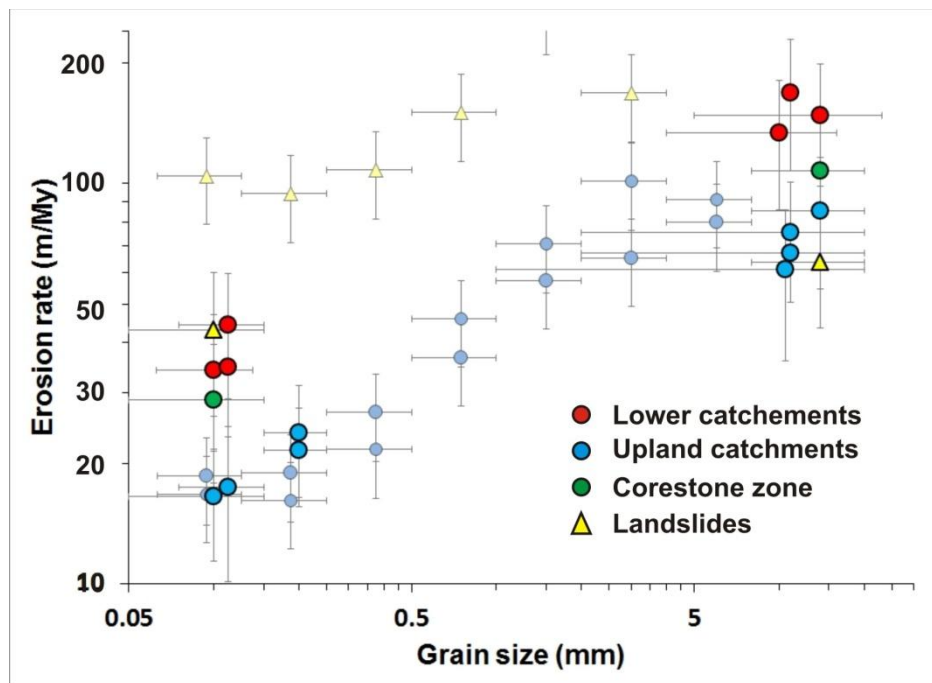


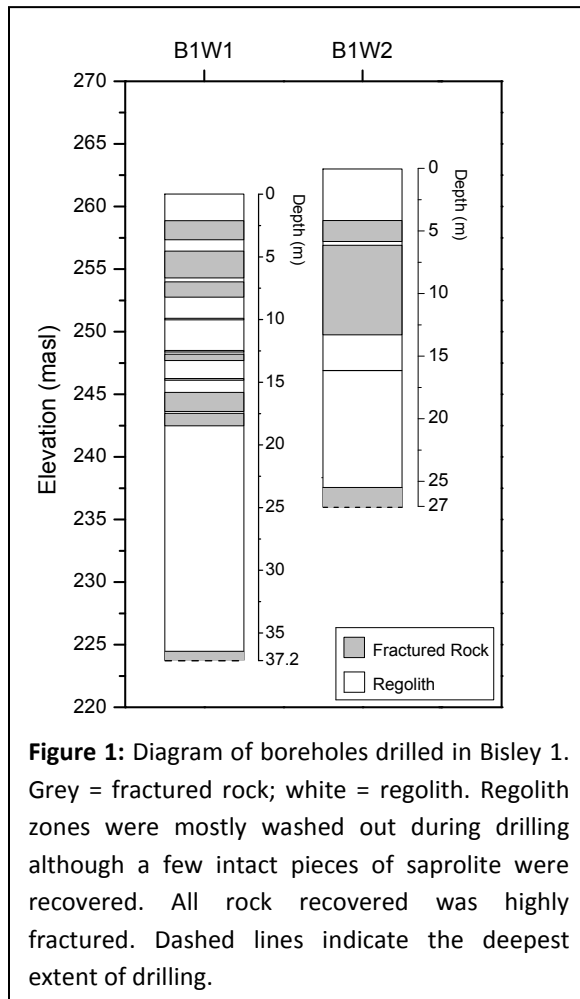
Figure 2. Distribution of ^{10}Be concentrations as a function of grain size in river sediment (faded colors: data from Brown et al., 1995, 1998).

Probing the Depths of the Critical Zone: Chemical and Physical Weathering of Deep Fractured Bedrock in the Bisley Watersheds

Heather L. Buss (H.Buss@bristol.ac.uk), Sue Brantley (Brantley@eesi.psu.edu), F.N. Scatena (fns@sas.upenn.edu), Marjorie Schulz (mschulz@usgs.gov), and a University of Bristol PhD student starting October 2012.

Key Science Questions Involved:

- Are weathering processes in the deep fractured bedrock represented by weathering data collected on rocks exposed at the surface (e.g., outcrops, corestones in the streams)?
- Does the size and distribution of corestones at the surface reflect the geometry of the bedrock-regolith interface at depth?



Sampling the Deep CZ

The rates and mechanisms of deep CZ weathering reactions are important in controlling weathering fluxes to rivers and oceans. This is especially true in the tropics where thick regolith contains few weatherable minerals. Furthermore, physical and chemical weathering processes in the deep CZ may control or impact watershed topography, hydrology, and subsurface ecology.

We are investigating the deep CZ in the Bisley watershed from two 9.6 cm diameter boreholes drilled with a hydraulic rotary drill to 37.2 and 27.0 m depth in late 2010 (a core was also drilled in Rio Icacos). Continuous core samples through coherent rock were taken using an HQ-wireline barrel. Exposed corestones were sampled with a hand-held paleomagnetic drill. A ~90 m landslide surface was also sampled with a rock hammer.

CZ Geometry

Drilled cores revealed repeated zones of highly fractured rock, identified as corestones, embedded within layers of regolith (Fig. 1). Some corestones

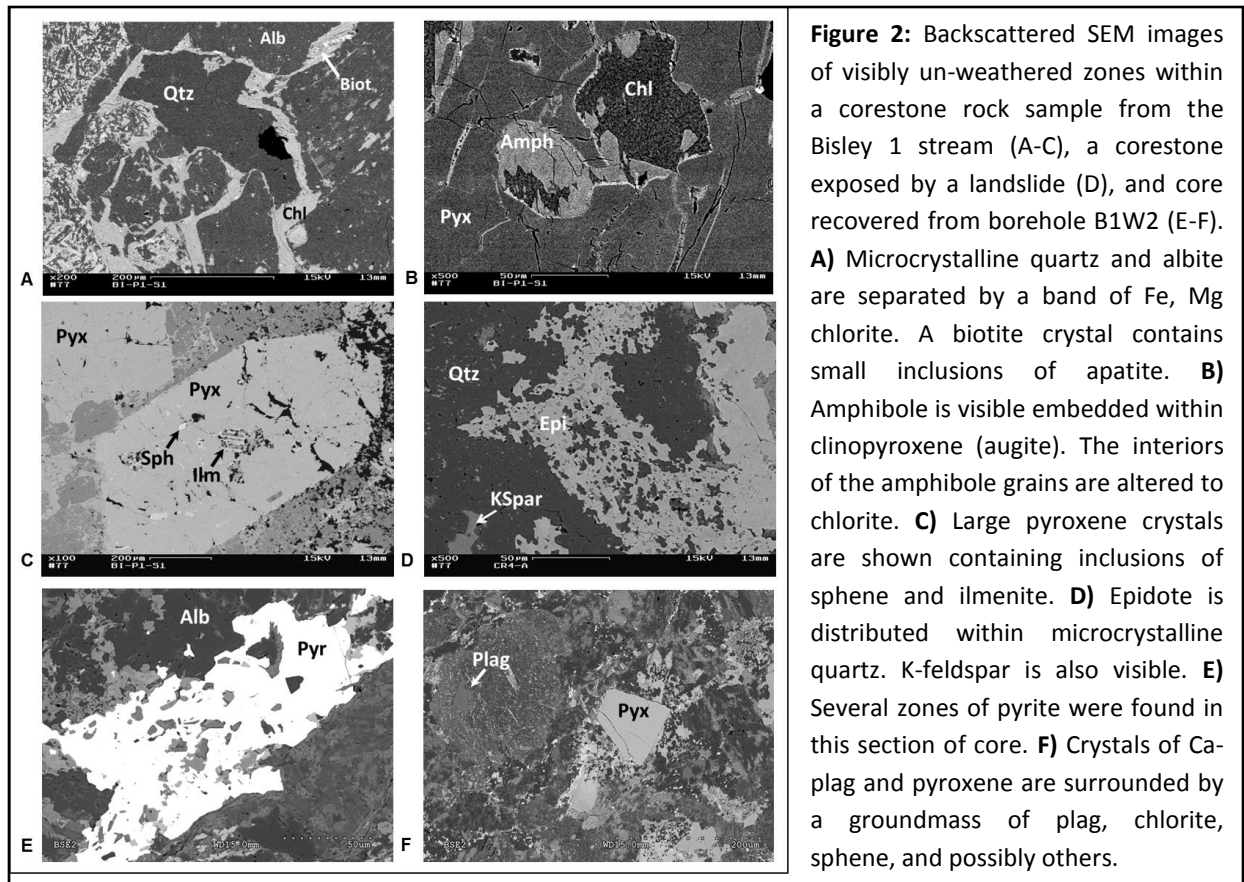
are massive and others are highly fractured. Subsurface corestones are larger and less fractured in the borehole drilled along the spine of a ridge (B1W2), compared to the borehole drilled near a stream channel (B1W1). As corestone size is thought to be a function of fracture spacing, the location of the valleys and ridges in the watershed may be controlled by the fracture spacing of the underlying bedrock.

Results are consistent with a model whereby weathering created a thick packet of regolith with embedded corestones. The Bisley I channel incised through this regolith package, exposing saprolite and corestones at the land surface.

Weathering

Weathered rinds developed on the surface of the exposed corestones and along fracture surfaces on subsurface rocks slough off of exposed corestones at <1 cm thickness, preventing corestone weathering from becoming diffusion-limited and leaving corestones angular rather than rounded. The absence of spheroidal weathering in these corestones (in contrast to the corestones in the Rio Icaos watershed) may reflect the very low biotite content of the volcanoclastic bedrock.

The weathering zone is well below the stream channel; thus weathering depth is not controlled by local base level. Furthermore, weathering rinds on fracture surfaces at depth indicate that water and O₂ are transported below the channel; thus not all of the water in the watershed is discharged to the stream. Ongoing work will identify weathering reactions occurring along fractures in the deep CZ (Fig. 2).



Additional funding sources: USGS WEBB Project, UK National Environmental Research Council (NERC)

Application of a Novel Mg-Li Dual Isotopic Tracer to Biogeochemical Cycles in the Critical Zone

Dr. Heather L. Buss (H.Buss@bristol.ac.uk); Ms. Maria Chapela Lara (M.ChapelaLara@bristol.ac.uk)

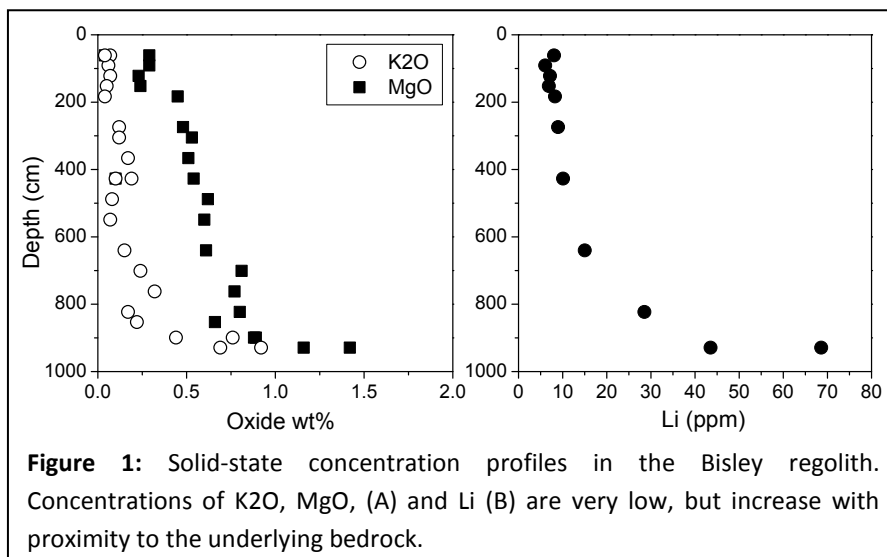
Key Science Questions Involved:

- Can Mg and Li isotopes be used as a dual tracer to separate and quantify the geochemical and biological components of the Mg cycle in the CZ?
- What fraction of the total Mg in the soil/regolith is recycled by vegetation or microorganisms?
- What fraction of biologically cycled Mg is sourced from minerals vs. precipitation and does this vary with lithology?
- To what extent does stream water Mg reflect deep weathering processes, surficial weathering processes, and/or biological processes; does this change during storm events; and does it vary with lithology?

Mg as an essential macronutrient and global weathering product

Losses of soil nutrients, such as Mg, threaten productivity in both agricultural and forested ecosystems. Mg is an essential macronutrient for all organisms, yet soils worldwide exhibit Mg deficiencies. In many temperate and tropical forests, including the LCZO, Mg is largely stored in the aboveground biomass. As a consequence, Mg supply in these soils is highly dependent on deposition via litterfall and precipitation. Thus Mg cycles worldwide are extremely sensitive to land use and climate change.

To date, most Mg isotope research has sought to quantify weathering fluxes to rivers and oceans. However, the role of CZ processes in governing these elemental and isotopic fluxes remains a



fundamental question in global biogeochemical and climate cycles. By analysing Mg and Li isotopes in tandem (Li is chemically similar to Mg, but is not a nutrient), we plan to disentangle and quantify the processes that transform, transport, add or remove these elements from the CZ.

Mg and Li in the LCZO catchments

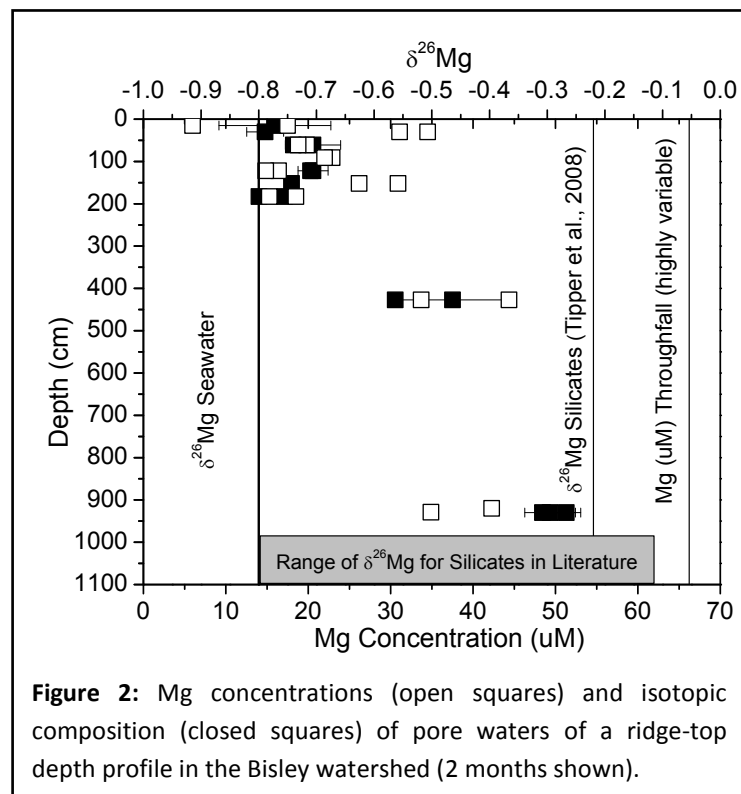


Figure 2: Mg concentrations (open squares) and isotopic composition (closed squares) of pore waters of a ridge-top depth profile in the Bisley watershed (2 months shown).

At the LCZO, we are investigating the Mg cycle as a function of depth, topography, and lithology in the Rio Icacos (Guaba Ridge) and Rio Mameyes (Bisley I) watersheds, focusing first on Bisley. Solid and solute concentrations of Mg, K, and Li are extremely low in the Bisley regolith; however, both increase with depth, with a dramatic increase near the regolith-bedrock interface (Fig. 1). Mg and K reside predominantly in chlorite and K-feldspar in the bedrock, with minor amounts in biotite, amphibole, and pyroxene. The only mineralogical Mg or K source in the regolith is residual biotite, which is in extremely low abundance. In the deepest samples, some chlorite and K-feldspar remain in the regolith. A small amount of exchangeable Mg was measured in the

Bisley regolith, but this is negligible compared to the total Mg. It appears that depth-dependent Mg trends in the regolith are related to chlorite dissolution at the bedrock interface and biotite dissolution in the overlying regolith, but that precipitation and biological cycling may strongly affect Mg trends in the pore water and at the surface.

We are measuring the Mg and Li isotopic composition of Bisley pore waters (Fig. 2), regolith, fresh and weathered bedrock, the NH₄-acetate exchangeable fraction, stream waters (base and storm flow), groundwater, openfall, throughfall, vegetation, and regolith microbial biomass. Mg and Li isotopes will be measured in Rio Icacos regolith, bedrock, and pore waters for comparison to Bisley. We hypothesize that Mg and Li isotopes will show similar trends for chemical weathering processes but will diverge when biological processes are significant, thus enabling quantitative separation of the biological and geochemical components of the Mg cycle using mass balance methods.

Additional funding sources: European Commission: Marie Curie Incoming International Fellowship to H.L. Buss, Consejo Nacional de Ciencia y Tecnología (CONACYT) postgraduate scholarship to M. Chapela Lara.

Lithological Influences on Weathering Processes and Rates

Heather L. Buss (H.Buss@bristol.ac.uk), Art White (afwhite@usgs.gov), Alex Blum (aebalum@usgs.gov).

Key Science Questions Involved:

- Do short-term and long-term weathering processes and rates vary as a function of lithology or landscape position?

Tropical Weathering

Rapid weathering and erosion rates in mountainous tropical watersheds lead to highly variable soil and saprolite thicknesses which in turn impact nutrient fluxes and biological populations. Even under near-identical conditions, weathering processes and rates can vary greatly due to differences in the underlying lithology. Here we are comparing weathering in two such watersheds.

Rio Icacos Weathering

Weathering processes in the granitic Rio Icacos watershed have been well studied by numerous researchers since the 1990's. Here, bedrock weathers spheroidally when oxidation of Fe(II) in biotite

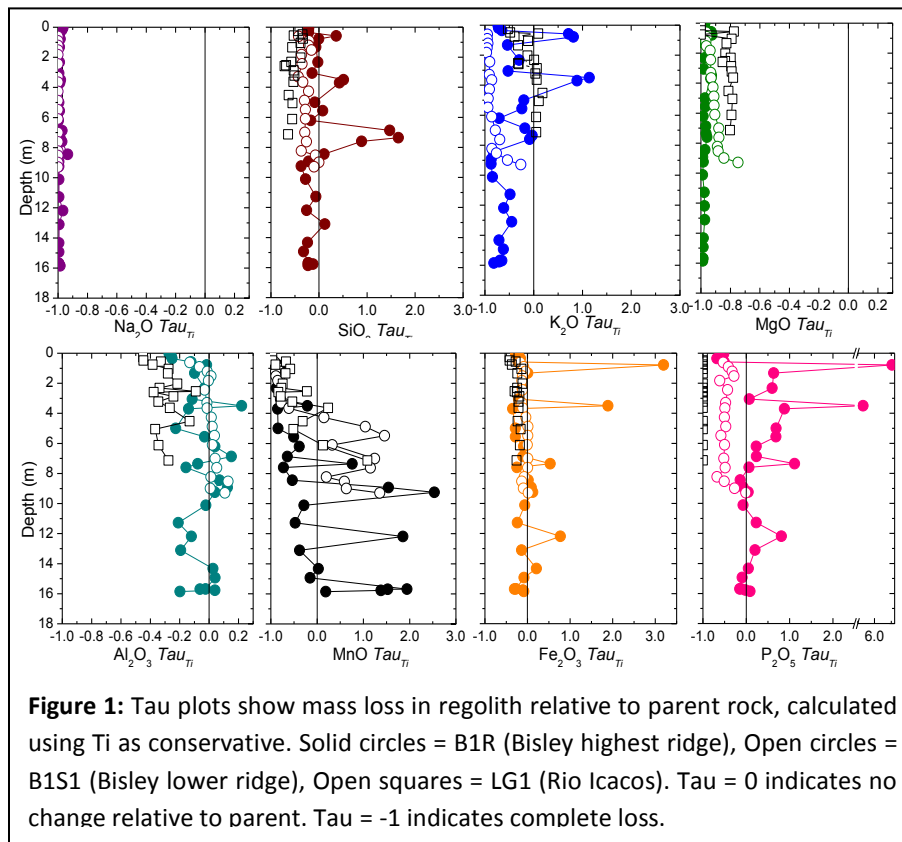


Figure 1: Tau plots show mass loss in regolith relative to parent rock, calculated using Ti as conservative. Solid circles = B1R (Bisley highest ridge), Open circles = B1S1 (Bisley lower ridge), Open squares = LG1 (Rio Icacos). Tau = 0 indicates no change relative to parent. Tau = -1 indicates complete loss.

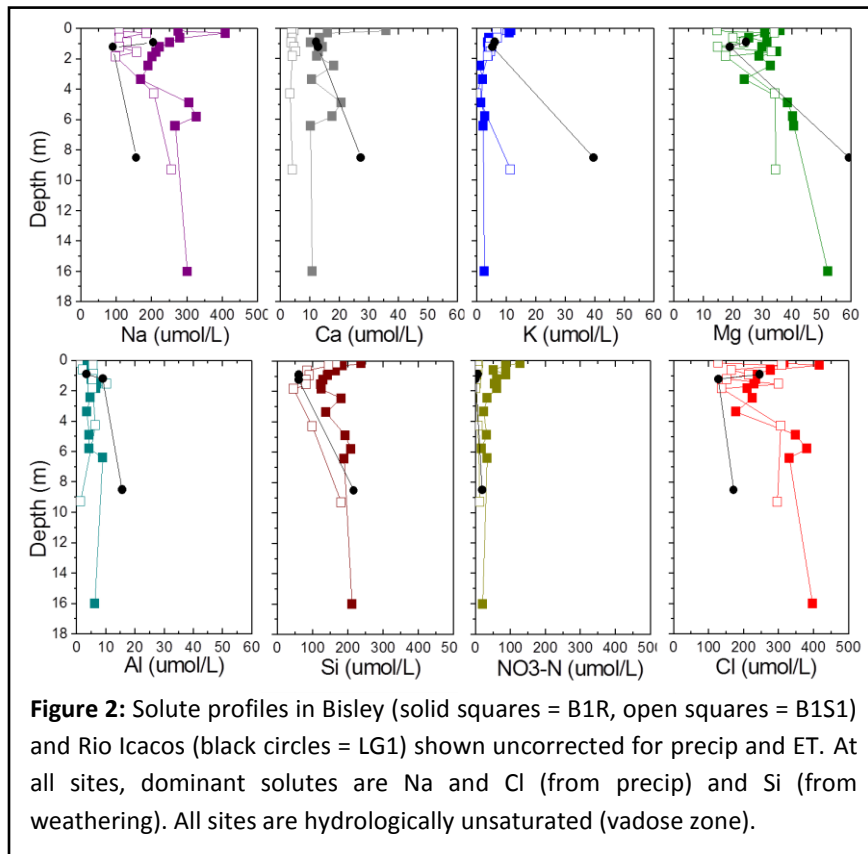
creates stress in the bedrock corestones until they fracture, forming rindlets (Fletcher et al., 2006). These fractures allow water to penetrate, which leads to further weathering such as rapid dissolution of hornblende at the rindlet-saprolite interface, which supports a deep microbial community of Fe(II)-oxidizing bacteria as primary producers (Buss et al., 2005; 2008; 2010). Within the thick, overlying saprolite (<9 m), biotite continues to weather, precipitating kaolinite and releasing Mg and K into the pore waters (Murphy et al.,

1998). The high quartz content of the bedrock forms a weathering-resistant matrix that supports isovolumetric weathering leading to saprolite development. Quartz eventually dissolves in the soil zone

(Schulz and White, 1999). A comparison of short-term and long-term weathering rates (deduced from solute and solid profiles, respectively) indicated that weathering at the site is in steady-state (White et al., 1998). A mechanism for maintaining a steady-state regolith thickness was proposed by Fletcher, Buss, and Brantley in 2006 whereby the weathering rate is controlled by transport of O₂ to the bedrock, which in turn is controlled by the thickness of the regolith.

Bisley Weathering in Comparison to Rio Icacos

Quartz content in the volcanoclastic Bisley bedrock is spatially variable and microcrystalline, indicating that it may have been deposited from Si-rich hydrothermal fluids. Thick saprolites (>30 m) on the Bisley ridges have a high quartz content (<65%) that could only have formed from the more quartz-rich bedrock, even considering relative enrichment due to mass loss of other minerals (Fig. 1). Bisley saprolite contains minute amounts of biotite, providing the only mineralogical source of Mg and K above the bedrock(or corestone)-saprolite interface, where Mg-rich chlorite weathers to completion.



Bisley bedrock also forms corestones, although these generally don't weather spheroidally (an exception being a bed of volcanic sandstone just east of the Bisley watersheds). Bisley corestones form oxidized weathering rinds that, when exposed, slough off at thicknesses <1 cm. Bedrock weathering rates in both watersheds have been estimated: for Rio Icacos, weathering proceeds at 43–58 m My⁻¹ (measured by ¹⁰Be and mass balance; Brown et al., 1995; White et al., 1998; Riebe et al., 2003), while the Bisley bedrock weathers at 334 m My⁻¹ (measured by U-

Th disequilibria, Dosseto et al, Subm.).

Additional funding sources: USGS WEBB Project

Stable isotopes of water as riparian indicators of flow frequency in a tropical montane stream network and the role of microclimates on stable isotopes of water

Jaivime Evaristo (evaristo@sas.upenn.edu), F.N. Scatena (fns@sas.upenn.edu)

Project Start and End Dates: March 2012 – September 2013

Key Science Questions to be addressed:

1. How do soil water and plant water source isotopic signatures along a vegetation sequence vary from the channel to hillslopes in different physiographic settings (Table 1)?
2. How is flow frequency at a series of long-term stream gages (Table 1) associated with temporal and spatial variations in soil water and plant water source isotopic signatures?
3. Can intra-annual soil water and plant water source isotopic signals be used as additional riparian features in approximating the magnitude and frequency of flows in fluvial systems?
4. What is the role of landscape stability, spatially heterogeneous biotic controls, and SOC accumulations (Pike, Scatena, and Silver 2011) on soil water and plant water source isotopic signatures?
5. How do apparent recharge areas of streams, groundwater and springs vary temporally and spatially between two contrasting lithologies of Luquillo?
6. What is the influence of microclimates on stable isotope signatures of water and how does this explain the hydrology of northeastern Puerto Rico? (Scholl et al. 2002)

Background:

The range of applications in isotope-related research in Puerto Rico has grown steadily between 1965 and 2011, led by the ubiquitous utility of stable isotope ratios in biogeochemical ($\delta^{13}\text{C}$, $\delta^{15}\text{N}$) and ecological ($\delta^{13}\text{C}$, $\delta^{15}\text{N}$, δD) research. Moreover, research in climatology has grown in recent years, spanning from the evaluation of the fidelity of isotope records ($\delta^{18}\text{O}$, $\delta^{13}\text{C}$) as an environmental proxy to the elucidation of multidecadal variability for paleoclimate reconstructions ($\delta^{18}\text{O}$ and Sr/Ca). On the other hand, in addition to using isotope ratios, hydrological studies in Puerto Rico have also used trace element data to answer flow source (δD , $\delta^{18}\text{O}$, $^{87}\text{Sr}/^{86}\text{Sr}$) and solute source (Ge/Si) questions, as well as in examining groundwater/surface flow relationships (^{222}Rn). Finally, various isotope data have been used in trying to understand geomorphological (^{10}Be , $\delta^{30}\text{Si}$) and geophysical (Pb, Nd, and Sr) phenomena. Figure 1 summarizes the range and number of isotopic studies performed in Puerto Rico between 1965 and 2011.

This study aims to answer the aforementioned key science questions by using the stable isotopes of water (D and ^{18}O) in investigations along an elevational and topographic gradient and between two contrasting lithologies of the Luquillo Mountains, NE Puerto Rico.

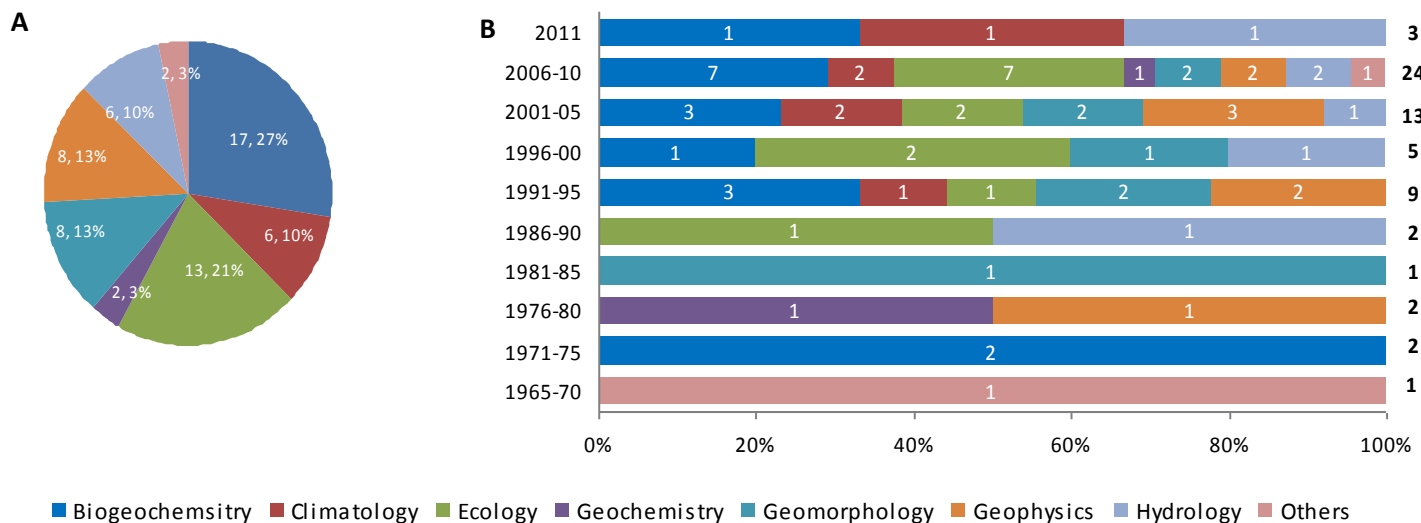


Figure 1. (A) Number and distribution of isotope studies in Puerto Rico per LCZO-relevant research area between 1965 and 2011. (B) Isotopic techniques have been applied in a growing variety of research areas in Puerto Rico between 1965 and 2011. Note: Figures on the RHS are total number of studies identified. Category “Others” includes Anthropology and Applied Isotopes (e.g. irradiation).

Hypotheses for Key Science Questions 1-4:

(1) Riparian zone soil water isotopic signatures show temporal variations as with periods of intra-annual inundation, and can therefore be used as an additional riparian feature in approximating the magnitude and frequency of flows in non-gaged streams. (2) Plant water source isotopic signatures, particularly riparian trees, on the other hand, show strong spatial variability that is influenced by species-specific attributes as well as elevation and topographic positions. Where fog/rainfall ratio is high, particularly in the cloud forests, δD and/or $\delta^{18}\text{O}$ signatures in trees as well as soil water are enriched relative to volume-weighted average rain samples.

Table 1 Estimated modern mean annual ^2H and ^{18}O composition of precipitation across an elevation gradient in northeastern Puerto Rico

USGS gage #	Gage name	Elevation (m)	$\delta^2\text{H}$	$\delta^2\text{H}$	$\delta^{18}\text{O}$	$\delta^{18}\text{O}$	
			(‰, VSMOW)	95% C.I. (‰)	(‰, VSMOW)	95% C.I. (‰)	
1	50063800	Rio Espiritu Santo nr Rio Grande	12	-12	2	-2.6	0.4
2	50071000	Rio Fajardo nr Fajardo	42	-12	2	-2.6	0.4
3	50064200	Rio Grande nr El Verde	50	-13	3	-2.7	0.4
4	50065700	Rio Mameyes at Mameyes	5	-12	2	-2.6	0.4
5	50065500	Rio Mameyes nr Sabana	84	-13	3	-2.7	0.4
6	50067000	Rio Sabana at Sabana	79	-13	2	-2.7	0.4
7	50063440	Quebrada Sonadora nr El Verde	375	-17	3	-3.3	0.5
8	50074950	Quebrada Guaba nr Naguabo	640	-21	3	-3.8	0.5
	50075000	Rio Icacos nr Naguabo	616	-21	3	-3.7	0.5

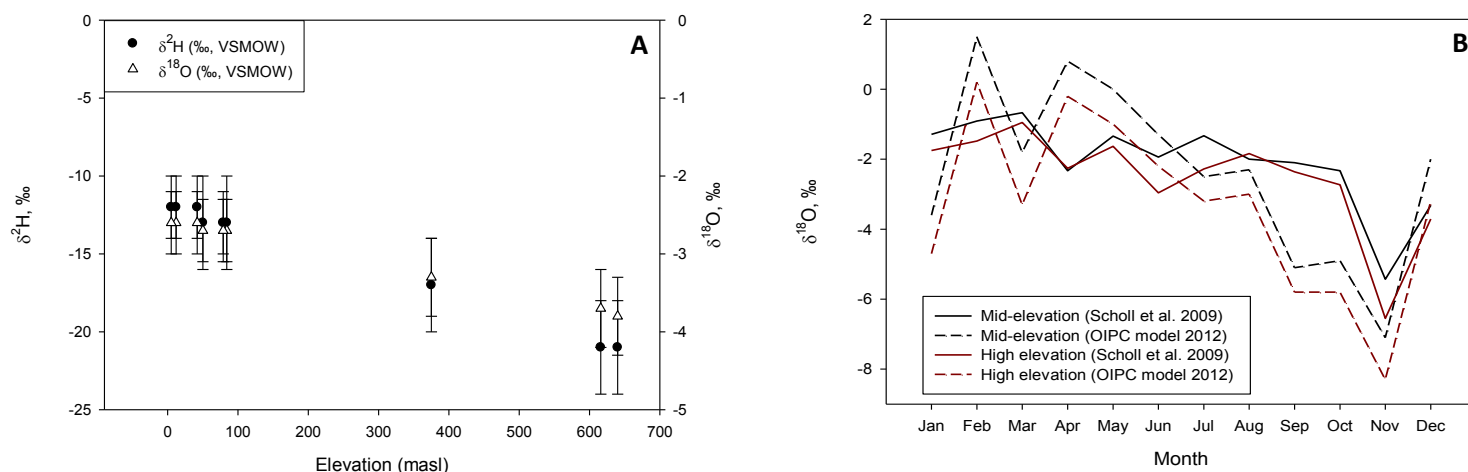


Figure 2. (A) Data source: Bowen, G. J. (2012) The Online Isotopes in Precipitation Calculator (OIPC), version 2.2. Estimated mean annual ^2H and ^{18}O isotope composition of rainfall from lowland to steepland gauged rivers in northeastern Puerto Rico. Error bars indicate 95% C.I. for estimated annual mean values (See Table 1 for details). (B) Comparison of monthly ^{18}O isotope composition at USGS gages Rio Mameyes nr Sabana and Rio Icacos nr Naguabo – mid-elevation and steepland river channels in NE Puerto Rico, respectively – between data from Scholl et al. (2009) and the OIPC Model v2.2.

Figure 1A shows the relationship between mean annual water isotope composition of rainfall and elevation from 5 masl to over 600 masl in NE Puerto Rico. Precipitation in the lowlands tends to be “enriched” relative to standard and “depleted” as elevation increases. The monthly water isotope composition of rainfall (Figure 2) across two elevational representative sites also reflects the effect of altitude as well as the intra-annual variations that tend to be enriched during the winter dry months and depleted during the summer rainy months in the area. Compared to the 2007 isotope data reported by Scholl et al. (2009), however, some temporal variations and disagreements with the OIPC model are apparent, particularly for the months of March through August. The OIPC-modeled values, therefore, may not strictly agree with instantaneous or time-averaged measurements of isotopic composition of precipitation; although the same may prove useful, at the very least, in building a fundamental understanding of the elevational and intra-annual variations of water isotope composition of precipitation over a given area. Thus, caution should be exercised when using these values for scaling as well as in granular studies, which often seek to elucidate the relationships between temporally diverse and spatially complex conditions (e.g. microclimates, presence of cloud forests, etc.).

Hypotheses for Key Science Questions 5-6:

Depending on flow source and flow path conditions within a watershed, non-riparian trees in leeward low-land and mid-elevations as well as streams, springs, and groundwater along the study area reflect water isotopic signatures of respective apparent recharge areas. Insights into the latter will help elucidate flow source and flow path characteristics of groundwater that may ultimately have practical implications for land use, especially in the “drier areas” of northeastern Puerto Rico.

References:

- Bowen, G. J. 2012. The Online Isotopes in Precipitation Calculator, version 2.2. <http://www.waterisotopes.org>
- Bowen G. J., Wassenaar L. I. and Hobson K. A. 2005. Global application of stable hydrogen and oxygen isotopes to wildlife forensics. *Oecologia* 143, 337-348, doi:10.1007/s00442-004-1813-y. (for monthly average values)
- Bowen G. J. and Revenaugh J. 2003. Interpolating the isotopic composition of modern meteoric precipitation. *Water Resources Research* 39(10), 1299, doi:10.129/2003WR002086. (for annual average values)
- Johnson, K. D., F. N. Scatena, and W. L. Silver. 2011. Atypical soil carbon distribution across a tropical steepland forest catena. *Catena* 87 (3): 391-7.
- Pike, A. S., and F. N. Scatena. 2010. Riparian indicators of flow frequency in a tropical montane stream network. *Journal of Hydrology* 382 (1-4): 72-87.
- Scholl, MA, SB Gingerich, and GW Tribble. 2002. The influence of microclimates and fog on stable isotope signatures used in interpretation of regional hydrology: East Maui, Hawaii. *Journal of Hydrology* 264 (1-4) (JUL 30): 170-84.
- Scholl, Martha A., James B. Shanley, Jan Paul Zegarra, and Tyler B. Coplen. 2009. The stable isotope amount effect: New insights from NEXRAD echo tops, Luquillo Mountains, Puerto Rico. *Water Resources Research* 45 (DEC 11): W12407.
- Link to data on <https://www.sas.upenn.edu/lczodata>

Linkages between redox processes and surface soil carbon cycling

Steven Hall and Whendee Silver
 UC Berkeley, Dept of ESPM, Ecosystem Science
 stevenhall@berkeley.edu, wsilver@berkeley.edu

Humid tropical soils are characterized by fluctuating oxygen (O₂) concentrations and periodic anaerobiosis caused by high soil moisture and biological O₂ demand. Iron (Fe) oxides provide an abundant electron acceptor for microbial metabolism under anaerobic conditions. Here, we explored interactions between Fe redox cycling and carbon (C) pools and fluxes.

Key Questions:

1. Does spatial and temporal variation in moisture, O₂ availability, and Fe reduction control soil C pools?
2. Does O₂ limitation constrain organic matter decomposition via microbial enzymes?
3. Does sequential Fe reduction and oxidation provide a novel mechanism for C decomposition?

We characterized spatial and temporal patterns of Fe, C, microbial enzyme activities, and oxidative capacity using field and laboratory experiments. In the field, patterns of reduced iron (Fe(II)) concentrations varied dramatically over space and time. Mean Fe(II) concentrations were highest on well-drained ridges and generally lower in riparian valleys (**Fig 1a**), corresponding with patterns of fine root biomass (**Fig 1b**) and soil C concentrations (**Fig 1d**), suggesting that *biological activity* may control Fe reduction, as opposed to soil moisture alone. Notably, C concentrations and hydrolytic enzyme activity (**Fig 1c**) correlated strongly with Fe(II) concentrations in ridge and slope topographic positions, but not in valleys, suggesting the importance of flooding in controlling valley soil C dynamics.

The “enzymatic latch” hypothesis proposes that anoxic conditions constrain oxidative and hydrolytic enzyme activity. In contrary, we found that *activity of five hydrolytic enzymes increased with soil Fe(II) concentrations*, an index of anaerobiosis (**Fig 1c**), providing further evidence of plant/microbial control of soil O₂ availability. Furthermore, we found strong relationships between soil oxidative activity (colorimetric assay with L-DOPA) and soil Fe(II) concentrations across a range of forest types in the LCZO (**Fig 2a**). *Solutions of Fe(II) alone generated oxidative activity in the absence of soil* (**Fig 2b**), suggesting an abiotic mechanism, possibly radical species generated via “Fenton reactions.” Fe(II) solutions did not affect hydrolytic activity.

Oxidative activity persisted or increased in autoclaved soils (**Fig 2c**). Adding Fe(II) solutions to replicate soils at a range of field concentrations stimulated short-term production of CO₂ under aerobic conditions (**Fig 2d**) but had little effect under anaerobic conditions, suggesting the potential importance of *sequential Fe*

reduction and oxidation as a novel mechanism for stimulating soil C decomposition.

We conducted a field water supplementation experiment to examine the influence of moisture on redox and C dynamics. Daily additions of 60 mm of water over 24 days maintained soils at field moisture capacity (**Fig 3a, back side**) but did not affect soil O₂ concentrations or CO₂ fluxes. Soil Fe(II) concentrations were largely static, but some plots showed considerable *net Fe reduction* (**Fig 3b**), likely associated with litterfall C inputs during a major storm.

Figure 1

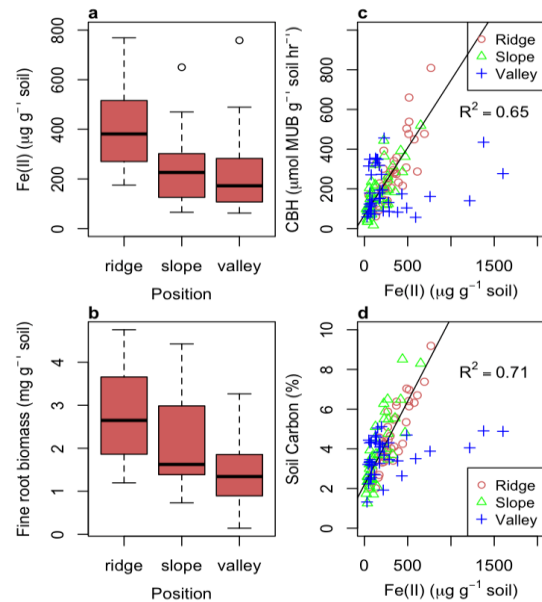


Figure 2

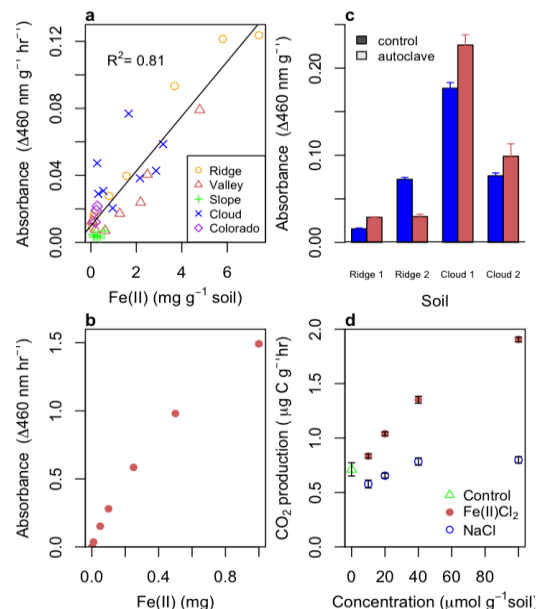
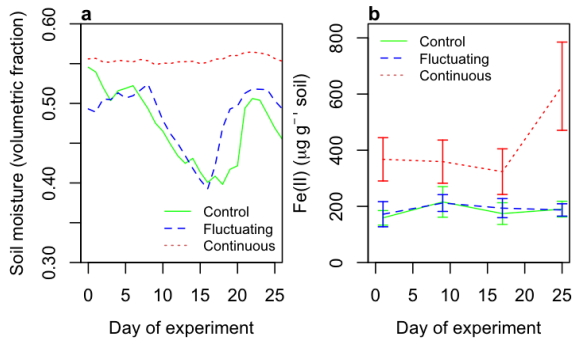


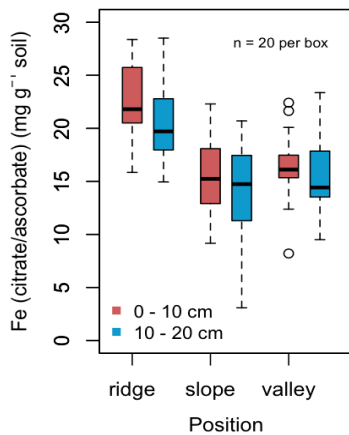
Figure 3



Linkages with LCZO collaborators

We found that nanoscale-order Fe oxides were highest in surface soils on ridges, and decreased with depth and landscape position (Fig. 4), following trends in fine root biomass (Fig. 1b). These landscape-scale measurements of soil Fe provide an ecosystem context for Fe mineralogy and dynamics measurements made by Wilmoth and Thompson (U. of Georgia). They found that specific Mossbauer spectral regions corresponded closely with Fe extractions (citrate/ascorbate). Their numerical model suggested that the frequency of redox oscillations was the best predictor of Fe dynamics, in agreement with our hypothesis that redox fluctuations structure biogeochemical function in this ecosystem.

Figure 4



Variation of soil oxygen concentrations with depth

(with Heather Buss, U. of Bristol)

Soil O_2 concentrations fundamentally constrain biogeochemical and weathering processes throughout the soil profile. We examined trends in O_2 with depth in granodioritic soils situated on a well-drained ridge in the Iacos Watershed. Concentrations of O_2 were measured at 30-minute timesteps for 18 months.

Key questions:

- How do soil oxygen (O_2) concentrations vary with depth over time?

- Do O_2 concentrations decrease monotonically from the soil surface, or could alternative delivery mechanisms supply atmospheric O_2 to deep soils?

Concentrations of O_2 typically declined from near-atmospheric levels (21 %) in surface soils to approximately 15% at 5 m depth (Fig 5). Surface soil (0 – 1 m depth) O_2 concentrations exhibited consistent temporal fluctuations on the scale of days – weeks (Fig 6). The largest fluctuations occurred at 0.5 m, where concentrations fluctuated as much as 3% over 30 minutes, and varied between 10 – 19 % over time .

Our finding that deep soil O_2 concentrations occasionally exceeded surface soil concentrations suggests the potential importance of O_2 supply to deep soils via fissures or other unexplored pathways. We will replicate this depth profile at multiple locations in volcanoclastic soils in summer 2012.

Figure 5

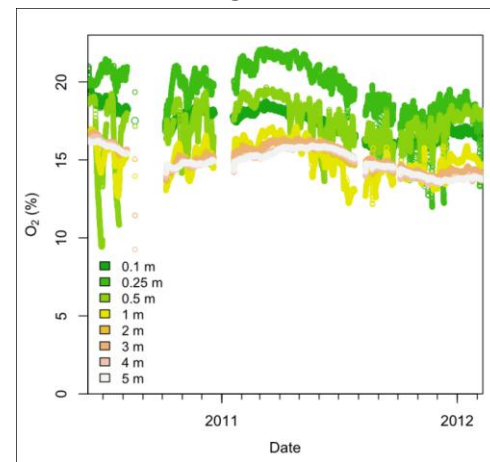
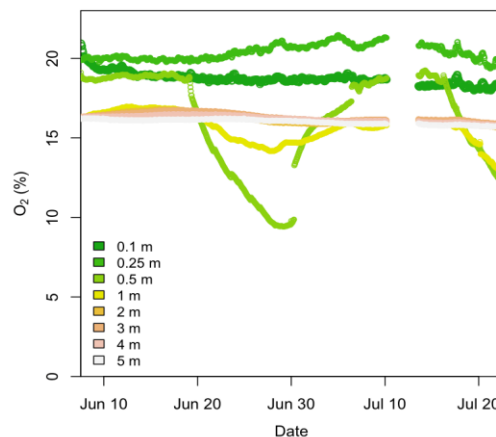


Figure 6



Additional support: This research is supported in part by the Department of Energy Office of Science Graduate Fellowship Program (DOE SCGF)

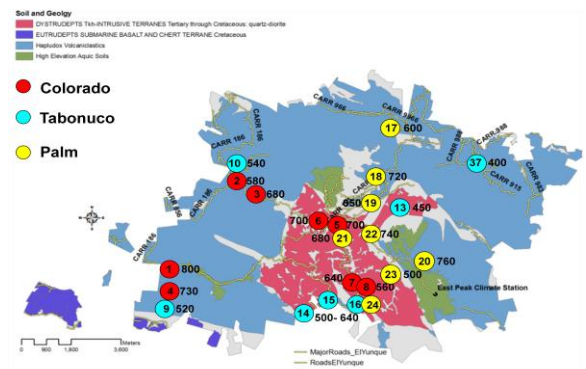
Landscape-Scale Controls on C, N, and exchangeable Ca⁺⁺, Mg⁺⁺ and K⁺ in Soils of the Luquillo CZO Forest

A.H. Johnson, Hao Xing Xing, F.N.Scatena. Department of Earth and Environmental Science, University of Pennsylvania.

Summary: We sampled soils from 216 profiles representing 24 sites in the El Yunque National Forest to determine amounts C, N and neutral-salt-extractable Ca⁺⁺, Mg⁺⁺ and K⁺. Following the classic paradigm, we assessed the influence of climate (modeled precipitation, modeled temperature and/or elevation as a surrogate variable for both), forest type (tabonuco, colorado, palm), parent material (quartz diorite, volcanics), and topography (catena positions ridge, slope, valley and % slope) on the distribution of these nutrients. To separate the effects of vegetation from those of climate, half of the sites were located between 500 and 700 m in the three forest types where rainfall and temperature were not significantly different. Using a combination of ANOVA (or Kruskal-Wallis) and univariate regression trees we determined that the amount of carbon in the top 80 cm of soil was influenced primarily by forest type ($c > p > t$) probably driven by differences in litter and/or root C:N ratios. Topographic position was significantly correlated with C amount ($v > s, r$), with the higher C amounts in the valleys probably driven by low O₂ levels. Bedrock type was significantly correlated with C amount in c and p stands, but not in the tabonuco type. N was strongly correlated with C as expected. Exchangeable Ca was different across forest types ($t > c, p$) and bedrock type ($qd > vc$). Mg and K were differed by forest type, but not by bedrock type ($t > c, p$) or any other variables.

The next phases of this project are (1) to determine levels of these nutrients below the root zone (80-140 cm) and the factors controlling their distribution; and (2) establish field experiments to test the results of the regression trees which indicate that the C:N ratio of litter and/or root inputs is the most important variable influencing C distribution. The latter represents a first step in exploring the usefulness of regression trees as a way of sorting out the relative importance of each of the state factors (climate, topography, organisms, parent material and time) in the classic paradigm relating environmental variables to soil properties.

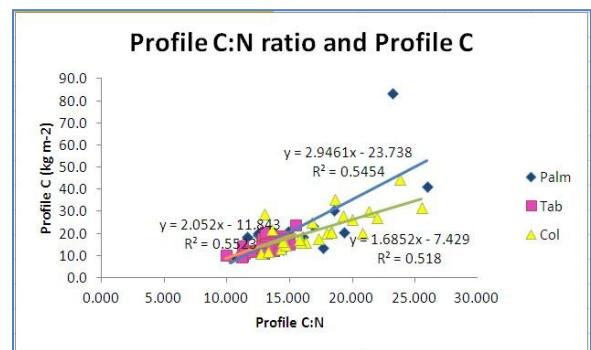
Sampling: 3 forest types x 2 lithologies x 4 independent sites x 3 replicate r, s and v pits (n=9) per site.



■ Quartz diorite of the Rio Blanco stock. Soils are Inceptisols. ■ Sedimentary volcanic rocks, mostly andesitic, soils are Oxisols. The contact zone is metamorphosed (hornfels).

Selected Results:

1. Soil Carbon

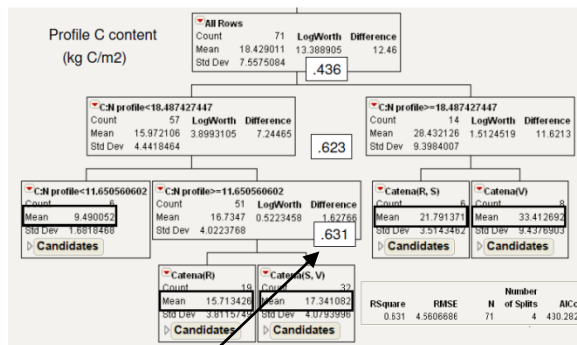


Mean C values(kg m⁻²):

Forest Type	Catena Position	Mean C (kg m ⁻²)	Litter C:N	Mean C (kg m ⁻²)
colorado	qd	19.9 ^a	colorado	38 ± 2
	vc	24.2 ^a		palm
palm	qd	16.3 ^b	tabonuco	30 ± 1
	vc	19.2 ^{ab}		
tabonuco	qd	13.5 ^c		
	vc	14.0 ^c		

Soil C differs markedly across forest types ($c > p > t$, $p < .0001$), and across catena positions ($v > s, r$, $p < .001$), but

not across bedrock types in spite of the higher clay content of soils derived from **vc**. C:N ratio (in any horizon, or in the whole profile) is the best predictor of soil C amount. The differences in soil C correspond to the differences in litter C:N. Tabonuco stands have the least soil C but the highest litter input rates ($c = 9.1$, $p = 7.2$, $c = 7.2 \text{ Mg ha}^{-1}\text{yr}^{-1}$, Weaver and Murphy, 1990, Frizano 1999, Lugo 1992) and Sullivan et al. (1999) measured substantially faster decomposition of tabonuco litter over 100d. Those findings support the idea that soil C amount is driven by differences in decomposition rate related at least in part to C:N ratios. Similar results were obtained in the 500-700m elevation band where only vegetation differs (soil C: $c = 21.5 \pm 3$, $p = 19.3 \pm 2$, $t = 14.7 \pm 1$). Univariate regression trees identify soil C:N ratio as the most important variable explaining soil C in all combinations of candidate predictor variables.



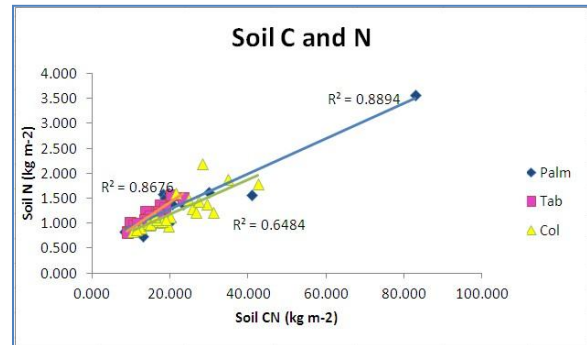
Sums of squares explained

For the past several decades, determining the influence of individual state factors on soil properties has been difficult due to the fact that some of the state factors are correlated with each other, and all 5 of the environmental variables can influence one soil property. Such problems are inherent in areas like the EYNF where vegetation changes along climate gradients. We plan to test the regression-tree result indicating that the C:N ratio of litter (and perhaps roots) is a more important control on decomposition rate than temperature and rainfall with field and laboratory incubations.

Valley soils have more C than ridge or slope soils. Depth profiles of soil C show equal C in the 0-20 cm layer across the catena, but greater amounts of C in the 20-80 cm layer in the valley soils (data not shown). This suggests a minimal role for down-slope movement of litter, and that the greater C content of valley soils is driven more by slower decomposition related to the lower O_2 levels measured in soil air in the valleys (Silver et al. xxxx).

2. Soil Nitrogen

Soil nitrogen and soil C are correlated within each forest type and across the study area, Attempts to find variables that might influence N amount other than forest type and the amount of organic C were unsuccessful.



3. Base cations

Neutral-salt-exchangeable Ca^{++} is different across forest types ($t > p$, c ; $p < .0001$) and bedrock types ($qd > vc$, $p < .0001$). XRD analysis indicates that some of the soils derived from **qd** have substantial amounts of feldspar (up to 60%, Zhou 2011) and this probably accounts for the difference related to bedrock type. Mg and K differ only across forest types ($t > p$, c , $p < .0001$ in each case) and not in response to any other variable. It is still unclear whether the high exchangeable cation amounts in the tabonuco forest soils are due to the rapid decomposition of organic matter or to the chance correspondence of weatherable feldspar in some of the the tabonuco stands growing on quartz diorite (or perhaps both).

Summary

In the top 80 cm of soils, vegetation type and the C:N ratio of litter (and roots?) are the most important controls on the quantities of C and N and on the amounts of exchangeable base cations. Bedrock influences are minor, and in the data analyzed thus far, confined to the amount of neutral-salt-exchangeable Ca (and the Ca:Mg ratio).

For more information please visit:

<https://www.sas.upenn.edu/lczodata/content/geological-controls-physical-and-chemical-properties-surface-soils-luquillo-critical-zone-ob>



A Geochemical Model of Redox Reactions in a Sandy Tropical Rain Forest floodplain Stream Riparian Zone: DOC Oxidation, Respiration and Denitrification

R.A. Jiménez, C. Mastropaolo, F.N. Scatena and W.H. McDowell

Key Science Questions: Biogeochemistry and redox- reactions across floodplains.

Abstract: A geochemical equilibrium model was used to quantify Dissolved Organic Carbon (DOC) electron donors during aerobic respiration and denitrification in a sandy tropical stream riparian zone underlain by Quartzdiorite in the Luquillo Experimental Forest, Puerto Rico. DOC electron donors were measured across three general redox zones (Oxic: slope, Transitional: slope-riparian interface and Anoxic: riparian-floodplain) of the Icacos watershed. Model results suggest that nitrate and oxygen are completely reduced after approximately 10.1 mg/L of DOC have reacted with an initial ground water solution. In order to reach the observed mean oxygen concentration of 3.79 mg/L in the Oxic zone from the modeled equilibrium oxygen concentration of 9.46 mg/L, approximately 5.33 mg/L of DOC need to be oxidized. Additionally, 2.06 mg/L of DOC are oxidized in order to reach the observed mean oxygen concentration of 1.6 mg/L in the Transitional zone. In order to reach the observed mean Anoxic zone oxygen concentration of 1.27 mg/L from the observed mean Transitional zone oxygen concentration, an additional 0.309 mg/L of DOC are oxidized. From modeled equilibrium concentrations of oxygen (9.46 mg/L), approximately 8.8 mg/L of DOC are oxidized by oxygen before nitrate becomes more thermodynamically favorable as the electron acceptor and begins decreasing in concentration. Model simulations suggest that 1.19 mg/L of DOC reduce the observed mean nitrate concentration of 0.47 mg/L found in the Oxic zone to the lowest observed mean nitrate concentration of 0.01 mg/L found in the Transitional zone. Differences between the observed DOC concentrations in the field and the modeled DOC concentrations needed to reach zone levels of oxygen and nitrate suggest that field reported values for DOC electron donors could represent residual or unused electron donors. Results also indicate that between 8.68 mg/L and 10.7 mg/L of DOC oxidation, 0.42 mg/L of dissolved N₂ are produced, HCO₃ increases from 0.33 mg/L to 2.64 mg/L and CO₂ concentrations decrease from 13.8 mg/L to 13.7 mg/L before continuing to increase. This pronounced interval of DOC oxidation at which denitrification occurs and beyond which CO₂ continues increasing suggests a specific range at which denitrifiers metabolize versus a larger range at which a general heterotrophic population metabolizes. The researchers are currently utilizing these modeling results in order to develop a geochemical modeling study that will compare redox reactions in two geomorphologically distinct watersheds underlain by Quartzdiorite and Volcaniclastic parent material.

Figure 1. Simulated concentrations of dissolved respiration and denitrification products across three general redox zones of the Icaos slope-riparian zone as a function of CH₂O reacted with an initial slope ground water solution at equilibrium. DOC electron donors were quantified in PHREEQC by modeling the oxidation of CH₂O, an approximation of organic matter as related to the Redfield stoichiometry for the average content of algae: (CH₂O) 106 (NH₃) 16 (H₃PO₄).

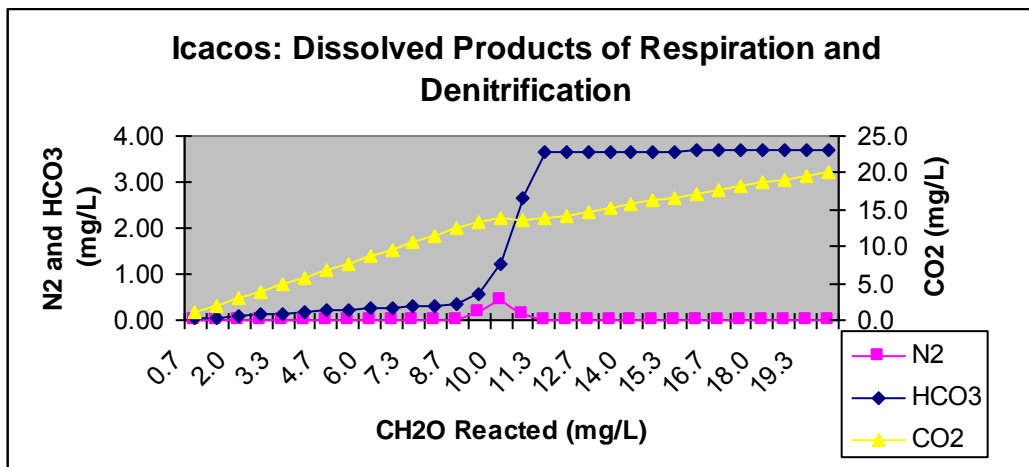


Table 1. Critical interval of DOC oxidation at which oxygen is completely reduced and denitrification begins. Product and reactant concentrations are shown in relation to pE and pH values.

CH ₂ O reacted (mg/L)	NO ₃ (N mg/L)	O ₂ (mg/L)	N ₂ (N mg/L)	CO ₂ (mg/L)	HCO ₃ (mg/L)	pE	pH
8.0	.47	0.9	0.0	11.5	.31	16.2	4.7
8.7	.47	0.2	0.0	12.5	.33	16.0	4.7
9.3	0.3	0.0	0.17	13.3	.57	14.9	4.9
10.0	0.05	0.0	0.42	13.8	1.22	14.3	5.2
10.7	0.0	0.0	0.14	13.7	2.64	-1.4	5.5
11.3	0.0	0.0	0.0	13.8	3.64	-2.3	5.7

References:

Jiménez RA (2011) A Geochemical Model of Redox Reactions in a Tropical Rain Forest Stream Riparian Zone: DOC Oxidation, Respiration and Denitrification. Masters Capstone and Thesis. University of Pennsylvania.

McDowell WH, Bowden WB, Asbury CE (1992) Riparian Nitrogen Dynamics in 2-Geomorphologically Distinct Tropical Rain-Forest Watersheds – Subsurface Solute Patterns. Biogeochemistry 18:53-75.

The reconstruction of Holocene sea level and paleoenvironmental change

Nicole Khan¹, Benjamin P. Horton¹, Christopher Vane², F.N. Scatena¹

¹Department of Earth and Environmental Science, University of Pennsylvania, USA

²British Geological Survey, Kingsley Dunham Centre, UK

Introduction

Sea-level changes on the time-scale of decades to millennia are driven, predominantly, by changes in climate. The recent transition of the earth system from a glacial to interglacial state produced a dramatic global sea-level response. Puerto Rico is distant from the major glaciation centers, thus is characterized by a sea-level rise of ~120 m since the Last Glacial Maximum due, largely, to the influx of glacial meltwater to the oceans. By comparing observations of sea-level changes to model predictions, it is possible to infer parameters relating to changes in climate, the rate and geographic source of meltwater influx, the rheological structure of the solid Earth, and the spatially variable vertical land motion, a key parameter for understanding mantle flow and the tectonic evolution of our planet. The key science objectives are:

1. To collect new Holocene sea-level data from mangrove peats involving a complete suite of paleoenvironmental indices, precise elevation measurements tied to sea level, state of the art analyses and data interpretation.
2. To synthesize existing and new data to produce a quality-controlled, spatially and temporally comprehensive sea-level database for Puerto Rico and the Caribbean during the Holocene.
3. To determine the nature and magnitude of vertical land motion within Puerto Rico and the Caribbean sea-level database.

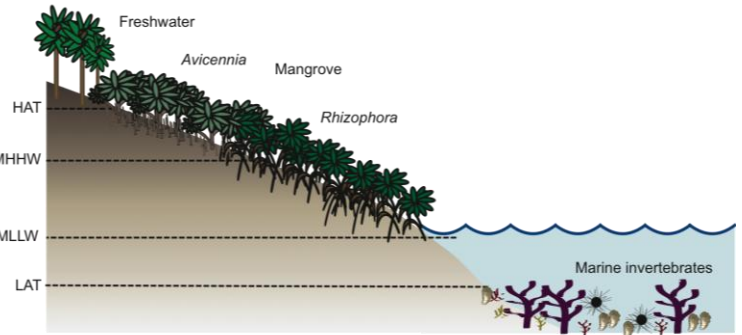


Figure 1. Mangrove zonation related to elevation in the intertidal zone

Sea-level Indicators: Carbon Isotopes

Holocene changes in RSL are commonly determined using microfossil sea-level indicators, which possess a systematic and quantifiable relationship to elevation with respect to the tidal frame. When the

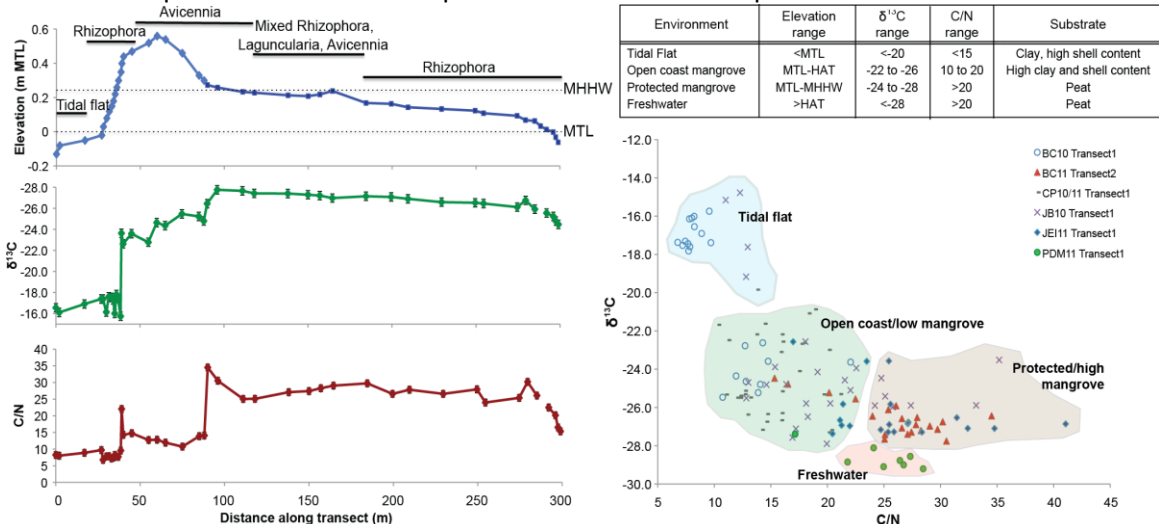


Figure 2. a) Variation in $\delta^{13}\text{C}$ and C/N along a transect near the Espiritu Santo River that extends from tidal flat up to high mangrove environments. There are 3-4 marked shifts in $\delta^{13}\text{C}$ and C/N occurring at the MHHW boundary at the transition from tidal flat/fringing Rhizophora to an Avicennia-dominated storm berm, again at the MHHW boundary at the transition to a protected, mixed Rhizophora/Avicennia environment, and finally at the MTL boundary. b) Biplot of $\delta^{13}\text{C}$ vs. C/N for transects from all 4 sites that defines the unique range of $\delta^{13}\text{C}$ and C/N of environments. c) The elevational and $\delta^{13}\text{C}$ and C/N range and associated substrate type for environments included in transects at the 4 sites.

relationship of such an indicator to present-day sea level is determined (Figure 1), it can be applied to samples in the stratigraphic record to determine the former position of sea level. Microfossils (e.g. diatoms, foraminifera) are, however, poorly preserved in tropical environments and therefore are of little use in paleoenvironmental studies in these locations. As an alternative we wish to examine if the stable carbon isotope chemistry of bulk organic matter, which varies with vegetation zones related to elevation in the tidal frame, holds utility as a sea-level indicator (Figure 2).

Constructing Chronologies in Mangrove Sediments

There is currently no consensus on the appropriate material to date in mangrove environments. Our initial results suggest that accurate chronologies can be obtained from these environments by dating leaf or wood fragments that fall *in situ* on the mangrove sediment surface (Figure 3). We will assess what components of mangrove peat should be dated to construct accurate and precise chronologies in mangrove environments.

RSL Reconstruction

We have collected a series of cores from the northern and southern coasts of the island to reconstruct RSL. Comparison of these records to glacio-isostatic adjustment (GIA) model predictions and other records in the Caribbean, and construction of our records from compaction-free basal peats, which minimize local effects, should enable us to estimate the impact of local tectonics on Puerto Rico's RSL history.

Additional funding sources

1. National Ocean Sciences Accelerator Mass Spectrometry Facility (NOSAMS) at Woods Hole Oceanographic Institution
2. British Geological Survey

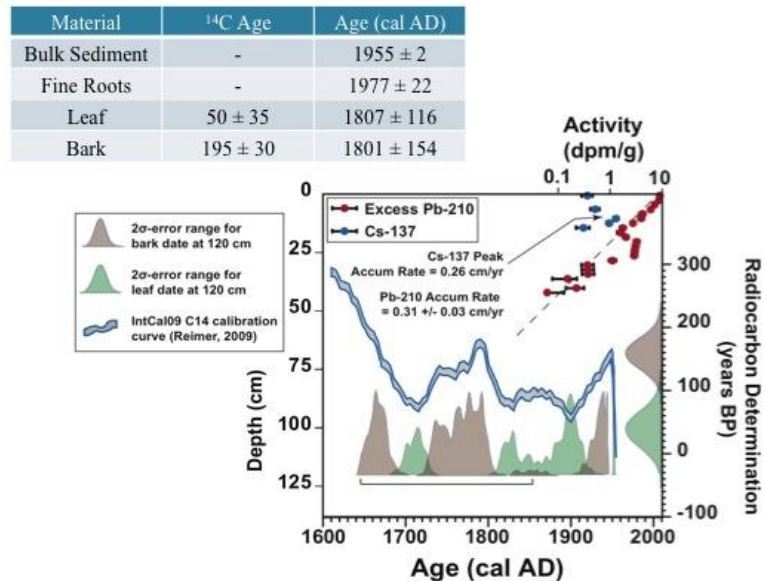


Figure 3. Radiocarbon dates obtained from bulk sediment, fine roots, leaf, and bark material sampled from 120 cm depth in a core collected near the Espiritu Santo. Modern roots penetrating to depth contaminate the ¹⁴C of dates from fine root and bulk sediment material. The radiocarbon dates obtained from the leaf and bark fragments are in general agreement with ²¹⁰Pb and ¹³⁷Cs accumulations and together, both methods constrain the depth of 120 cm to correspond to an age between 1650 and 1860 cal AD



A $\delta^{44}\text{Ca}$ based comparison of Ca cycling in tropical and temperate ecosystems

Andrew Kurtz, Associate Professor
Boston University – Earth Science Dept.
675 Commonwealth Ave.
Boston, MA 02215
Phone: (617) 358-2570 Fax: (617) 353-3290
Email: kurtz@bu.edu

Kenneth Takagi, PhD Candidate
Boston University – Earth Science Dept.
675 Commonwealth Ave.
Boston, MA 02215
Phone: (860) 818-1239 Fax: (617) 353-3290
Email: katakagi@bu.edu

Key Science Questions Involved:

What can Ca stable isotopes tell us about the differences between Ca cycling in tropical and temperate ecosystems, and the role vegetation plays in regulating the export of calcium in streams?

This project was conceived in response to the CUAHSI Pathfinder Graduate Student Fellowship request for proposals, which encouraged graduate students to go beyond a "one site, one view" approach to research. This is accomplished by spending extended time at an additional research site to broaden the research experience of the student and/or adding an interdisciplinary dimension to their project. Our ongoing research has focused on furthering the development of Ca stable isotopes as a tracer of Ca cycling in forest ecosystems. Recent work on forest ecosystems has confirmed that vegetation and near-surface organically bound-Ca is isotopically light (enriched in ^{40}Ca) compared to both soil and bedrock, likely reflecting preferential uptake and incorporation of light calcium isotopes into actively growing portions of biomass. The isotopic differences between various Ca pools potentially provides a means for Ca stable isotopes to identify the source of Ca in streamwater and quantify the flux of Ca into and between different forest Ca pools.

We are currently utilizing Ca stable isotopes as a tracer of Ca to investigate the mechanism of increased streamwater calcium export following a harvesting experiment at Hubbard Brook Experimental Forest (HBEF) in New Hampshire. HBEF Watershed 5 (W5) underwent a whole tree harvest between the fall of 1983 and spring of 1984 that removed 93% of all aboveground biomass (Mann et al., 1988; C.E. Johnson et al., 1991, 1997). A four-fold increase in cation nutrient export via streamwater was observed, as well decreases in soil and streamwater pH. The source of this increased cation export is uncertain as Johnson et al. (1991, 1997) observed no significant depletion of the exchangeable cation pool in Watershed 5 either 3 or 8 years post-harvest, and Ca:Na ratios indicated no increase in weathering of bedrock or till in Watershed 5 (Bailey et al., 2003).

Taking advantage of archived water samples, we measured Ca stable isotopes in W5 streamwater collected, before, during and after the harvest. We initially hypothesized that we would observe a resolvable shift toward negative (^{40}Ca -enriched) $\delta^{44}\text{Ca}$ ratios following harvesting, which would be indicative of elevated export of near-surface organically bound-Ca by the stream. Though we did observe $\delta^{44}\text{Ca}$ variability outside the range our external precision, there was no clear shift in $\delta^{44}\text{Ca}$ values associated with the harvesting.

Interestingly, we find a statistically significant relationship between $\delta^{44}\text{Ca}$ and discharge. At high discharge periods (spring snow melt and large rain events), stream water $\delta^{44}\text{Ca}$ shifts toward negative

(⁴⁰Ca-enriched) isotope ratios (figure 1). We interpret this shift to indicate elevated export of near-surface, biologically fractionated Ca during high discharge, possibly due to the activation of near-surface flow pathways. In the context of calcium retention by vegetation, this result suggests that the forest ecosystem at HBEF is not strongly retaining Ca in the upper soil profile, as the thin soil mantle (typically less than 1m) and relatively young soil (<15,000 y.o.) can provide vegetation direct access to unweathered minerals, which may be an important source of Ca to vegetation.

In contrast, in tropical environments, such as LCZO, that experience high precipitation rates and have highly weathered, nutrient poor saprolite extending beyond the rooting zone, tight cycling of nutrients is of utmost importance. Saprolite at LCZO, which can exceed 15m on ridgetops and has exchangeable Ca concentrations as low as 3ppm, coupled with the isovolumetric weathering of saprolite that maintains low infiltration rates, can act as an effective barrier restricting the flux of Ca between

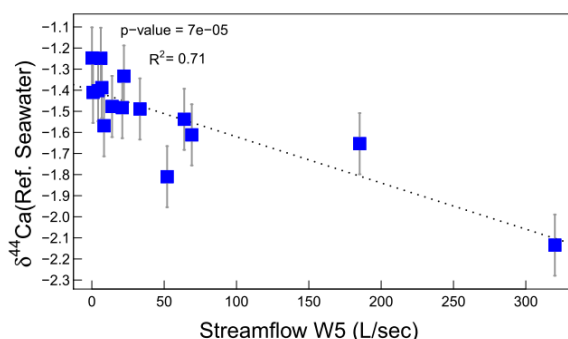


Figure 1. Streamwater $\delta^{44}\text{Ca}$ vs. Streamflow at HBEF Watershed 5.

the near-surface and deeper Ca pools. In fact, unlike at HBEF, there may be two physically distinct Ca cycles operating at LCZO, a deep, bedrock-derived Ca cycle that is the dominant supply of Ca to streams, and a biologically controlled Ca cycle operating at the near surface, dominated by atmospheric deposition and biological recycling of Ca. This decoupling maybe be apparent in the Ca concentration-discharge relationships. At LZCO, streams exhibit a rainfall dilution effect, suggesting that during high discharge little additional calcium beyond the baseflow contribution is exported. In contrast, at HBEF, Ca streamwater concentrations remain relatively constant even at high discharge, suggesting an increasing supply of Ca as discharge increases.

We hypothesize that at LCZO, unlike at HBEF, the tight cycling of nutrients by vegetation will limit the export of near-surface biologically fractionated Ca and restrict the range of stable Ca isotopes ratios observed in stream water during high flow periods. Secondly, tight cycling and preferential retention of shallow Ca by vegetation will result in vegetation that is more strongly fractionated and shallow soil pools that are less fractionated than their respective counterparts at HBEF. To test these hypotheses, we will sample and measure streamwater $\delta^{44}\text{Ca}$ from storm event sequences in the Bisley and Iacos watershed, as well as potential streamwater endmembers (soil water, groundwater, precipitation) to constrain the sources of streamwater Ca. Additionally, isotopic measurements of soil exchangeable Ca will allow us to assess the depth to which Ca is biologically fractionated, and determine the extent to which shallow and deep Ca pools are decoupled by the presence of a thick, Ca-poor saprolite.

Additional funding sources: Consortium for the advance of hydrological Sciences, Inc. (CUAHSI) Pathfinder Grant; Geological Society of America-Graduate Research Grant; National Science Foundation Critical Zone Observatory Program.

Real time rainfall-induced landslide risk assessment System for the Luquillo Mountains of Puerto Rico

M. Leon, F.N. Scatena; Department of Earth and Environmental Science,
University of Pennsylvania.

A prototype real time landslide warning system has been developed for the Luquillo Mountains and is available at landslidepr.com. The warning system incorporates results from Larsen and Simon 1993, which established a rainfall intensity for inducing landslides in Puerto Rico. Rainfall intensity is calculated based on National Weather Service radar and ground based precipitation measurements and compared to a threshold of $I > 91.45 D^{-0.82}$ if I , the measured intensity, is greater than 91.45 times duration raised to -0.82 than a landslide warning is issued for that area.

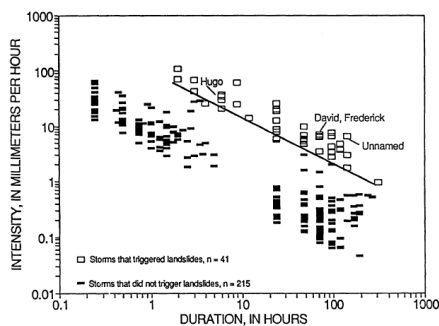


Figure 1: Rainfall Intensity Duration Threshold for inducing landslide events.

The Warning system incorporates background landscape risk maps based on frequency ratio analysis and Logistic Regression analysis of factors related to landslide risk from Lepore 2011. The logistic regression was redone with similar datasets for just the northeastern portion of Puerto Rico, instead of the entire Island and similar results were achieved. The variables used to explain landslide occurrence are Slope (in degrees), Precipitation, Aspect,

Annual Geopotential Energy from falling rain, and if a location is within 85 meters of a road or not. These factors are used to explain the occurrence of past landslides which have been mapped. Users of the website can view the results of this analysis of background landslide risk in addition to the computed rainfall totals and warnings.

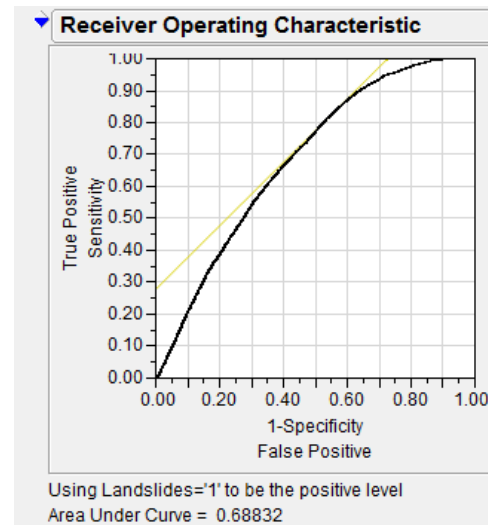


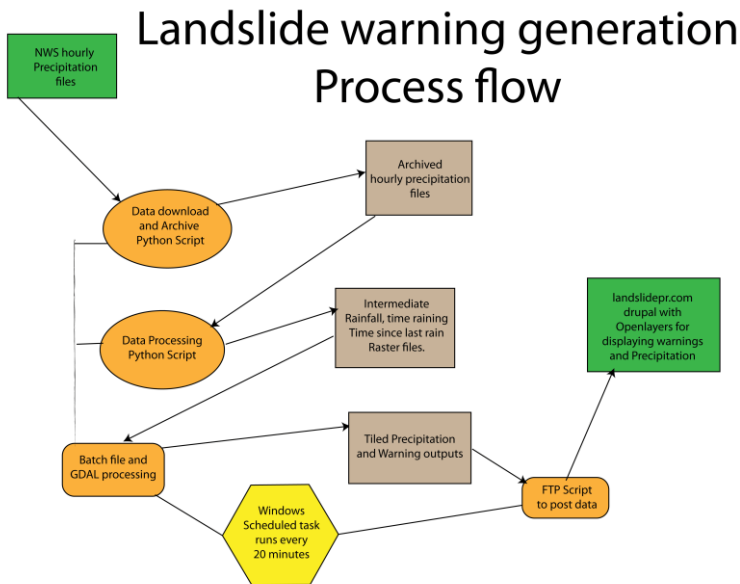
Figure 2: Logistic regression results for north eastern Puerto Rico with an AUC of .688.

In order to determine if the rainfall intensity duration threshold has been met, radar precipitation raster data needs to be analyzed on a per pixel basis. Every twenty minutes a one hour precipitation raster is downloaded and compared to the previously downloaded one. If for a particular cell, precipitation has occurred, then a total precipitation raster is updated by adding this amount. If no precipitation has occurred then a separate time between precipitation raster is

updated. If the new total time between precipitation value is greater than or equal to six hours then the total precipitation and total time raining rasters are updated to 0. This has the effect that for each individual grid cell, rainfall intensity is tracked separately and reset when appropriate for that cell. The total time raining and precipitation values are then compared with the rainfall intensity threshold for inducing landslides, if it has been exceeded a warning raster is updated to indicate increased risk of landslides for that particular cell. Finally landslide warning and total precipitation rasters are processed for presentation on the web via a series of GDAL (Geospatial data abstraction

Total Precipitation, background landslide risk, and computed landslide warnings are presented on the web via a drupal content management system with openlayers. Google maps are used for the base layers and additional information about the computed warnings, the statistics used for generating the risk assessment and background materials are presented for users to learn more about landslides in Puerto Rico.

The functioning of the site has been confirmed through corroboration of warnings with large rainfall events through the summer and fall of 2011.



layer) commands and uploaded to the web.

Figure 3: Data process flow for creating landslide warning products for the web.

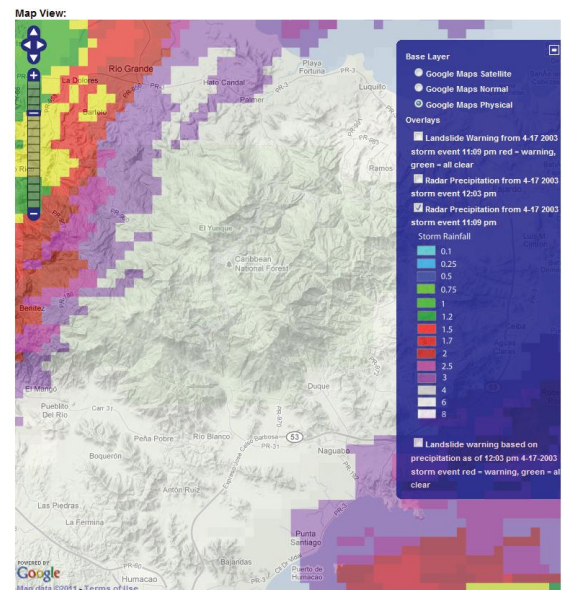


Figure 4: Computed rainfall totals presented on the web based on NWS radar.

Larsen, M.C., Simon, A. A Rainfall Intensity-Duration Threshold for Landslides in a humid-tropical Environment, Puerto Rico. *Geografiska Annaler* (1993) p13-23

Lepore, C. Kamal, S. A., Shanahan, P. Bras, R. L., Rainfall-induced landslide susceptibility zonation of Puerto Rico. *Environmental Earth Science*, 2011. DOI 10.1007/s12665-011-0976-

Microbiota versus geochemistry in regolith in the Rio Icacos and Bisley watersheds

LAURA LIERMANN¹, SUSAN BRANTLEY¹, ISTVAN ALBERT¹, HEATHER BUSS², MORGAN MINYARD³

¹ Penn State University, lj18@psu.edu,

sxb7@psu.edu, iaa1@psu.edu

²University of Bristol, School of Earth Sciences, Bristol, UK, h.buss@bristol.ac.uk

³U.S. Defense Threat Reduction Agency

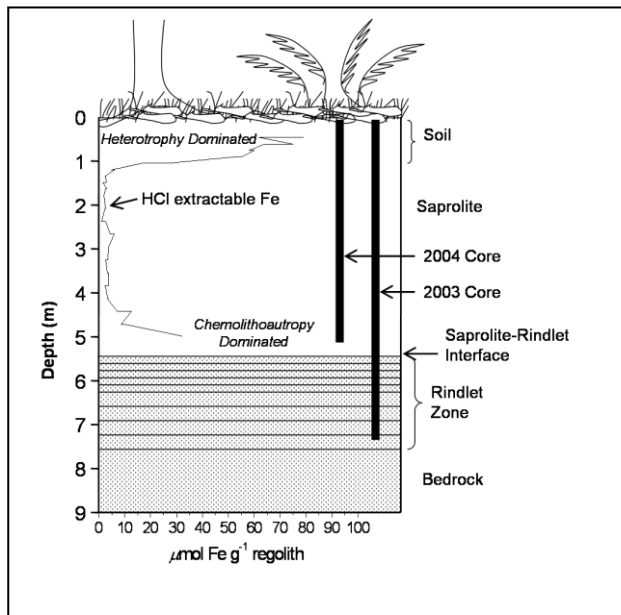


Figure 1. Cartoon depicting regolith on the Rio Blanco quartz diorite at site LG1. The quartz diorite is overlain by 2-8 m of saprolite and topped by 50-100 cm of soil. The bedrock weathers spheroidally, forming a zone of partially weathered rock layers termed *rindlets*. A shallow ecosystem (upper 2 m) based upon heterotrophic metabolism and a deeper ecosystem (deeper than 4 m) based upon autotrophic metabolism were both identified. The deeper ecosystem may be metabolizing ferrous iron released by weathering of the bedrock (Buss et al., 2005; 2008; Minyard et al., 2011; Bruns et al., 2011).

lower density of heterotrophs (relative to the surface) at the bedrock-regolith interface. We have also inferred the presence of iron-oxidizing bacteria near the regolith-bedrock interface in the Susquehanna Shale Hills Observatory in central Pennsylvania (USA). Thus, we are hypothesizing that Fe-related chemolithoautotrophic microorganisms may play a role in the disaggregation of intact bedrock to regolith. In the quartz diorite, oxidation of Fe in biotite is the deepest reaction that we have observed in the bedrock (Buss et al., 2008), and may be driving the spheroidal fracturing of the rock (Fletcher et al., 2006). We are now testing this hypothesis in 9.2 m deep regolith developed on volcanoclastic material of the Fajardo formation in the Bisley watershed.

Key Science Questions:

- How does the abundance, distribution and metabolism of micro-biota change as a function of depth in weathering regolith down to bedrock in the two watersheds?
- Are surface and subsurface microbial communities decoupled?

Previous research. In previous studies in the Rio Icacos watershed, we have observed a pattern of decreasing heterotrophic and total bacterial cell numbers with depth in regolith (quartz + kaolinite + Fe oxides + biotite) from surface to bedrock (quartz + feldspar + biotite + accessories).

However, an increase in cell density was observed at the regolith-bedrock interface (Fig 1). Biochemical tests for iron-oxidizing microorganisms document Fe-oxidizing bacteria along with a

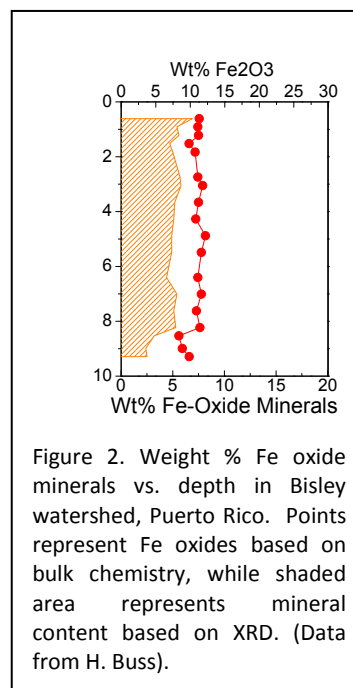


Figure 2. Weight % Fe oxide minerals vs. depth in Bisley watershed, Puerto Rico. Points represent Fe oxides based on bulk chemistry, while shaded area represents mineral content based on XRD. (Data from H. Buss).

Bisley regolith. The Fajardo formation consists of volcanoclastic sediments that contain quartz, plagioclase, chlorite, pyroxene, epidote, K-feldspar, and tourmaline with minor prehnite, biotite, calcite and illite (Buss et al., 2012). The dominant mineralogical reaction – also the reaction that correlates with disaggregation of rock – is transformation to kaolinite. Buss et al. (in prep.) cored regolith on a local ridge overlooking the Bisley 1 stream gage from the northeast (site B1S1) for mineralogical and microbiological analysis. Kaolinite and Fe oxides are present from the surface down to 8.3 m, while the weathered primary minerals chlorite and feldspar were only detected at depths between 8.3 and 9.2 m (i.e., the bedrock, see Fig. 2). Microcrystalline quartz is found throughout the profile.

Microbiology. Cell counts for all bacteria and heterotrophs generally decrease from the surface down to ~9 m, with higher densities correlating with lower clay content (Liermann et al, in prep). Cell densities that grew in iron-oxidizing media decreased with depth, but increased near the weathering front at 8.3 m depth.

Using next-generation sequencing and metagenomics analysis tools, bacteria community composition and structure were assessed in the context of chemical and mineralogical characteristics. At all depths analyzed, 4 phyla were dominant – Proteobacteria, Acidobacteria, Planctomycetes, and Actinobacteria (Table 1). Sub-phylum groups containing known iron-oxidizing microorganisms (e.g. subclass Acidimicrobiae, shown in grey in Table 1) were found as a greater percentage of identified sequences near the regolith-bedrock interface compared to shallower depths, consistent with chemolitho-autotrophic bacteria playing an important role in disaggregation of bedrock.

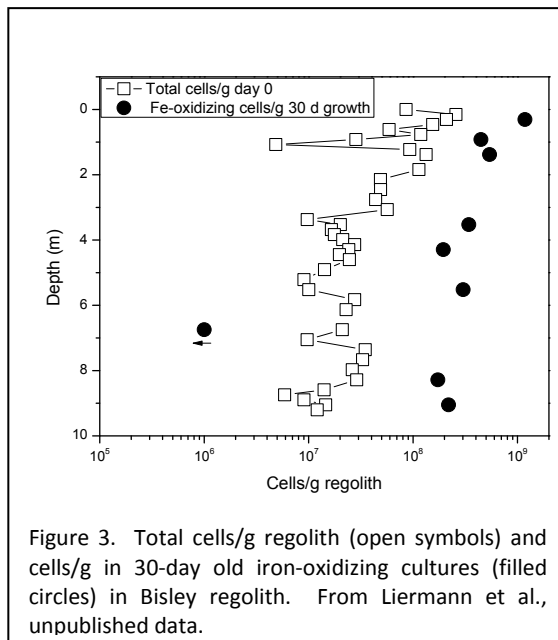


Figure 3. Total cells/g regolith (open symbols) and cells/g in 30-day old iron-oxidizing cultures (filled circles) in Bisley regolith. From Liermann et al., unpublished data.

Table 1. Percent of all sequence reads classified as specified phyla, and percent sub-phylum taxa¹ with known iron-oxidizers.

Taxon	Depth (m)						
	1.4	3.5	4.4	5.5	6.8	8.3	9.0
Phylum Proteobacteria	34.2	13.4	12.7	34.8	43.4	41.1	43.7
Class β-Proteobacteria unclassified	29.2	94.8	90.3	45.2	5.75	16.8	19.7
Class γ-Proteobacteria unclassified	81.4	55.4	56.8	77.6	89.7	90.2	87.8
Phylum Acidobacteria	36.9	42.8	37.2	34.7	33.5	34.2	31.2
Phylum Actinobacteria	2.6	1.2	1.3	5.1	4.4	3.0	3.0
Subclass Acidimicrobiae	33.1	37.9	18.0	11.1	26.9	44.6	46.2
Phylum Planctomycetes	7.2	4.0	1.4	2.4	4.7	3.4	5.4
Unclassified bacteria	15.5	35.4	44.8	17.3	10.9	14.9	13.3

¹ Sub-phylum percentages are the percent of sequences within a particular phylum that are classified as the indicated sub-phylum.

Iron-reducing groups (e.g. *Geobacter*, *Anaeromyxobacter*) were also detected at 8.3 m and 9.0 m, as well as at 1.4 m and 6.8 m. The data are consistent with the hypothesis of an iron-cycling community that in turn supports heterotrophs at 8.3 m

depth and contributes to disaggregation of bedrock.

Additional funding sources: Department of Energy grant DE-FG02-05ER15675 and the Penn State Astrobiology Research Center grant NNA04CC06A.



References:

Buss, H.L., Bruns, M.A., Schultz, M.J., Moore, J., Mathur, C.F., Brantley, S.L. (2005). The coupling of biological iron cycling and mineral weathering during saprolite formation, Luquillo Mountains, Puerto Rico. *Geobiology*, 3: 247-260.

Buss, H.L., Sak, P.B., Webb, S.M. and Brantley, S.L. (2008). Weathering of the Rio Blanco quartz diorite, Luquillo Mountains, Puerto Rico: Coupling oxidation, dissolution, and fracturing. *Geochimica et Cosmochimica Acta*, 72(18): 4488-4507.

Buss H.L., Brantley S.L., Scatena F.N., Bazilievskaya E.A., Blum A., Schulz M., Jimenez R., and White A.F. Probing the deep critical zone beneath the Luquillo Experimental Forest, Puerto Rico. *Submitted to Earth Surface Processes and Landforms*.

Buss H.L., White A.F., Blum A.E., Schulz M.S., Fitzpatrick J. and Bullen T.D. Lithological influences on weathering processes and rates at the Luquillo Critical Zone Observatory. *In prep. for GCA*.

Fletcher, R.C., Buss, H.L. and Brantley, S.L. (2006). A spheroidal weathering model coupling porewater chemistry to soil thicknesses during steady-state denudation. *Earth and Planetary Science Letters*, 244: 444-457.

Liermann, L.J., Albert, I., Brantley, S.L., Buss, H.L., and Minyard, M. Relating microbial community structure and geochemistry in a watershed on volcanoclastic sediments in the Luquillo Mountains, Puerto Rico. *In prep for Geomicrobiology Journal*.

Relative importance of sediment abrasion in downstream fining of grains and production of fine sediment.

Kimberly Litwin and Douglas Jerolmack; Department of Earth and Environmental Science, University of Pennsylvania

Key Science Questions Involved:

1. What is the relative importance of abrasion versus selective transport in causing downstream fining of river sediments?
2. What is the fraction of fine material that is produced by abrasion of gravel?

The process of abrasion is defined by the production of fine sediments and sand that occurs by saltation of gravel, where particle-to-particle collisions supply the energy required to break apart grains (Figure 1). Although previous work has shown that lithology, grain shape, and energy of collision are contributing factors that control abrasion rates of river-bed

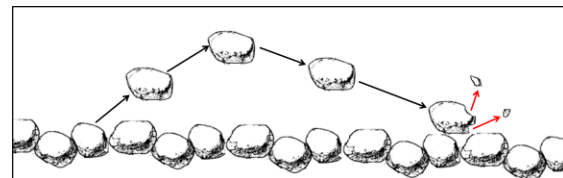


Figure 1 Schematic showing abrasion due to saltation of bedload.

material, little is known regarding the relationship between these factors and diminution rates. Without such knowledge, it is not possible to estimate the contribution of in-stream abrasion to determining grain sizes of river sediments, relative to the better-studied processes of chemical weathering and sorting by transport. In this project, we are investigating the controls on abrasion rates and the products of the abrasion process. The Luquillo Critical Zone Observatory (LCZO) in Puerto Rico is an ideal setting to study sediment abrasion because of the two different lithologies, volcanoclastic and quartz diorite, that comprise the channel sediments in the two otherwise similar study watersheds of the Rio Mamayes and Rio Icacos, respectively. The volcanoclastic watershed produces a wide range of river-bed grain sizes, whose distribution changes gradually downstream. Streams draining quartz diorite lithologies are rich in sand and boulders but are lacking in intermediate grain sizes. We hypothesize that

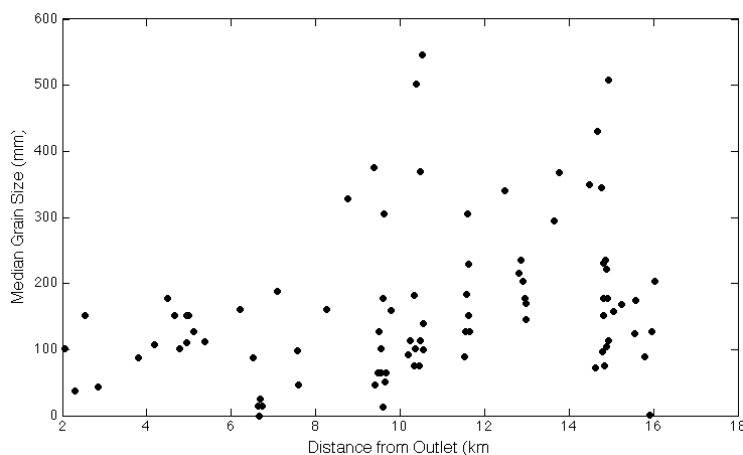


Figure 2: Median grain size with distance from headwaters for Rio Mamayes watershed.

in steep mountain sections of streams, sediment storage capacity is minimal while collision energies are higher; thus, abrasion should dominate over size-selective sorting for determining grain size fining downstream. Conversely, alluvial plain river sections with higher storage capacity should show strong size-selective sorting, while the importance of abrasion is reduced.

Pike et al. (2010) measured grain size at over 45 locations within the Mamayes watershed, with results

indicating an overall fining of grains with distance from headwaters (Figure 2). In order to explain this downstream fining, we measure the shape of channel sediments in both watersheds to determine their downstream evolution. Results from experiments conducted by Durian et al. (2006) of abrasion of a two dimension square pebble in a rotating drum showed that areas of pebble that protruded, marked by high curvature values, tended to abrade faster. As the protruding corners of the square abraded away, the pebble became rounder causing abrasion rates to decrease (Durian et al., 2006). Since shape has been shown to control abrasion rates of grains, we are using this parameter as a proxy for observing the abrasion process. We assume that any rounding of the river sediments will be solely due to abrasion. We characterize grain shape with standardized shape parameters, as well as Fourier analysis, which allows us to track changes in grain roughness at a variety of length scales. Preliminary results of shape analysis of 36 locations within the Rio Mamayes watershed shows a distinct pattern of rounding in the last 10 km of the river (Figure 3). In order to further examine the mechanism behind abrasion, we will determine the mobility and collision energy of gravels that are transported by floods using results from the work Colin Phillips and Douglas Jerolmack are conducting on tracking the transport of grains using radio-tracer particles. Additionally, we can calculate the amount of fine sediments that should be produced by abrasion and compare them to hillslope sediments produced by chemical weathering. Using results from the sediment fingerprinting project being completed by Marcie Occhi and Jane Willenbring, we hope to determine the fraction of fines that are derived from the abrasion process. Laboratory experiments are being conducted at the University of Pennsylvania to tease apart the controls of lithology, collision energy and grain shape on the rates and styles of abrasion. Experiments will allow us to link the mechanics of granular collisions to parameters such as grain size and shape distributions that can be measured in the field. The results of this research will enable us to isolate the effects of in-stream abrasion on the downstream fining of grains in a river, and to understand the specific control that bedrock lithology exerts on this process.

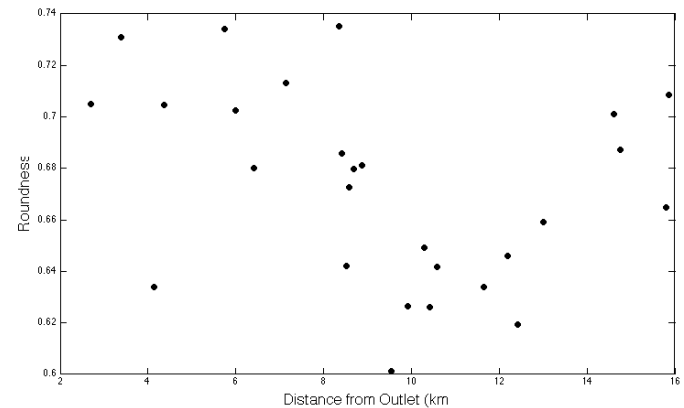


Figure 3: Bulk shape parameter, roundness, averaged from 40 samples at different locations along the Rio Mamayes as a function of distance.

Landscape connectivity indices of Luquillo Watershed

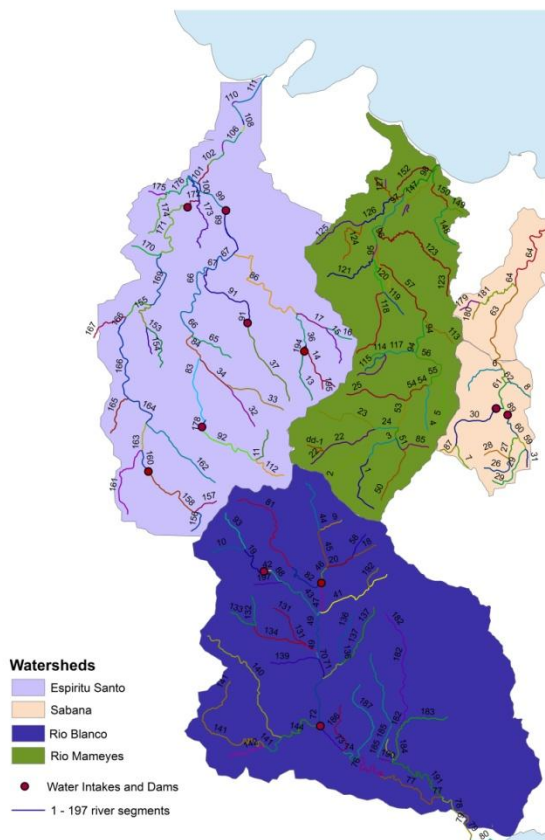
Urmila Malvadkar, F.N. Scatena, M.C. Leon. Department of Earth and Environmental Science, University of Pennsylvania.

Key Science Questions Involved: Quantifying connectivity between different landscape units; Relationship between connectivity measures and ecological/geological structure

Start and End Date: Jan 2012-Jan 2013

Natural differences in the morphology of drainage nets as well as dams, culverts, and land use may fragment and disconnect habitats, reduce effective habitat size, and ultimately reduce the population viability of riverine species. Previous research indicates these impacts can be assessed through “connectivity metrics” that quantify the connectedness of populations and landscapes. Some of the measures characterize an entire landscape (or riverscape), while others describe connectivity at a point. The level of connectedness of either a landscape or a point generally depends on the physical structure of the landscape; however, these measures also can include information about the dispersal ability of the organism or material.

While dozens of connectivity metrics have been proposed and used in the ecological literature, little is known about how these metrics vary between watersheds of different sizes, structures, lithologies, or land covers or if these metrics are related to hydrologic and mass fluxes from watersheds. This study investigates the use of connectivity metrics on the drainage net of the Luquillo Critical Zone Observatory and will eventually test their sensitivity to differences in watershed morphology, geology, land use, and hydrological and material fluxes. Specific questions being tested include how various metrics are correlated to each other and to the transport of material and organisms across the landscape; and how connectivity varies across watersheds. The following metrics are being tested.



Betweenness Centrality (BC), which measures the number of paths that go through a given point;

Integral Index of Connectivity (IIC), which measures the amount of reachable habitat from a patch, scaled by number of links between patches.

Coincidence Probability (CP), the probability that an individual can move between any 2 randomly chosen points;

Eigenvector Centrality (EC), the long-term equilibrium number of individuals in a branch, assuming random movement

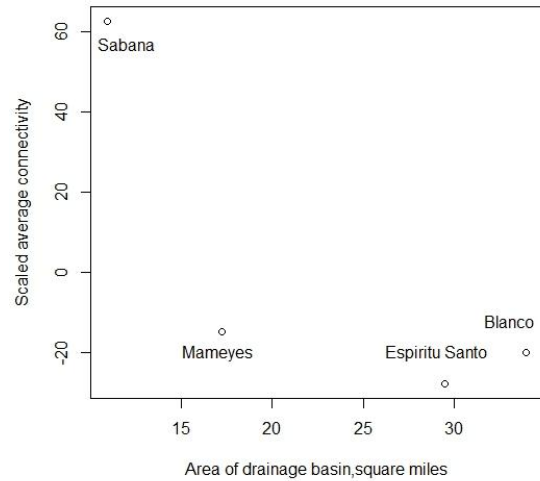
Probability of Connectivity (PC), the probability that an individual would travel the distance between any 2 points. This requires a value reflecting dispersal distance, called alpha; thus, this measure is species-specific.

$1/(N^2\text{var}(EC))$ and $1/(N^2\text{var}(BC))$. These are new watershed-based metrics developed in this study, in order to apply information from node-based connectivities to whole watersheds.

BC and EC produce a connectivity value for each node. IIC, CP and PC give a value for the entire watershed, but can be modified to evaluate the connectivity at a point: the point-wise connectivity value can be defined as the change in the metric when that point is removed, as a fraction of the intact landscape.

Initial results indicate that all of the point-wise connectivity metrics are significantly correlated, with correlations ranging between 0.5 and 0.99. These results contrast with those found in Estrada and Bodin (2008) who were working on forest patches in Madagascar. Of the 15 pairwise combinations of the 5 metrics they use to determine patch connectivity, only 3 were significantly correlated. This indicates that connectivity metrics appear to be more correlated on riverscapes than on forests, which could result from the structural constraints on graphical representations of watersheds.

The connectivity of the four watersheds can be compared using five metrics-- $1/(N^2\text{var}(BC))$, IIC, $1/(N^2\text{var}(EC))$ and PC ($\alpha = 0.01$) and PC ($\alpha = 10$). These metrics consistently show that the Sabana is the most connected; they fairly consistently (all but IIC) rank Rio Espiritu Santo as the least connected. Thus, for most measures the connectivity of the watershed decreases with the area of the watershed.



The connectivity of the subbasins can also be used to compare the five metrics themselves. All the metrics decrease exponentially with the number of nodes in the subbasin, except for $PC_{\alpha = 0.01}$, which decreases linearly. Likewise, the connectivities of the watersheds given by each metric are correlated at levels of greater than 0.9, except for $PC_{\alpha = .01}$. Thus, for alpha large enough (that is, for constrained dispersal), the metrics appear to be consistent.

Ultimately the value of these metrics depends on how well they can predict the distribution of organisms and inorganic material. Future research will involve testing these metrics on wider range of streams and subwatersheds, either actual or randomly-generated; comparing them to populations, simulations, water quality indices/exports, and sediment delivery ratios.

Determining the Provenance of Suspended Sediment: Storm Sampling in NE Puerto Rico

Marcie E Occhi*, Dr. Jane Willenbring*, F.N. Scatena*, Dr. Martha Scholl^a, Dr. Jamie Shanely^b, Dr. Jim Kaste^c, Dr. Gilles Brocard*, Hyejung Lee*

*Department of Earth and Environmental Science, University of Pennsylvania, ^aUSGS, Reston, VA, ^bUSGS, Montpelier, VT, ^cDepartment of Geology, The College of William and Mary.

Motivation for study:

1. How does a single precipitation event erode a landscape?
2. Can we determine provenance of suspended sediments during a flood event?
3. Do source areas contributing suspended sediments vary over the course of a hydrograph?

Landscape evolution is largely determined by weathering/erosion rates and subsequent transportation of material. However, it is unclear what controls total denudation, as no strong correlation exists between climate and total denudation. For this project I am interested in identifying possible sediment source regions to better understand weathering and erosion on a short time scale. To do this, we apply multiple isotopic tracers (meteoric ¹⁰Be and ⁷Be) to suspended sediment samples collected from multiple watershed locations at various stages over course of a storm hydrograph.

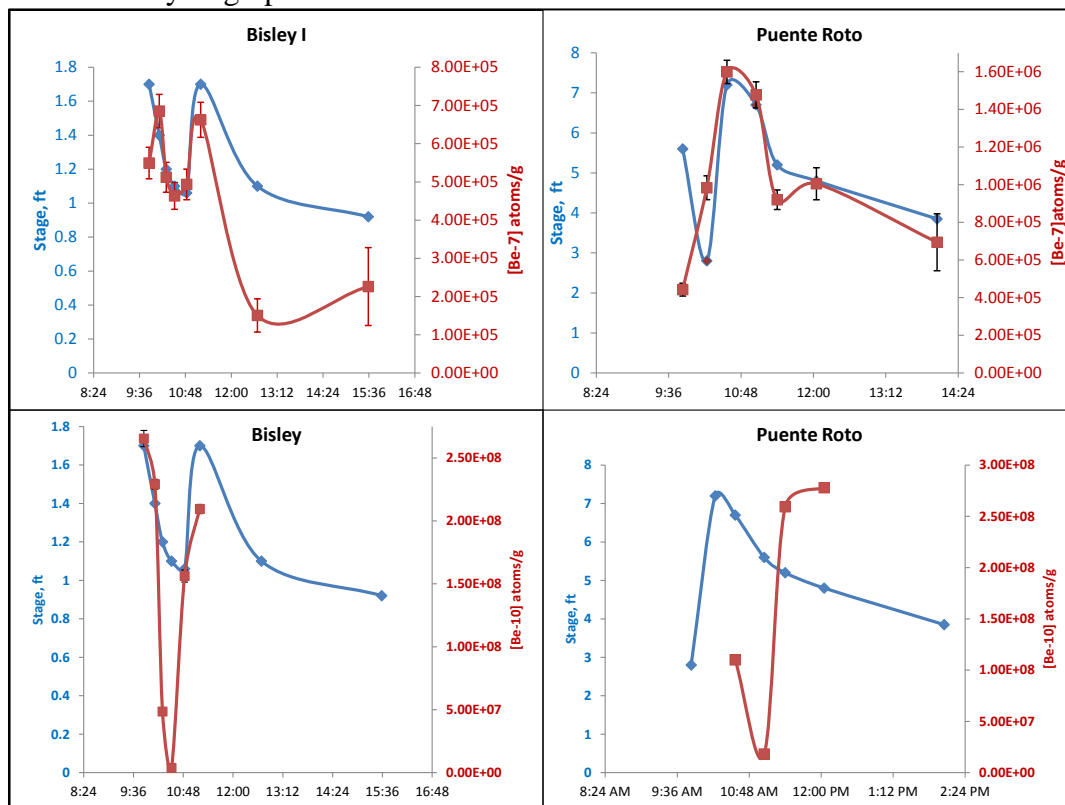


Figure 1: ⁷Be and ¹⁰Be concentrations with river stage from two sample sites.

We are also interested in understanding if sediment sources change over the course of the storm hydrograph due to variations in rainfall magnitude and intensity and changes in flow paths. This isotopic fingerprinting of suspended sediment coupled with proper characterization of source

regions will provide a clear and robust understanding of active sediment source regions present throughout the watershed, which could prove key to pinpointing sources of fine sediment pollution, as it is estimated that over 90% of sediment export through river systems in Puerto Rico is through suspended load.

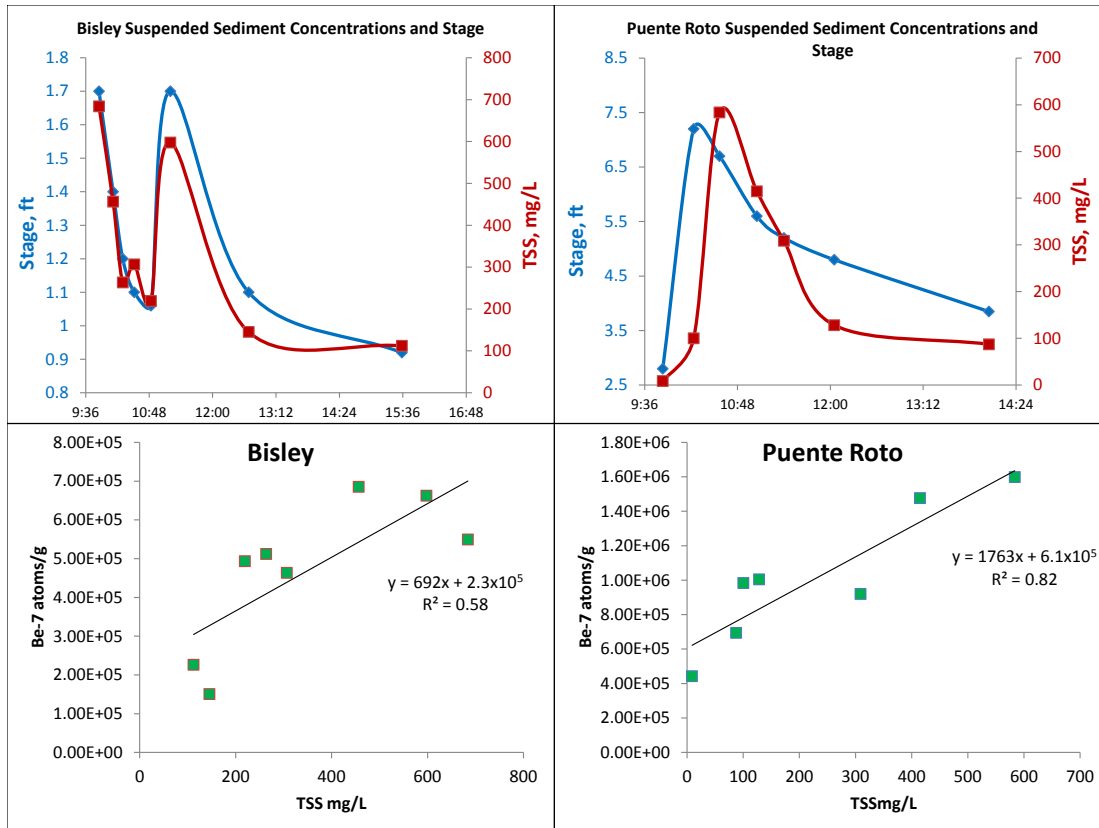


Figure 2: shows how stage correlates with total suspended solids (TSS) for both sampling sites. Also shown is the relationship between ⁷Be concentrations and TSS.

Last summer we collected multiple suspended sediment samples during a high flow event on June 7th, 2011 at three sites; Puente Roto (Mameyes watershed), Bisley I (upper Mameyes watershed), and Rio Icacos (Icacos watershed). This large-scale suspended sediment collection effort was aided by many participants actively conducting research in the Mameyes and Icacos watersheds. In an effort to determine sediment sources and constrains on the amount contributed by each source, we are currently considering a two end-member contribution to suspended sediment during high flow - stable sources, such as ridge top crests and unstable sources, such as landslide scars. Sediments from possible source regions (including ridge top crests and landslide scars) were also collected last summer to compare with the isotopic signals collected in high flow suspended sediment samples (figs. 1 and 2).

Future work will include synthesizing multiple data sets (water stable isotope measurements, Hg analysis, organic matter carbon isotopic composition, etc.) for the same storm event, collecting more high flow suspended sediment collections along with possible source characterization samples in both the Rio Mameyes and Rio Icacos watersheds.

The architecture of the weathering zone in the Rio Icacos watershed.

Joe Orlando (jjo167@psu.edu); Susan Brantley (sxb7@psu.edu) (both at Penn State); Heather Buss (h.buss@bristol.ac.uk; Univ of Bristol); Xavier Comas (xcomas@fau.edu, Florida Atlantic University); Fred Scatena (Univ of Penn)

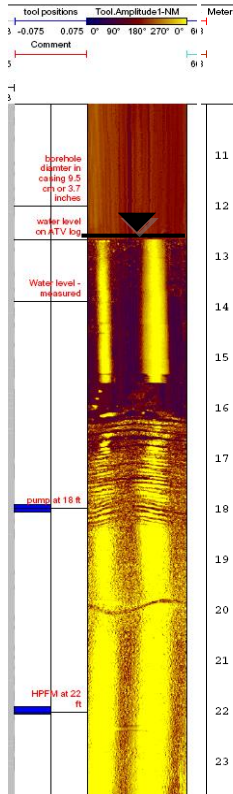


Figure 1: Televviewer image from the LGW1 borehole drilled on Rte 191 in the quartz diorite by H. Buss showing rindletting at about 5 meters below land surface (645 masl) and the deepest fracture at ~644 masl. Rindlets make up a zone that is ~0.5 m thick. The image also shows the water table above the rindlet zone. Baseflow in the Rio Icacos contains Na and Si from plagioclase weathering; however plagioclase is not found in saprolite, only in rindlets and bedrock. These observations were used to propose an architecture for a high-permeability zone in the subsurface (Fig. 2). Also, pyrite is observed in the core below 20 m depth (630 masl, not shown).

Key Science Questions Involved:

- What is the architecture of the weathering layer that overlies quartz diorite bedrock and hornfels within the upper Rio Icacos watershed?
- How does the rock and water chemistry vary with depth, and especially how do rindlets that form around corestones channelize water flow and control water chemistry?

The oxidation of biotite in corestones of Rio Blanco quartz diorite apparently drives formation of spheroidal fractures in the subsurface (Fig. 1). The spheroidal fracturing creates rindlets (cm-thick, onionskin-like layers) that wrap around corestones. In the saprolite above rindlets, we have observed that all the feldspar has weathered away: in fact, feldspar dissolves across the rindlet sets. Thus, the rindlets are the reaction front for feldspar. Since the river water contains solutes from feldspar weathering, it is thought that the zone of rindlets is a zone of fluid flow (*the corestone routing zone*, i.e. CRZ, Fig. 2).

Previous work on spheroidal weathering at the LCZO (TURNER et al., 2003; FLETCHER et al., 2006; BUSS et al., 2008; BUSS et al., 2010) was largely confined to corestone-rindlet complexes exposed at a road cut on Rte 191. To investigate the subsurface CRZ, Buss and coworkers drilled a borehole (LGW1) on Rte 191 into the quartz diorite (Fig. 1). The bottom of the corestone routing zone – the corestone baseline -- where corestones begin to “emerge” from less fractured/altered bedrock was encountered at 644 masl (see Fig. 1). In contrast, up-gradient from that borehole, Art White, Heather Buss, and other researchers observed the depth of refusal for augering at 671-675 masl. This elevation has been inferred to represent the upper envelope of the corestone routing zone at that location. We have projected those elevations to a cross-section across the Rio Icacos to conceptualize the CRZ (Fig 4). Also shown is the water table, assuming that it lies just above the corestone baseline (as observed in LGW1, Fig. 1).

For comparison to the West-East cross section, we also show a longitudinal profile for the Rio Icacos (Fig. 3). We are currently hypothesizing that the flat point in the river above 600 masl represents where the river has incised down to the corestone baseline. Consistent with this, corestones are observed in the bottom of the river at that point. According to this thinking, the knickpoint in the river corresponds to where the river is incising fractured bedrock rather than corestones + saprolite.

To further investigate the lateral extension of the CRZ within the subsurface we have performed some preliminary surveying to explore the ability of Ground Penetrating Radar, GPR, to image rindlet zones and the presence and extent of corestones. Figure 5 shows a GPR profile across the 3 to 4 m high outcrop characterized by Fletcher et al. (2006) and Buss et al. (2008). The outcrop contains large corestones (on the order of meters) and rindlet zones characterized by 5- to 10-cm thick fracturing. Vertical resolution of 9 cm was achieved with 200 MHz antennas: GPR allowed rindlet imaging as characterized by continuous reflections with high relative amplitudes. GPR profiling also showed promise in detecting the lateral extent of corestones as shown in the image by areas with amplitude attenuation and lack of reflections.

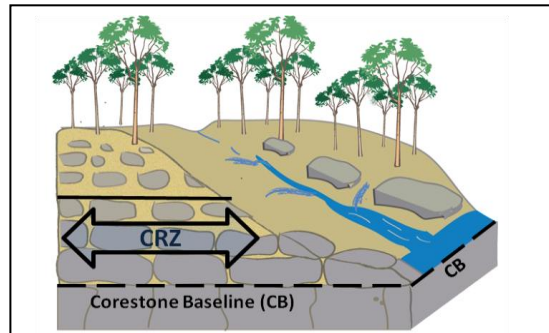
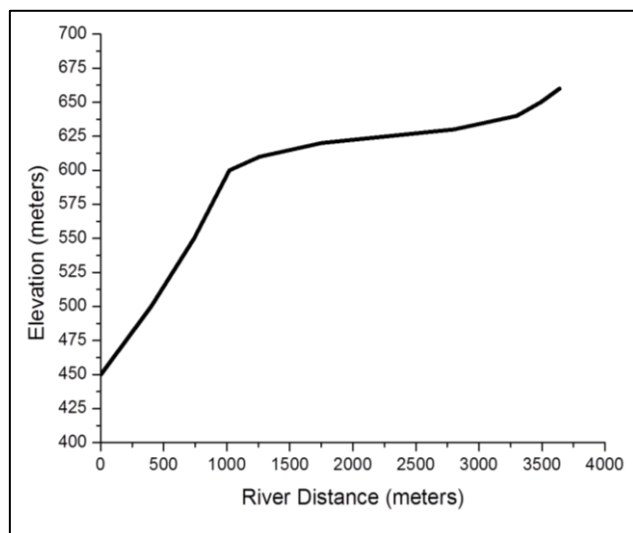
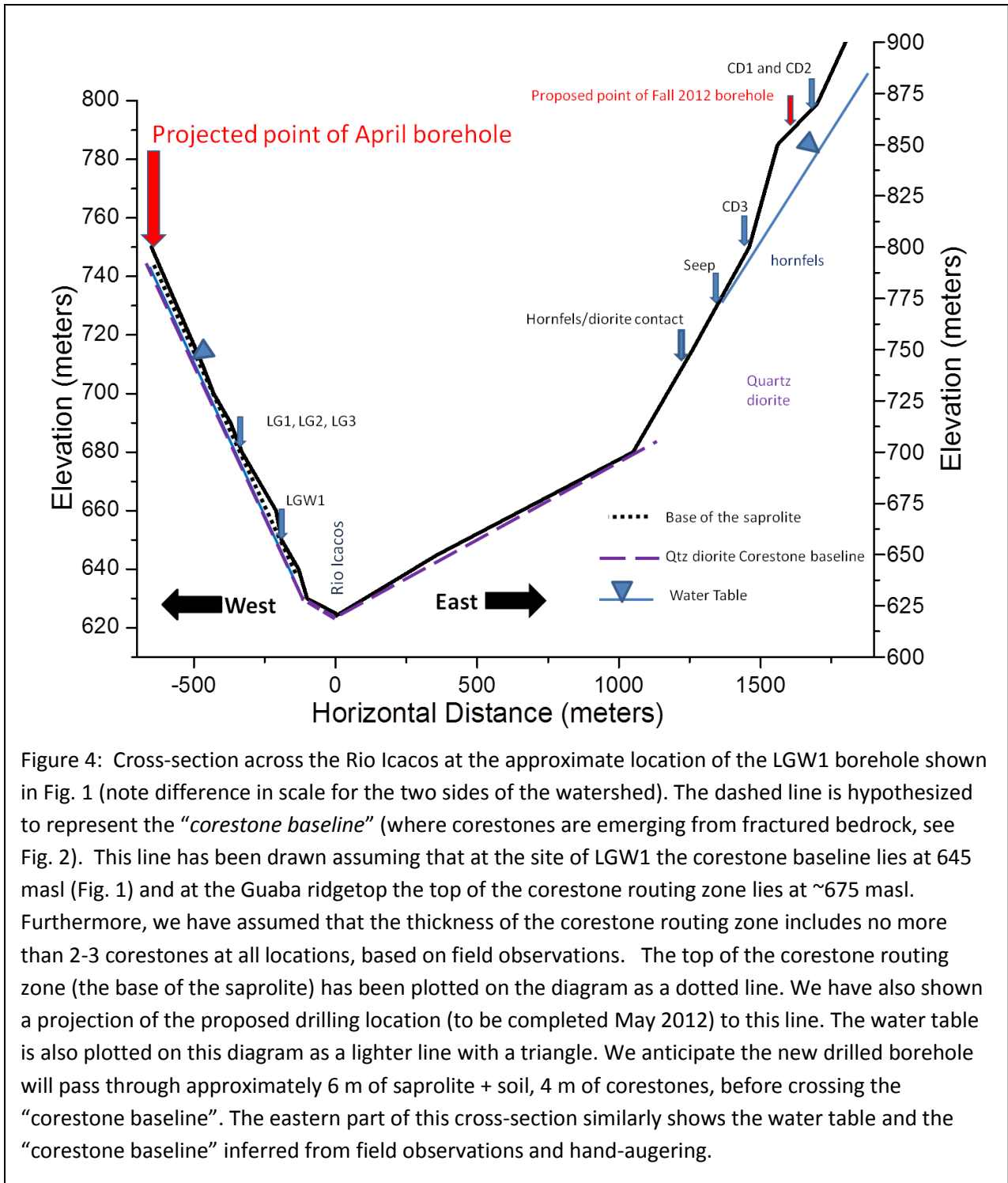


Figure 2: A conceptualization of the subsurface in the Rio Icacos watershed showing fractured bedrock topped by corestones and, at the top, saprolite/soil. We define the “corestone routing zone” as the high-permeability zone of corestones + regolith and the interface between the fractured bedrock and the corestones as the “corestone baseline”. Channel incision causes exposure of corestones that are forming in the subsurface. This regolith scenario could represent either a previously weathered zone that is now being incised, or a system that is both incising and weathering rapidly today such that today’s rate of corestone formation = the rate of incision.

Figure 3: A longitudinal profile for Rio Icacos starting on the left at 450 meters above sea level. We hypothesize that the knickpoint at about 600masl marks the point in the river that we are calling the corestone baseline.





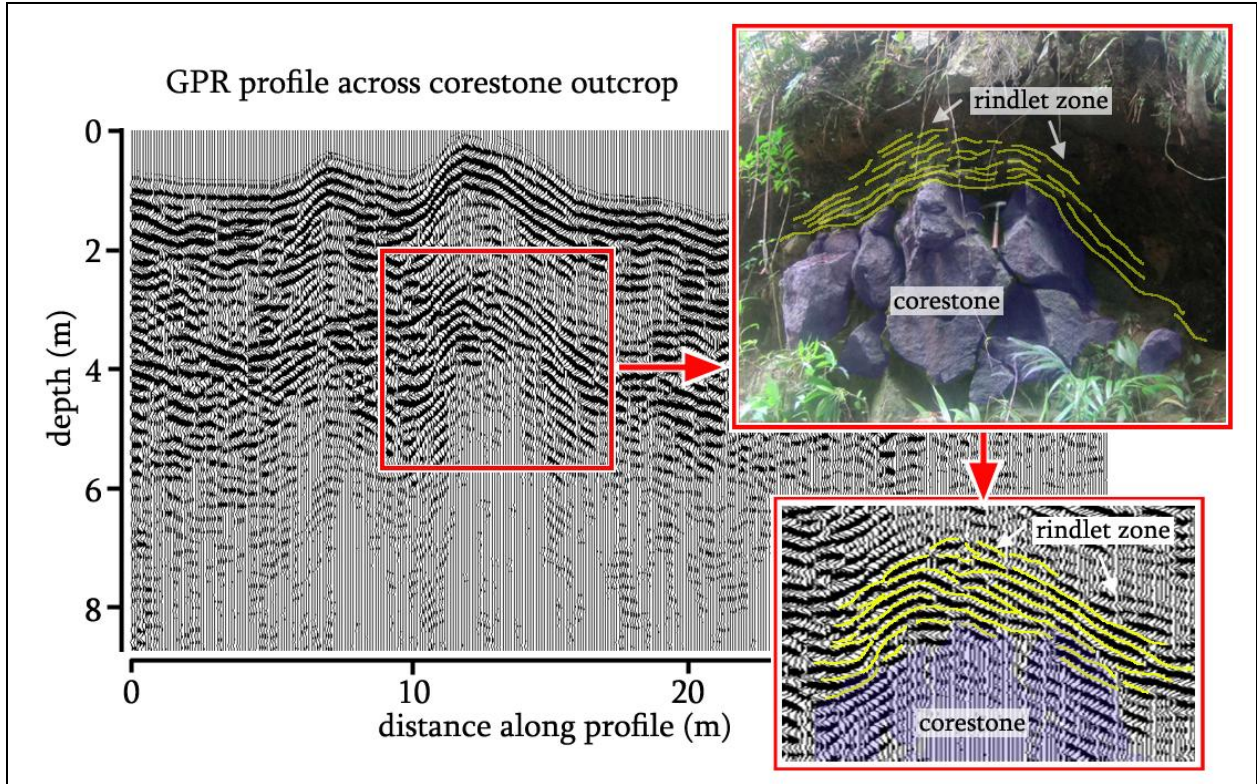


Figure 5: GPR profile using 200 MHz unshielded antennas across a 30 m outcrop with presence of corestones and rindlet zones. The reflection record shows rindlet zones as characterized by continuous reflections and corestones characterized by reflection attenuation.

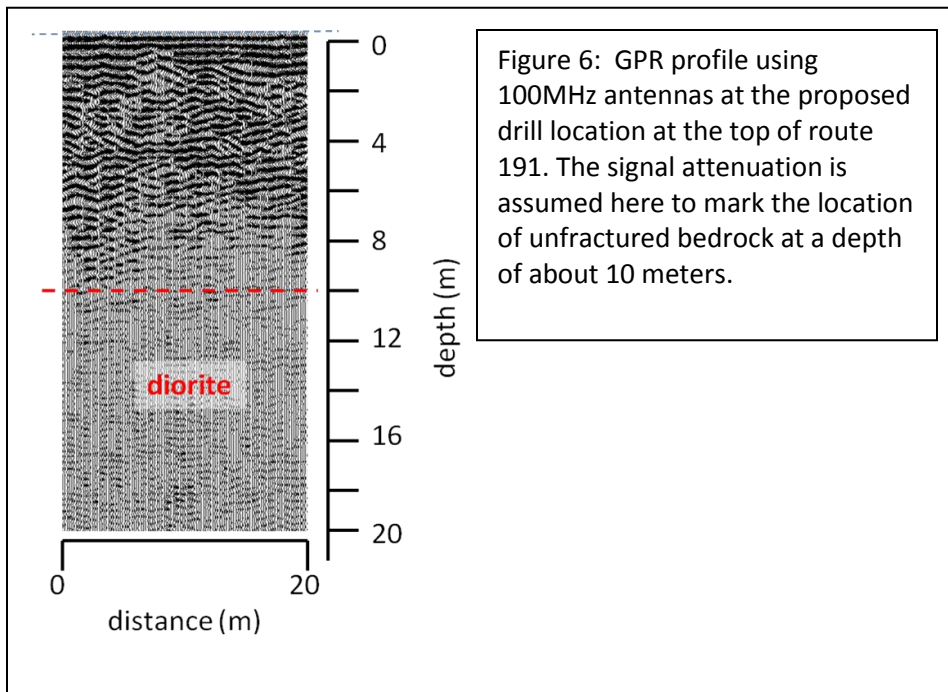


Figure 6: GPR profile using 100MHz antennas at the proposed drill location at the top of route 191. The signal attenuation is assumed here to mark the location of unfractured bedrock at a depth of about 10 meters.



- Buss, H. L., Mathur, R., White, A. F., and Brantley, S. L., 2010. Phosphorus and iron cycling in deep saprolite, Luquillo Mountains, Puerto Rico. *Chemical Geology* **269**, 52-61.
- Buss, H. L., Sak, P., Webb, R. M., and Brantley, S., 2008. Weathering of the Rio Blanco quartz diorite, Luquillo Mountains, Puerto Rico: Coupling oxidation, dissolution and fracturing. *Geochimica et Cosmochimica Acta* **72**, 4488-4507.
- Fletcher, R. C., Buss, H. L., and Brantley, S. L., 2006. A spheroidal weathering model coupling porewater chemistry to soil thicknesses during steady-state denudation. *Earth and Planetary Science Letters* **244**, 444-457.
- Turner, B. F., Stallard, R. F., and Brantley, S. L., 2003. Investigation of in situ weathering of quartz diorite bedrock in the Rio Icacos basin, Luquillo Experimental Forest, Puerto Rico. *Chemical Geology* **202**, 313-341.

Stream channel response to urbanization in the humid tropical region of NE Puerto Rico

Colin B. Phillips* and F. N. Scatena

Department of Earth and Environmental Science, University of Pennsylvania

[*colinp@sas.upenn.edu](mailto:colinp@sas.upenn.edu)

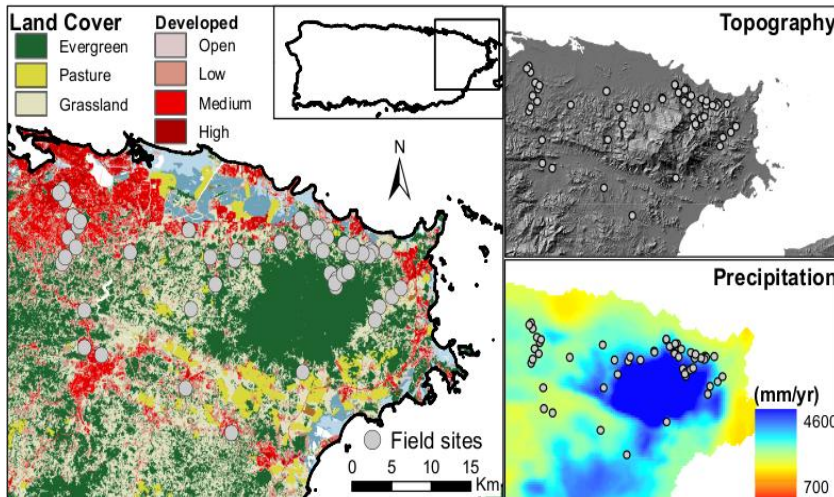


Figure 1. Land use, topography, 30 year normal precipitation, and field site locations for NE Puerto Rico.

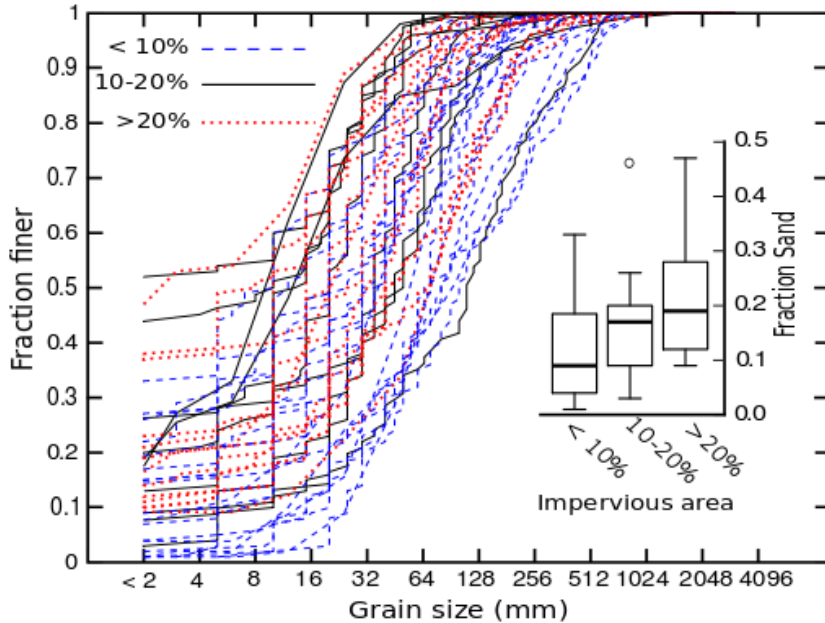


Figure 2. Cumulative grain size distributions for field sites. Blue dashed lines, black solid lines, and red dotted lines represent rural, mixed, and urban land uses based on impervious cover respectively. 2.Inset. Fraction of sand versus percent impervious cover in the drainage area. Urban land use streams are enriched in fine grained sediment compared to rural streams.

Key science question:

- How does stream channel morphology respond to the addition of impervious cover in a humid tropical region adjusted to frequent large storms?

Streams in the NE region of Puerto Rico are adjusted to frequent sediment mobilizing flows. The frequent high magnitude flows and steep coarse grained nature of these streams is one of the primary factors explaining their low levels alteration with drastic changes in land use. Field sites are located in a variety of land use ranging from high density urbanized areas in San Juan, to pristine evergreen forests in the Luquillo Mountains (Fig. 1). The regional climatic regime exerts a strong control on channel morphology. First order differences observed between field sites are explained by differences in precipitation and drainage area. Field sites were split into three classes of land use determined by the percent of impervious cover (<10%, 10-20%, >20%) within the field site's catchment. At the grain scale rural sites were found to have slightly coarser grain size distributions than comparable urban sites (Fig. 2). When grain size distributions are standardized by drainage area the differences between groups were not statistically significant at the 95% confidence level. Urban sites were found to be enriched in fine sediment (Fig. 2. Inset). Channel geometry metrics are commonly compared at a bank full flow. For mountain streams in the NE PR region a topographic expression of the bank full flow is often absent or obscured. Previous work in the Luquillo Mountains by Pike and Scatena (2010) established that the level that large woody vegetation occurs at on the channel bank is analogous to bank full flow. We further established two additional reference flow depths based on sediment transport

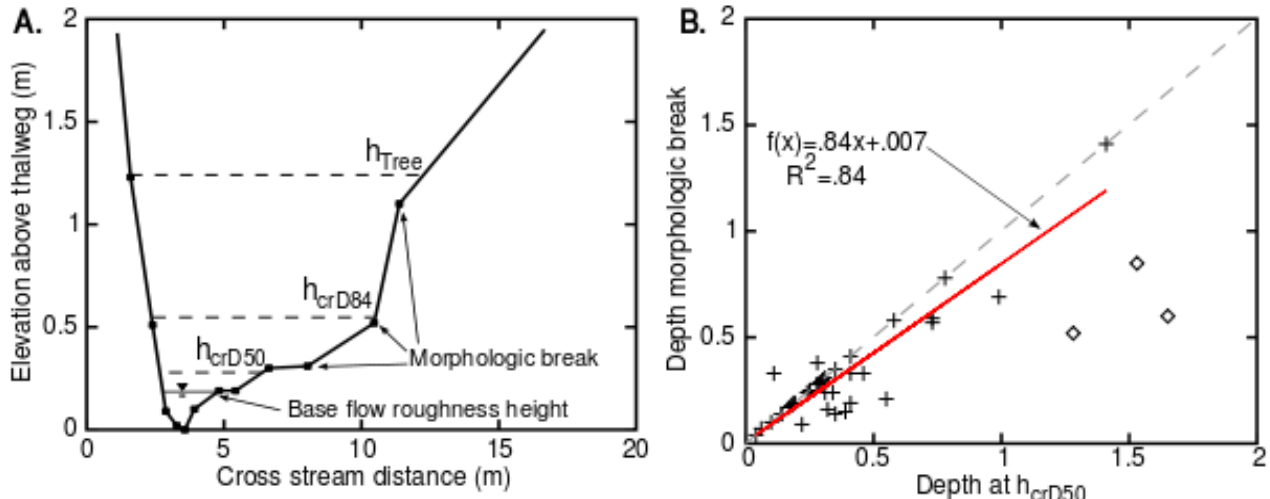


Figure 3. A. Survey cross section annotated with relevant reference levels which correspond to low, medium, and high flow depths, labeled h_{crD50} , h_{crD84} , and h_{Tree} respectively. B. Relationship between the depth at h_{crD50} and the depth at the first morphologic break in the channel. Diamonds represent outliers excluded from regression line. The dashed line represents the one to one line.

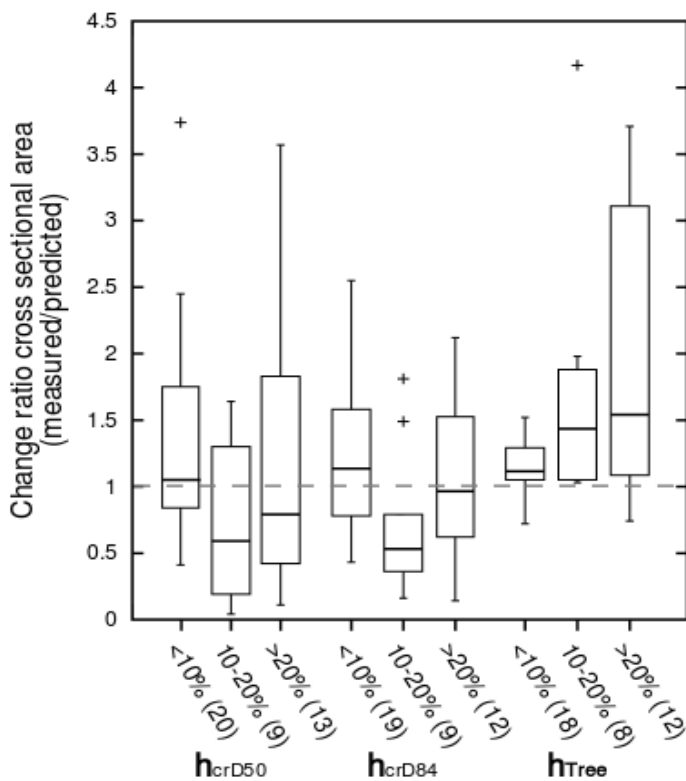


Figure 4. Change ratios for cross sectional area for all three reference levels within the channel cross section. The reference depths are split into three groups based on the percent of the drainage area covered in impervious cover (sample size).

The additional reference depths represent a low and medium depth to complement the high flow depth of the woody vegetation level (Fig. 3.A). Channels alteration occurs through the erosion and deposition of sediment. The low and medium flow depths correspond to the flow depth necessary to initiate motion of the median grain (h_{crD50}) size and the grain size for which 84% of the bed is finer (h_{crD84}). The h_{crD50} depth is further found to be closely related to the first morphologic break in the channel cross section (Fig.3.B), which was found to be coincident with riparian flow indicators established by Pike and Scatena (2010). We use these three flow levels to compare channel metrics across the three classes of impervious area. Change ratios (Fig. 4) represent the measured channel cross sectional area divided by the predicted cross sectional area. The predicted channel cross area is determined from relations for comparable rural streams accounting for both drainage area and precipitation. Differences between the three groups within each reference level are not statistically significant. Overall urban streams have a greater degree of variability in cross sectional area at the highest reference flow when compared to similar rural catchments. The high variability is a result of channelization in the high impervious class.

Coarse sediment tracers and flood scale bed load transport

Colin B. Phillips* and Douglas J. Jerolmack
 Department of Earth and Environmental Science, University of Pennsylvania
[*colinp@sas.upenn.edu](mailto:colinp@sas.upenn.edu)

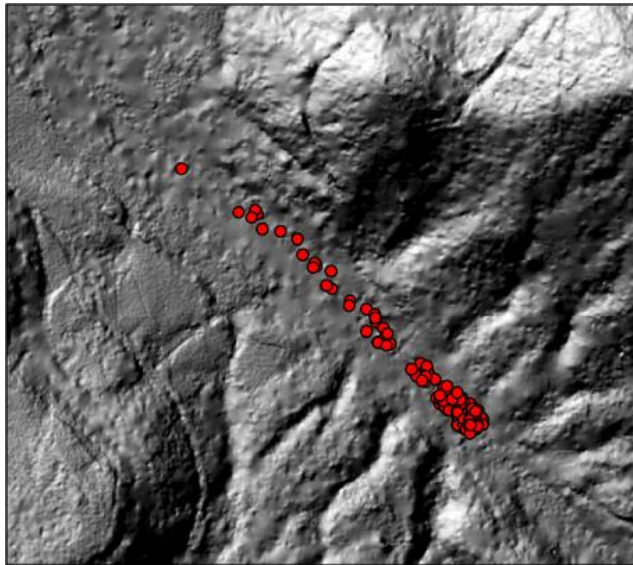


Figure 1. LiDAR of lower Rio Mameyes River with RFID tagged tracer particles (overlaid circles). The plume of tracers is 300 meters long.

Key science questions:

- How do the transport lengths of mobile sediment tracers depend on flood duration and magnitude?
- Can sediment tracer transport lengths at the individual flood scale predict annual tracer travel distances and bed load flux?

Coarse sediment particles were equipped with Radio Frequency Identification tags (RFID); their position is subsequently tracked after individual floods and on an annual basis. Tracers particles were installed in the Rio Mameyes River (300 tracers), and two smaller tributaries (25, 50 tracers). Tracers in the main channel of the Rio Mameyes River have experienced the highest mobility (Fig. 1) with the farthest transport distance recorded at 300 meters. From repeat tracking of tracers at the individual flood scale we determine the mobile/immobile particles, and transport distances. The critical shear stress for initiation of motion for our tracers can further be determined based on the fraction of mobile and immobile tracers (Fig. 2) for a given flood.

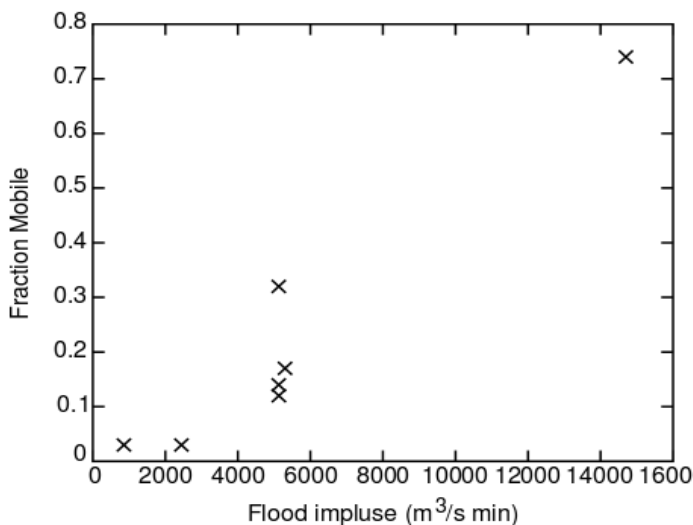


Figure 2. Fraction of mobile tracers for each resurvey with integrated flood discharge.

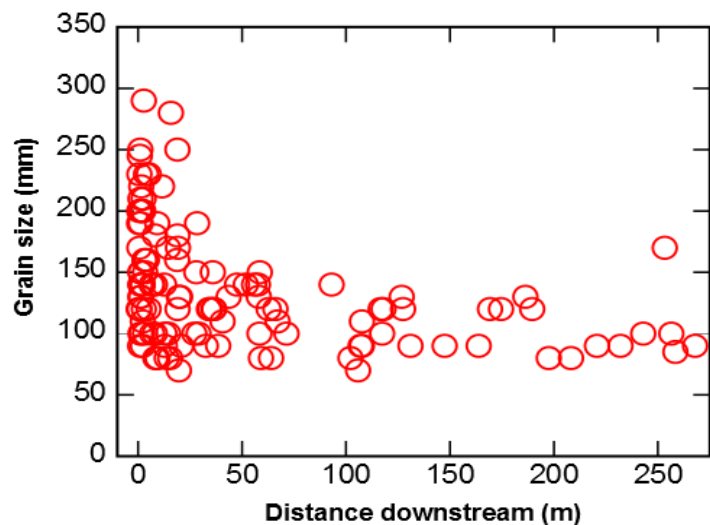


Figure 3. Tracer particle total travel distance and grain size after one year.

At the individual flood scale transport distances are weakly affected by grain size, while at the annual scale the smallest particles travel the furthest (Fig. 3). Transport distances are analyzed against the flood impulse as a way to determine the dependence of transport lengths on flood magnitude and duration. Bed load transport rates at the flood scale are determined by the fraction of mobile tracers, the characteristic transport distance, and the stream bed area.



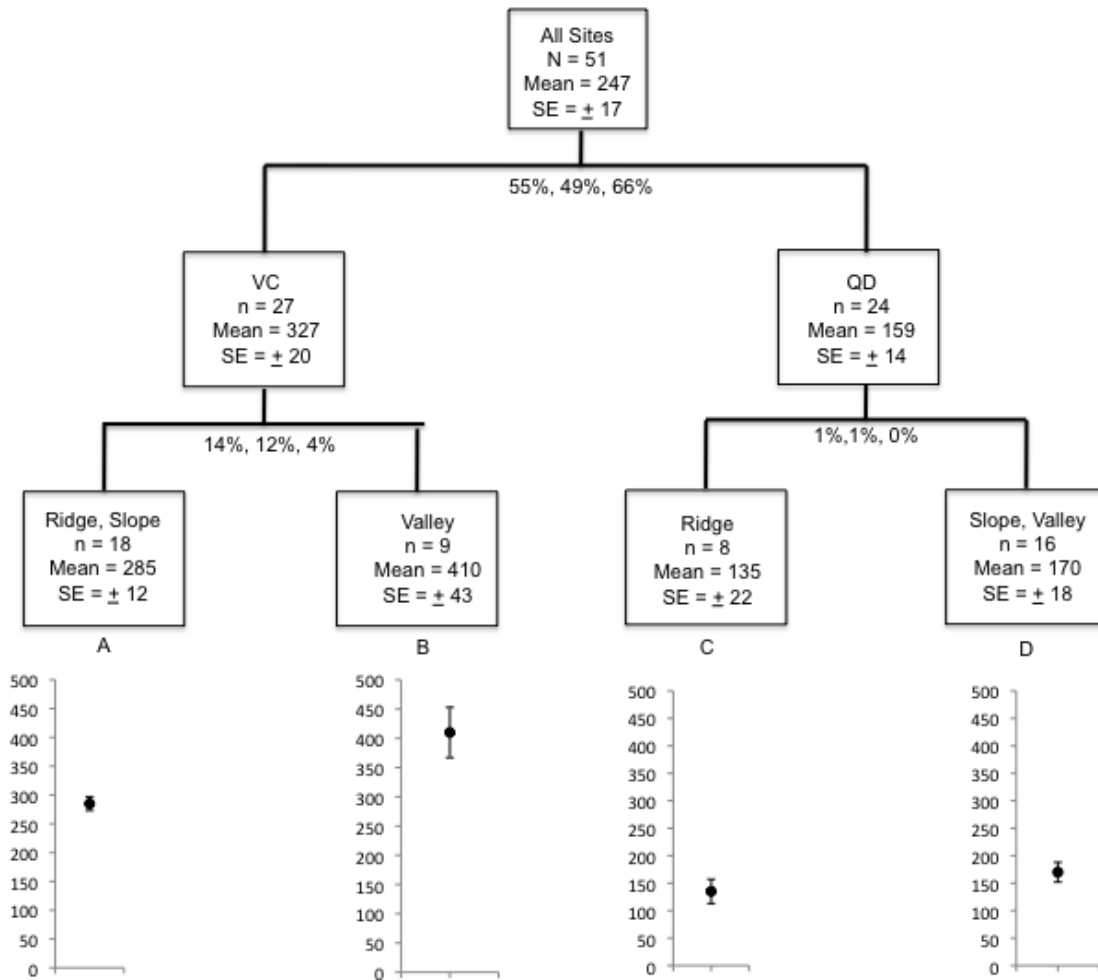
Parent material and topography drive soil P status across the Luquillo Mountains.

Stephen Porder PI (stephen_porder@brown.edu), Susanna Mage (susanna_mage@brown.edu).

Key Science Questions Involved: What factors are most important in driving soil phosphorus status across this tropical montane landscape?

Soil phosphorus (P) availability is assumed to influence primary production and decomposition in many tropical forests, yet the underlying controls of soil P status in these biogeochemically diverse ecosystems are still poorly understood. We explored the influence of three state factors (parent material, topographic position, forest type) on total soil P concentrations, P forms, and the loss of P relative to bedrock in the Luquillo Mountains of Puerto Rico. We sampled soils (0-80cm) from at least four replicate catenas across a full factorial combination of two parent materials (quartz diorite and volcanoclastic), three topographic positions (ridge, slope, valley), and two forest types (Tabonuco and Colorado, which occur across an elevation gradient). Volcanoclastic parent material had significantly higher P (~600 ppm) than did quartz diorite parent material (~300 ppm; $P < 0.001$). Similarly, total soil P concentration was 2x higher in volcanoclastic than quartz diorite-derived soils ($P < 0.001$). Within a rock type, valleys had up to 40% higher total P concentrations than slopes/ridges ($P < 0.001$). Volcanoclastic-derived soils also had slightly higher NaHCO_3 and NaOH-extractable P, but this difference was small relative to the 2.5x higher concentrations in valleys versus ridges. The fraction of recalcitrant P (P not removed by NaHCO_3 , NaOH, or HCl) was 2x higher in the clay-rich volcanoclastic-derived soils ($P < 0.01$) and this fraction did not change significantly downslope ($P > 0.05$). Finally, the loss of P relative to parent material, as measured by indexing to an immobile element (niobium), was higher in volcanoclastic than quartz diorite-derived soils ($P < 0.001$). Forest type had no significant effect on the concentration of P in any form. These data indicate that parent material can influence the P status of soils both directly through concentration and indirectly by driving the soil characteristics (e.g. mineralogy, iron content) that shape the trajectory of the P cycle during soil development.

Figure 1: Multiple regression tree for total soil P in the Luquillo Mountains. VC = volcaniclastic and QD = quartz diorite parent material. Percentages at each split show the variance explained for 0-20, 0-50 and 0-80cm depth intervals respectively. Note that parent material explains >49% of the variance in total soil P, with topography of secondary importance. This pattern is reversed for the more readily available P accessed by extraction with NaHCO₃, which is more influenced by topographic position than rock type.



Additional funding sources: The Andrew Mellon Foundation and NSF DEB 0918387 to S.P.

Isotope Hydrology Research in the Luquillo Critical Zone Observatory

Martha Scholl, U.S. Geological Survey, National Research Program, Eastern Branch, Reston, VA. mascholl@usgs.gov. Collaborators: F.N. Scatena, W.H. McDowell, J. Shanley, S. Murphy, H. Buss, T. Coplen, T. Heartsill-Scalley, C. Estrada, M. Rosario, A. Torres, S. Torres, M. Occhi, H. Qi, J. Lorenz, B. Buck.

Key Science Questions Involved: How can we utilize stable isotopes of water as tracers of precipitation from different climate patterns through the hydrological cycle? If the climate pattern in the Caribbean changes to dry periods punctuated by intense storms, how will the water supply be affected? We can use the strong isotopic signature generated in low pressure systems to partition the water from these storms into runoff and infiltration, to better understand the storage dynamics of the watersheds. Puerto Rico has also been an ideal site to develop the correlation between precipitation and atmospheric temperature, by using radar echo top altitudes to determine where rain originates in the atmosphere.

In 2005, regular sampling of cloud water, rainfall, and streamflow for stable isotope analysis began in the Rio Mameyes and the Rio Icacos--Rio Blanco watersheds; soil water, groundwater and throughfall have also been measured. Temporal records of isotopic composition in rain show a 'reverse seasonality' compared to higher latitudes, with higher isotopic values in the winter and lower values in the summer. Rain isotopic values correlate strongly with local and mesoscale weather patterns and with cloud altitude (and therefore atmospheric temperature). This correlation allows us to assign isotopic signatures to different sources of recharge, and to investigate which climate patterns contribute to streamflow and groundwater recharge.

Precipitation has a wide range of stable isotope values, from fog/cloud water with $\delta^2\text{H}$, $\delta^{18}\text{O}$ averaging +3 ‰, -1.7 ‰ to tropical storms with rain values as low as -155 ‰, -20.4 ‰.

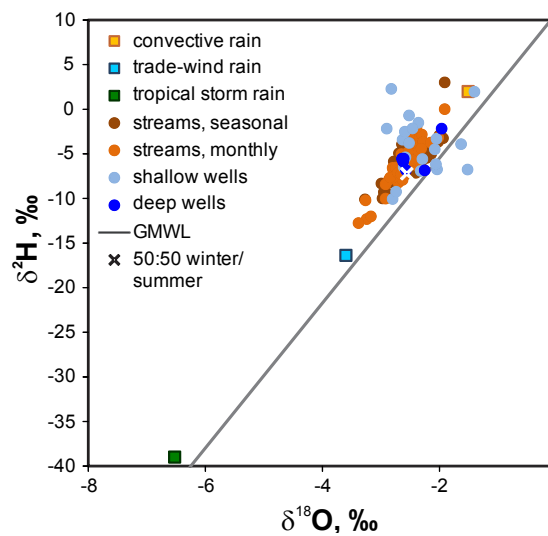


Fig. 1. Stream and groundwater isotopic composition shows higher contribution of trade-wind orographic rain, though convective rain makes up a larger proportion of total rainfall.

Rainfall in the Luquillo mountains is frequent and streams are flashy, indicating little short-term storage capacity in the watersheds. Contributing factors may be thin or low-permeability soils and consistently high saturation levels. Long-term average streamflow isotopic composition indicates a disproportionately large contribution of trade-wind orographic precipitation to streamflow and groundwater, highlighting the importance of this climate pattern to the hydrology of the watersheds. The climate pattern in the Caribbean is projected by ensemble GCM results to change to dry periods punctuated by intense storms. Determining how the water supply of Puerto Rico and other locations in the region may be affected will be relevant to management of water resources in the future.

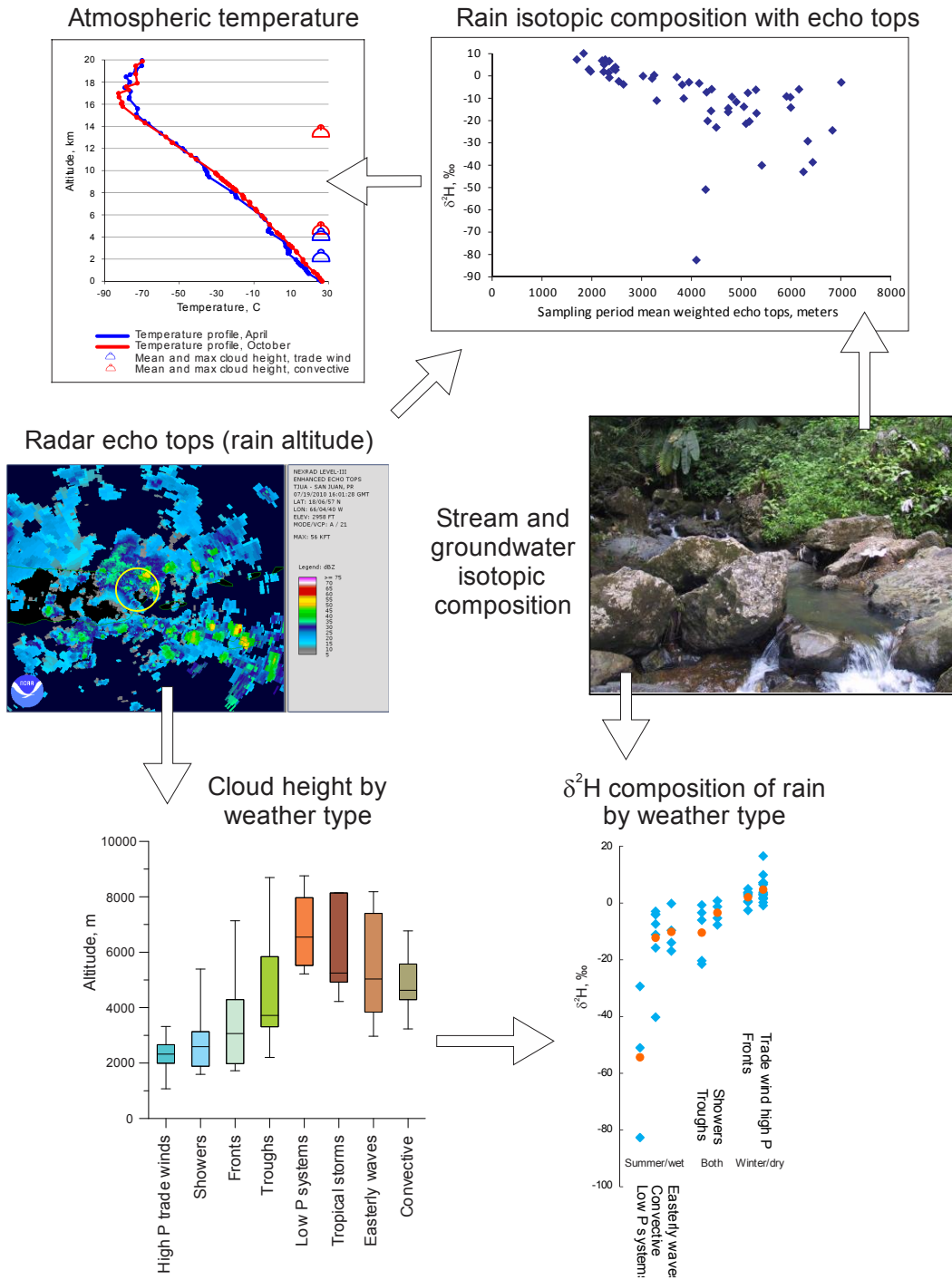


Fig. 2. Using echo top measurements, we can link precipitation stable isotopes to atmospheric temperatures and weather patterns. This provides a direct link between groundwater recharge, streamflow and climate patterns. The data can be used to determine effects of projected climate change on water supply, and the isotope-temperature link can contribute to paleoclimate studies.

Reference: Scholl, M.A., Shanley, J.B., Zagarra, J.P., and Coplen, T.B., 2009, The stable isotope amount effect: New insights from NEXRAD echo tops, Luquillo Mountains, Puerto Rico, *Water Resources Research*, 45, W12407, doi:10.1029/2008WR007515.

Additional funding sources: U.S. Geological Survey Climate and Land Use Change Program

Mercury research at Luquillo Critical Zone study

Shanley J.B. - USGS

Synopsis

Mercury (Hg) loading in precipitation is surprisingly high at the Luquillo CZ site. Its setting in northeastern Puerto Rico is influenced primarily by “clean” easterly to northeasterly Trade Winds, and is far downwind from point sources of Hg emissions. The high Hg in deposition is reflected in high stream Hg transport, but Hg in biota is relatively low.

Hg in Deposition

The U.S. Geological Survey established a Hg deposition station in the Luquillo Experimental Forest (LEF) in April 2005. Weekly wet-only deposition samples are collected following the protocols of the Mercury Deposition Network (MDN). Hg loading in wet deposition during the first two years was the highest in

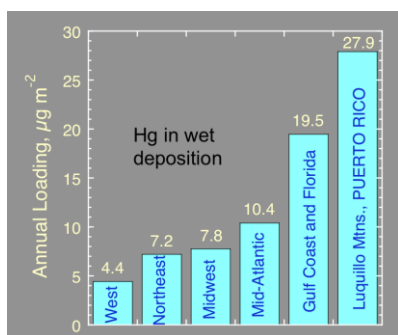


Figure 1. Hg in wet deposition in USA regions.

the USA (Figure 1). This result was unexpected, given the lack of proximal upwind Hg emission sources. The leading explanation for the high Hg deposition is that the high cloud tops during tropical storms (Scholl et al., 2009) scavenge Hg from the pool of reactive gaseous mercury (RGM) known to exist in the upper free troposphere (Shanley et al., in review). Mercury has about a one-year residence time in the atmosphere and this RGM is formed from the global Hg pool. The high Hg deposition at this site removed from point sources underscores the global reach of Hg contamination.

Hg in Streams

The high Hg in deposition was matched by one of the world’s highest documented stream Hg loadings in the Río Icacos (Shanley et al., 2008). The high riverine Hg flux is driven by both high runoff and high Hg concentrations. Stream Hg flux is strongly dominated by particle-associated Hg during high-flow events (Figure 2). The stream Hg study was limited to Río Icacos, set on granodiorite on the southern side of LEF. However, preliminary results suggest similar high-flow Hg concentrations and patterns with flow at Río Mameyes in volcaniclastic rocks on the northern side of LEF (Shanley, Willenbring, and Occhi, unpublished data). If further sampling confirms similar dynamics in the two basins, this would support atmospheric deposition source rather than a geologic source of the Hg in streamwater.

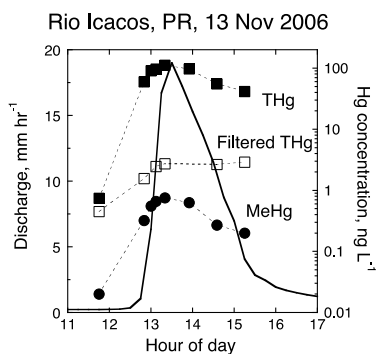


Figure 2. Total Hg (unfiltered), Filtered Hg, and Methyl Hg during a large storm. Note log scale.

CZ research will more fully document the dynamics of stream Hg not only through extending sampling in the Mameyes basin, but also through its support of real-time sensors in the Icacos basin. Sensors are measuring turbidity, a proxy for particle Hg, and fluorescing dissolved organic matter (FDOM), a proxy for dissolved Hg. In addition, CZ researchers are focusing on the mechanisms of Hg movement from watershed to stream. A fundamental question is the residence time of Hg in the watershed: is Hg in streamwater newly deposited Hg entering the system in the current or recent events, or is it Hg that has cycled through vegetation and biota possibly for years or decades? If the former, CZ response to changes in deposition and other factors such as climate will be rapid; if the latter, response will be lagged.

CZ researchers are assessing Hg residence time using beryllium (Be) isotopes. ⁷Be enters the watershed in precipitation and has a half-life of 53 days. Like Hg, Be has a strong affinity for organic matter. Assuming its mobility is similar to that of Hg, it is a good indicator of “young” mercury. By measuring ⁷Be in precipitation and streamwater, researchers can ascertain the relative age of Hg in the stream.

Hg in the Food Web

Hg is a potent neurotoxin. One of the main pathways of Hg assimilation by humans is through fish consumption, as some fish species are top predators in a large food web that bioaccumulates mercury at each step. For mercury to bioaccumulate, it must first be converted to the organic or methylmercury form. Methylation is a microbially-mediated process that occurs in sub-oxic or anoxic conditions in the presence of ample Hg, sulfur, and organic carbon. Despite the abundance of Hg on the LEF landscape, Hg content of the biota is relatively low, presumably because the Hg methylation efficiency is low. Shanley et al. (2008) found that only 0.5% of the Hg in streamwater was methylated, compared to typical values near 2%. USGS and CZ researchers are currently quantifying methylation rates to test the hypothesis that low methylation rates are limiting uptake of Hg in the LEF food web.

Citations

Shanley, J.B., M.A. Engle, D.P. Krabbenhoft, R. Brunette, M.A. Scholl, M.L. Olson, J.W. Troester. In review. High mercury deposition in the Luquillo Mountains, Puerto Rico. Intended for ES&T

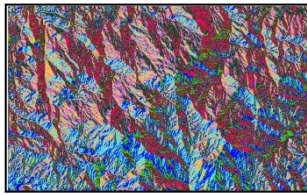
Scholl, M. A., J. B. Shanley, J. P. Zegarra, and T. B. Coplen. 2009. The stable isotope amount effect: New insights from NEXRAD echo tops, Luquillo Mountains, Puerto Rico, *Water Resour. Res.*, 45, W12407, doi:10.1029/2008WR007515.

Shanley, J.B., M.A. Mast, D.H. Campbell, G.R. Aiken, D.P. Krabbenhoft, R.J. Hunt, J.F. Walker, P.F. Schuster, A. Chalmers, B.T. Aulenbach, N.E. Peters, M. Marvin-DiPasquale, D.W. Clow, and M.M. Shafer, 2008. Comparison of total mercury and methylmercury cycling at five sites using the small watershed approach. *Environmental Pollution* 154, 143-154.

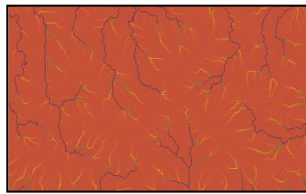
Influences of bedrock lithology and vegetation on flow hydrology in the Luquillo Mountains.

Lauren Stachowiak, Dr. Frederick Scatena, Dr. Edward Doheny, Dr. Dana Tomlin
 Key Science Questions: Relationships between lithology and drainage patterns

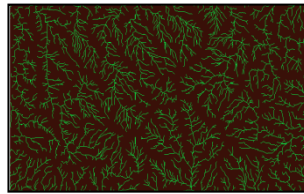
Drainage networks of streams in tropical ecosystems are the result of an advanced inter-connected system of relationships, including both abiotic and biotic influences. It was the goal of this study to analyze the extent to which bedrock lithology and vegetation control stream bifurcation and networking in a tropical montane ecosystem. More specifically, a GIS was created to model drainage densities of low-order streams within the study area to extract precise differences among different rock and forest types.



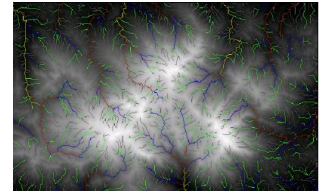
Flow Direction



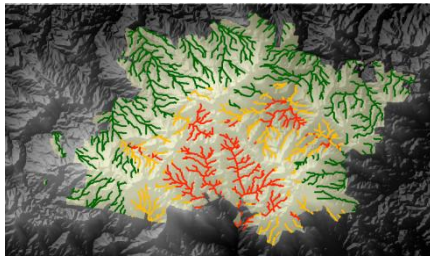
Flow Accumulation



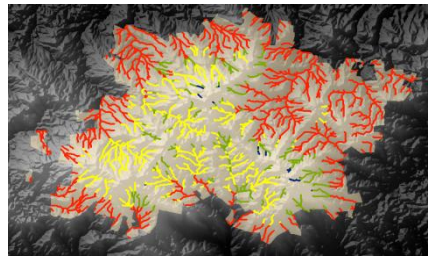
Critical Area Threshold



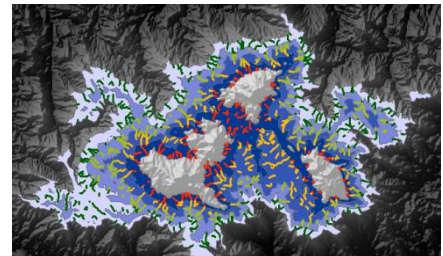
Stream Order



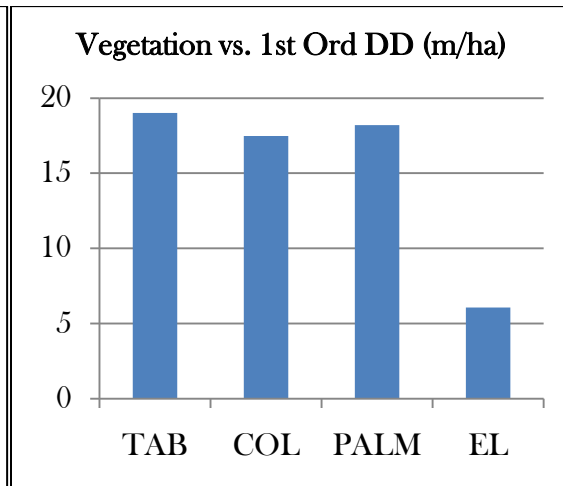
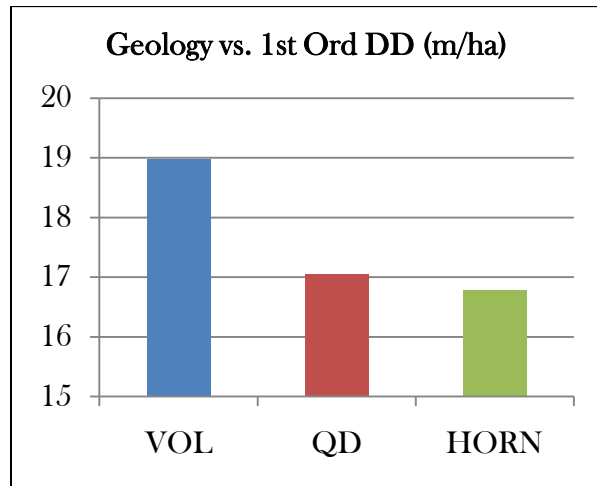
Streams by Geology

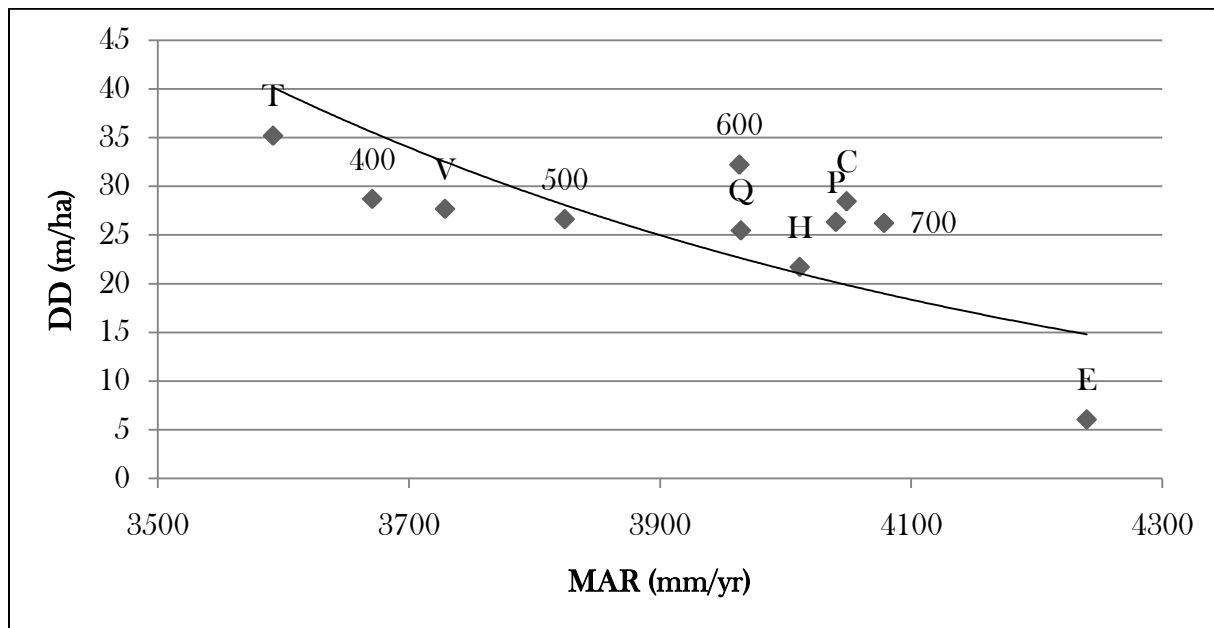
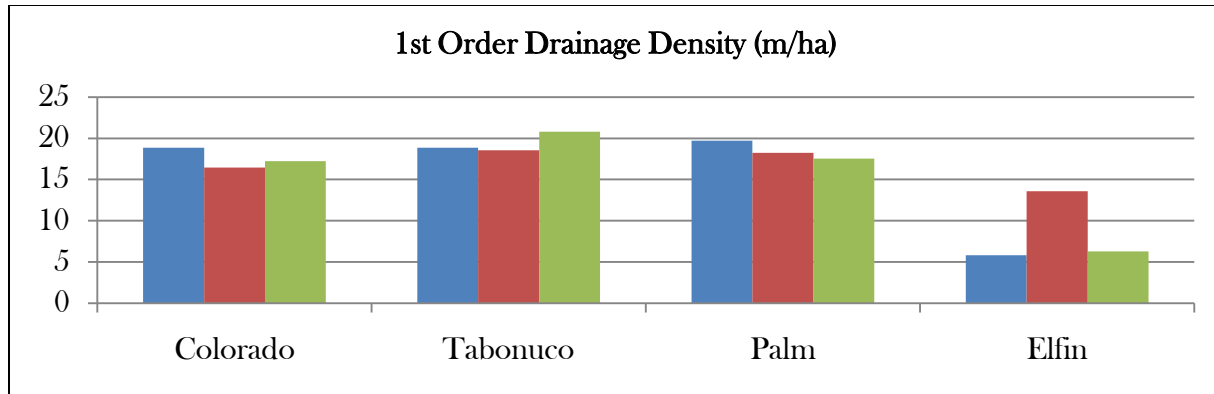


Streams by Vegetation



Streams by Elevation





- Volcanoclastic bedrock weathers into a clay-rich soil, thereby impeding water infiltration rates promoting overland flow. Such flow characteristics favor greater stream densities than quartz diorite which weathers into sandy soil and the weather resistant contact metamorphic hornfels. This is supported by the data.
- Elfin forests have low DD due to low overall distribution. Tabonuco and Colorado forests favor spatial areas similar to volcanoclastics and have high DD. Palm forests are found nestled in stream valleys and have high total stream length values creating high DD values.
- Elevation can be used as a proxy for mean annual rainfall and micro-climates. As can be seen in the data, no strong significant relationship between MAR and DD exists.



Soil organic matter quantity, quality and microbial activity in deep soil profiles

Madeleine Stone (madstone@sas.upenn.edu; PhD)

Lydia Ali (prali@sas.upenn.edu; undergraduate)

Alain Plante (aplante@sas.upenn.edu, co-PI)

Key Science Questions Involved:

- 1) How does the quantity and quality of soil organic matter change as a function of soil profile depth:
 - in old, highly weathered oxisol profiles versus younger, granitic inceptisol profiles?
 - in three different forest types: Tabunuco, Colorado and sierra palm?
- 2) How do soil microbial community structure and functional characteristics change with depth across contrasting parent materials and forest types?
- 3) Can we relate microbial community characteristics to SOM quantity and quality?

Background

The “critical zone” is defined as the region of the Earth where rock meets life. Soils, consisting of a heterogeneous mixture of dead organic matter, live microbial decomposers and inorganic rock-derived minerals, represent a part of the critical zone where rock and life directly interact. From the forest floor down, a soil profile represents a continuum of actively cycling energy in the form of organic carbon (C) and nutrients that supports the most diverse communities of microorganisms on earth. Despite the importance of deep (1-2 m) SOM as a long-term sink of C from the biosphere, most studies that aim to characterize SOM focus on the upper 20-30 cm (Jobbagy & Jackson 2000). In addition, little is known about how microbial communities change with depth (Fierer *et al.* 2003), and few studies attempt to explicitly link SOM properties with microbial community characteristics.

This study aims to describe how SOM and microbial community characteristics are related and how they change with depth in across the two parent materials and three forest types that comprise the Luquillo CZO. Due to rapid decomposition of surface litter in these tropical soils, we expect the chemical composition of SOM to be relatively decoupled from overlying vegetation and that SOM residence time will increase with depth. We expect deep soil microbial communities to be less diverse than surface communities, possibly exhibiting greater substrate specialization and different metabolic strategies.

Experimental Approach

We collected soil at six sites at similar elevations that represent two parent materials (sedimentary volcaniclastic and igneous quartz-diorite) and three forest types (Tabunuco, Colorado and sierra Palm) that characterize the Luquillo CZO. Five soil profiles were dug along catenas such that for each site, one ridge, one valley and three slope profiles were dug. Approximately 70% of Luquillo soils exist on sloping terrain (Scatena & Lugo 1995) and we therefore biased our sampling design to incorporate more slope

profiles than ridges or valleys. Each soil profile was dug down to 140 cm (or bedrock) and sampled aseptically at 10 cm intervals. Aliquots of each sample were frozen for microbial analysis. The rest of the soil was air dried and sieved to 2mm.

A suite of biological, chemical and physical techniques will be used to compare and contrast SOM composition and stability with depth across the different parent materials and forest types. Microbial communities will be examined using fingerprinting approaches, including DGGE and qPCR, to broadly assess community richness and evenness, and GeoChip microarray analysis to measure the presence and metabolic activity of ecologically functional organisms. A suite of hydrolytic and oxidative C-acquiring enzymes, as well as several nitrogen and phosphorus acquiring enzymes will also be measured in order to link community structure to carbon and nutrient cycling.

Preliminary Results

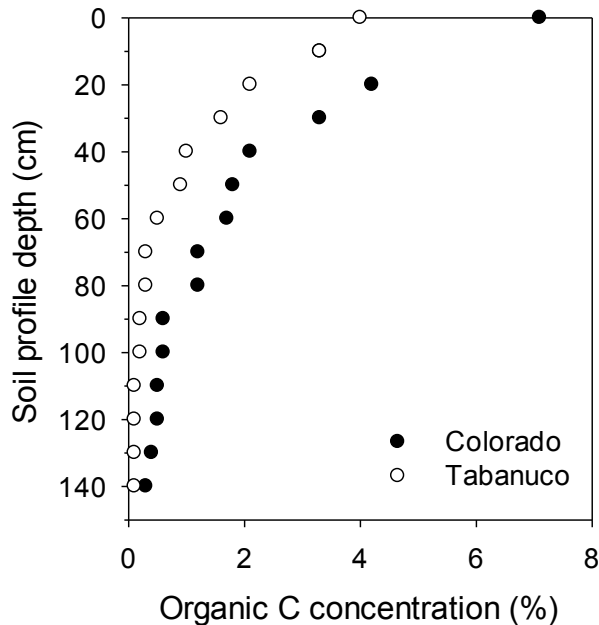


Figure 1: Soil organic carbon concentration as a function of depth in a single replicate soil profile from Oxisol soils under Colorado and Tabanuco forests.

Additional funding sources: National Science Foundation Graduate Research Fellowship to M. Stone.

References

Fierer N., J.P. Schimel, and P.A. Holden 2003. Variations in microbial communities through two soil depth profiles. *Soil Biology Biochemistry*, **35**, 167-176.

Jobbagy, E. G., and R. B. Jackson. 2000. The vertical distribution of soil organic carbon and its relation to climate and vegetation. *Ecological Applications*, **10**, 423-436.

Scatena F.N, and Lugo A.E. 1995. Geomorphology, disturbance, and the soil and vegetation of two subtropical wet steepland watersheds of Puerto Rico. *Geomorphology*, **13**, 199-213.



Redox cycling and Fe atom exchange in the Bisley Watershed

PIs: Aaron Thompson¹, Christof Meile² and Michelle Scherer³ **Post Docs:** Brian Ginn¹ and Viktor Tishchenko¹

Grads: Tim Pasakarnis³ and Jared Wilmoth¹

¹University of Georgia (Crop and Soil Sci.); ²University of Georgia (Marine Sci.); ³University of Iowa (Civil and Environ. Engineering)

Our overall goal is to delineate the functional roles of iron (Fe) in soils characterized by variable redox conditions. We focus first on the dynamics of microbially-labile Fe and second on the coupled roles of phosphorus (P) and carbon (C).

Research Questions

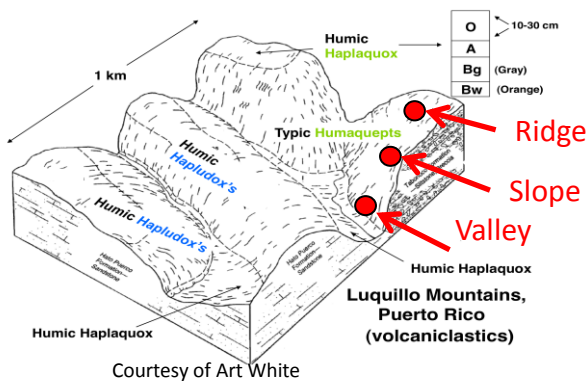
- (1) What governs the amount of reactive soil Fe?
- (2) How do dynamic redox conditions impact Fe, C and P cycling?
- (3) Can the elemental response *across a range of redox oscillations* be captured in a model?

Objectives

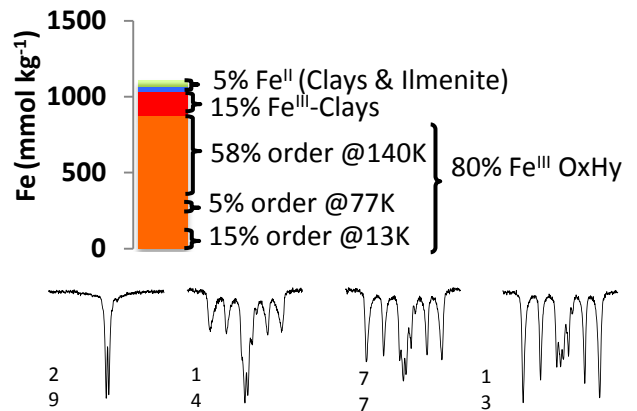
To examine the behavior of Fe in redox-dynamic soil from the Bisley watershed, we:

- (1) Characterize the reactivity of solid-phase Fe using microbial, chemical, spectroscopic, and isotopic tools.
- (2) Track soil Fe (along with P and C) behavior across a range of variable redox oscillation parameters imposed in the lab.
- (3) Construct a process-based numerical model of Fe behavior.

Bisley Watershed sampling sites



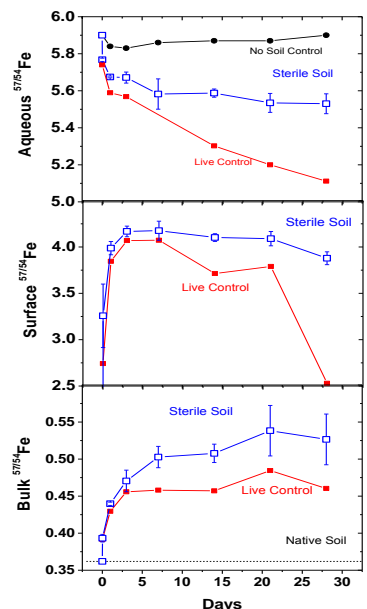
Solid-phase Fe reactivity (valley location)



The maximum microbially-reducible Fe (~180 mmol kg⁻¹) and citrate-ascorbate extractable Fe coincides with the amount of nano Fe (oxyhydr)oxide requiring a temperature between 13K and 77K to magnetically order in a Mössbauer experiment.

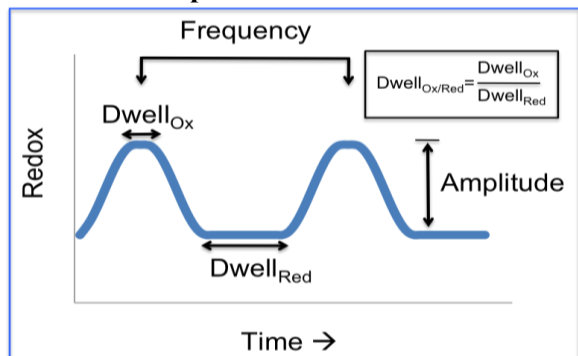
Fe atom exchange

Atom exchange was studied by following the fate of ⁵⁷Fe added as Fe²⁺(aq) to soil slurries. In the sterile (Hg₂Cl) treatments, Fe²⁺(aq) was constant following an initial sorption event, while the live control exhibited an Fe²⁺ increase. A decrease in aqueous ^{57/54}Fe ratios and an increase in ^{57/54}Fe ratios of the solid-phase pools was also observed. The presence of Fe reducers in the live control decreased the rate of atom exchange in the bulk Fe pool.



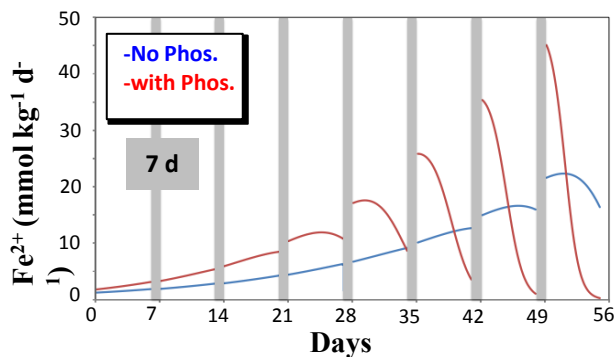
Laboratory Redox Oscillations

Imposed redox conditions



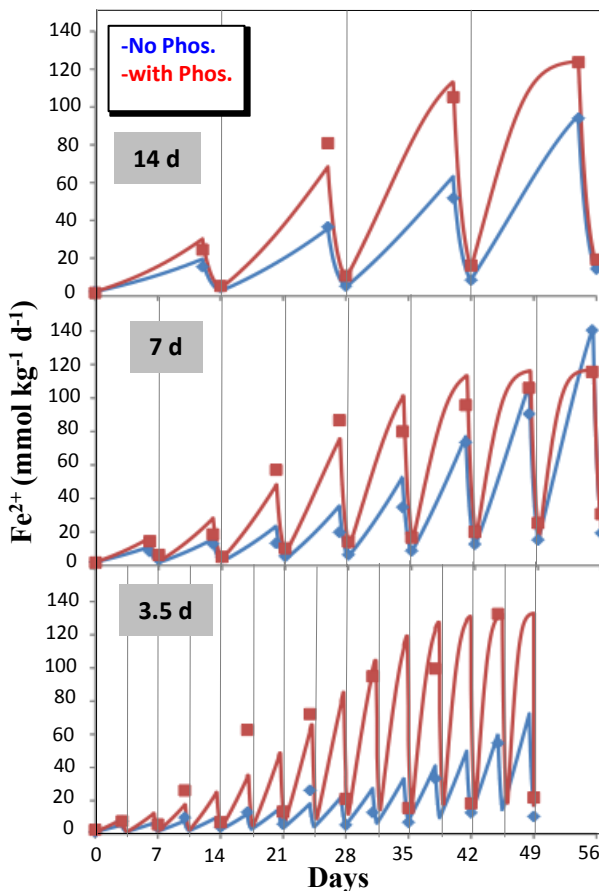
Variation in redox status is imposed by manipulating the supply of oxygen to a slurry leading to oscillations of defined frequency, amplitude and duration (dwell). The presented research examines modulation of redox frequency on Fe dynamics. Ongoing work explores modulation of the other two parameters.

Rates of Fe^{II} Reduction



Modeled rate of Fe²⁺ reduction: The rate of Fe^{II} reduction (P & no P amendment) increased dramatically as the experiment progressed. The current model uses a single pool of reducible Fe^{III}-oxide and implies higher cell-specific reduction rates for the P addition treatment. Ongoing work investigates the role of iron pools with different reactivities.

Fluctuating Fe^{II}



Observed and modeled Fe²⁺ dynamics: Comparison of simulated (lines) and measured (symbols) Fe^{II} during redox oscillations with frequency = 3.5 d, 7 d or 14 d. All reactors had $Dwell_{Ox/Red} = 1/6$ at full amplitude (21% O₂ during the oxic cycle). The P amended treatments approached the maximum Fe^{II} concentration at earlier oscillation cycles than the unamended treatments, but after 2 months all but the 3.5 d unamended treatment reached similar Fe^{II} oscillation amplitudes.



Differences in soil organic matter quality by biological, chemical and physical fractionation

Elizabeth Wordell (ewordell@sas.upenn.edu; MSAG)

Tsutomu Ohno (ohno@umaine.edu)

Alain Plante (aplante@sas.upenn.edu, co-PI)

Key Science Questions Involved:

1. What is the most appropriate method to characterize soil organic matter (SOM) quality in tropical soils?
2. Does SOM quality differ based between the parent materials, forest types, and slope positions in the LCZO?

Background

While other projects aim to determine the *quantity* of SOM in the surface soils of the LCZO, our goal was to characterize the *quality* of SOM in these soils. We define SOM quality in terms of its resistance to microbial decomposition due to various stabilization mechanisms, and therefore the term can be used interchangeably with SOM stability. Characterization of SOM quality is essential to identify potential responses in SOM quantity due to disturbance such as land use change or to global climate change. Characterizing the SOM quality typically involves the empirical separation of relatively unstable or labile fractions from relatively stable fractions. To identify these two fractions, a number of biological, physical, and chemical fractionation techniques have been developed. There is no definitively best method to identify or isolate labile SOM because each method uses different properties to define the fractions. In addition, these fractionation methods were largely developed using temperate soils, raising the question if they are applicable to tropical soils. Previous studies on temperate soil fractionations showed positive correlations between methods, meaning methods may be able to serve as a proxy for one another or to verify data consistencies between multiple methods, but also showed large differences in the sizes of the labile pools (McLauchlan and Hobbie, 2004).

The purpose of this study was to compare biological, physical, and chemical fractionation methods in tropical soils to identify differences in SOM stability. The design of the LCZO study also allowed for a comparison between parent material, forest type, and slope position, to identify environmental characteristic that may play a role in SOM stability in tropical soils.

Methods

Biological fractionation was performed using a 60-day laboratory incubation at 25°C. CO₂ measurements were taken periodically to determine respiration rates and cumulative CO₂ evolved. The biologically labile pool of SOM is the proportion of initial C respired (%C respired, g CO₂-C/g soil C). Physical fractionation was performed by separating the free and particulate OM from the mineral-bound OM by density using a sodium polytungstate solution (SPT) of density 1.6 g/cm³. The physically labile pool of SOM is the proportion of initial C in the light fraction (%LFC). Two chemical fractionations were performed: hot-water extractable organic carbon (HWEOC) and sodium pyrophosphate extractable C (py C). Hot-water extractions were performed at 70°C for 18 h, and sodium pyrophosphate extractions were

performed by shaking in 1.0 M solutions for 18 h. The chemically labile pools of SOM are the proportions of initial C in the HWEOC and pyrophosphate-extractable pools (% HWEOC and % py C).

Results

Table 1: Proportion of the labile soil organic matter pool determine by biological (%C Respired), physical (% LFC), and chemical (%HWEOC and %py C) fractionations

Parent Material	Forest Type	Catena Position	% C Respired	% LFC	% HWEOC	% py C
Granodiorite	Colorado	Ridge	2.2 ± 0.8	25.1 ± 1.9	3.7 ± 0.4	32.8 ± 4.4
		Slope	2.0 ± 0.5	32.3 ± 5.4	3.1 ± 0.3	27.6 ± 3.4
	Tabanuco	Ridge	1.7 ± 0.4	23.3 ± 5.9	2.8 ± 0.3	28.2 ± 1.4
		Slope	2.4 ± 0.7	30.2 ± 1.6	3.4 ± 0.6	39.5 ± 1.6
Volcaniclastic	Colorado	Ridge	1.8 ± 0.2	34.4 ± 0.7	3.8 ± 0.7	33.4 ± 0.2
		Slope	3.2 ± 0.1	30.5 ± 2.5	3.5 ± 0.8	31.9 ± 1.6
	Tabanuco	Ridge	1.4 ± 0.1	33.2 ± 5.2	4.6 ± 0.0	37.6 ± 3.5
		Slope	2.5 ± 0.7	34.2 ± 1.7	3.1 ± 0.2	34.9 ± 3.9

The three fractionations showed that the largest pool of labile SOM was in the light fraction of the density fractionation, with a range of 23-34%. The smallest labile pool was the respired pool, with only 1-3% of initial C, but this is a function of the relatively short incubation time. Because the three fractionation methods remove different pools of labile SOM, the percentages of extracted C from the soils may not be the best way to determine whether one fractionation method is better than another for tropical soils. However, the values are worth noting because the actual quantities of extracted C may have a strong correlation between fractionation methods. This correlation has been shown in previous studies performed on temperate soils in the past (McLauchlan and Hobbie, 2004) but has not yet been shown in tropical soils.

Standard 3-way analyses of variance (ANOVA) for each fractionation method showed no significant differences between parent material, forest type, and position, with one exception. The proportion of SOM in the light fraction was significantly different between parent materials, with samples from volcaniclastic bedrock containing an average of 33.2% and samples from granodiorite bedrock containing an average of 27.7% ($P = 0.02$). The results suggest that SOM quality was generally consistent across the LCZO. This is somewhat surprising given the variability in the landscape variables and may be attributable to low sample numbers or to the fact that these relatively coarse-scale methods are unable to distinguish more subtle differences in SOM quality.

McLauchlan KK, Hobbie SE (2004) Comparison of labile soil organic matter fractionation techniques. *Soil Sci. Soc. Am. J.* 68(5): 1616-1625